PB82-109372

Nearshore Marine Trace Metal Geochemistry

Rhode Island Univ., Narragansett

Prepared for

Environmental Research Lab.
Narragansett, RI

Aug 81

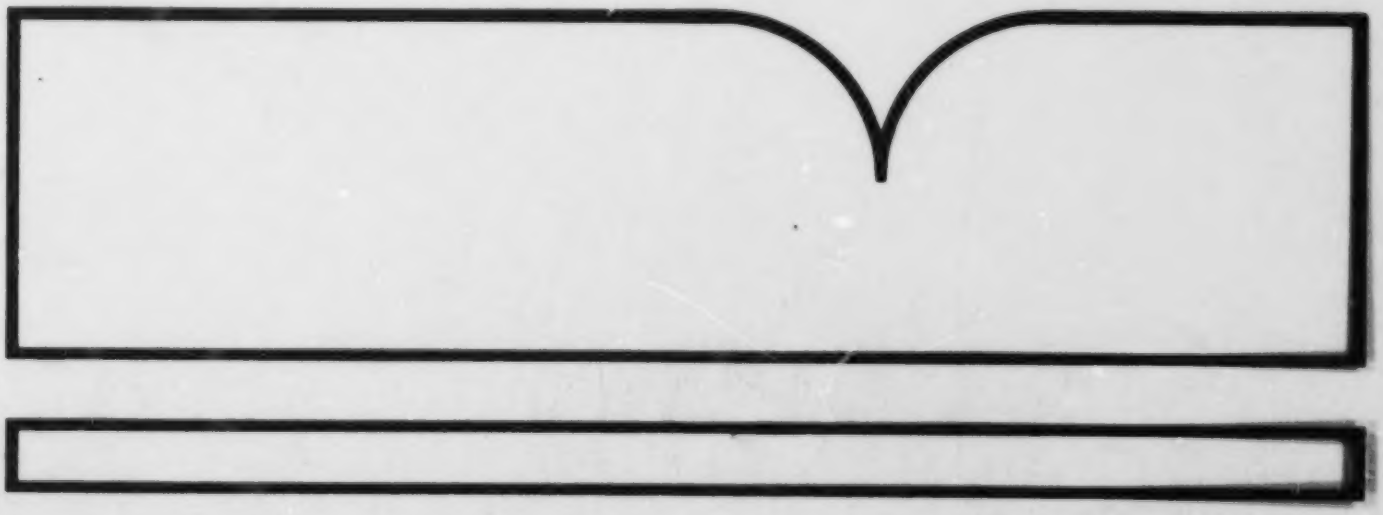

U.S. Department of Commerce
National Technical Information Service
NTIS.

PB82-109372

EPA 600/3-81-050

August 1981

NEARSHORE MARINE TRACE METAL GEOCHEMISTRY

by

Michael L. Bender
Graduate School of Oceanography
University of Rhode Island
Kingston, R.I. 02881

Project Officer

Earl Davey
Environmental Protection Agency
Environmental Research Laboratory
Narragansett, R.I. 02882

ENVIRONMENTAL RESEARCH LABORATORY
OFFICE OF RESEARCH AND DEVELOPMENT
U.S. ENVIRONMENTAL PROTECTION AGENCY
NARRAGANSETT, RHODE ISLAND 02882

Grant R-803243

Submitted June 1980

REPRODUCED BY
NATIONAL TECHNICAL
INFORMATION SERVICE
U.S. DEPARTMENT OF COMMERCE
SPRINGFIELD, VA 22161

TECHNICAL REPORT DATA (Please read Instructions on the reverse before completing)		
1. REPORT NO. EPA-600/3-81-050	2. ORD Report	3. RECIPIENT'S ACCESSION NO. PB82 109372
4. TITLE AND SUBTITLE Nearshore Marine Trace Metal Geochemistry		5. REPORT DATE August 1981
		6. PERFORMING ORGANIZATION CODE
7. AUTHOR(S) Michael L. Bender		8. PERFORMING ORGANIZATION REPORT NO. ERLN-X11
9. PERFORMING ORGANIZATION NAME AND ADDRESS Graduate School of Oceanography University of Rhode Island Narragansett, Rhode Island 02882		10. PROGRAM ELEMENT NO. AARB1A
		11. CONTRACT/GRANT NO. R 803243
12. SPONSORING AGENCY NAME AND ADDRESS EPA Environmental Research Laboratory South Ferry Road Narragansett, Rhode Island 02882		13. TYPE OF REPORT AND PERIOD COVERED Final Grant Report
		14. SPONSORING AGENCY CODE EPA/600/05
15. SUPPLEMENTARY NOTES		

16. ABSTRACT

In this final report, we summarize a number of studies aimed at understanding several aspects of the nearshore geochemistry of trace metals which give information on consequences of trace metal pollution attending nearshore waste disposal.

We have studied the distribution of dissolved and particulate trace metals in the Hudson River Estuary; pore water nutrient, carbon and metal geochemistry in Narragansett Bay; trace metal adsorption in Narragansett Bay sediments; and benthic fluxes of transition metals out of Narragansett Bay sediments.

Our key findings are that dissolved Mn, Ni, Cu, Cd and Zn tend to remain dissolved during passage through an estuary; that reducible metals (Mn and Fe) are released at rapid rates from reducing estuarine sediments; and that other divalent cations forming insoluble sulfides are sequestered in reducing nearshore sediment pore waters.

17. KEY WORDS AND DOCUMENT ANALYSIS		
a. DESCRIPTORS	b. IDENTIFIERS/OPEN ENDED TERMS	c. COSATI Field/Group
Sediments, trace elements, pore waters, Narragansett Bay, Hudson River Estuary		
18. DISTRIBUTION STATEMENT unlimited	19. SECURITY CLASS (This Report) unclassified	21. NO. OF PAGES 100
	20. SECURITY CLASS (This page) unclassified	22. PRICE

EPA Form 2220-1 (9-73)

ABSTRACT

In this final report, we summarize a number of studies aimed at understanding several aspects of the nearshore geochemistry of trace metals which give information on consequences of trace metal pollution attending nearshore waste disposal.

We have studied the distribution of dissolved and particulate trace metals in the Hudson River Estuary; pore water nutrient, carbon and metal geochemistry in Narragansett Bay; trace metal adsorption in Narragansett Bay sediments; and benthic fluxes of transition metals out of Narragansett Bay sediments.

Our key findings are that dissolved Mn, Ni, Cu, Cd and Zn tend to remain dissolved during passage through an estuary; that reducible metals (Mn and Fe) are released at rapid rates from reducing estuarine sediments; and that other divalent cations forming insoluble sulfides are sequestered in reducing nearshore sediment pore waters.

DISCLAIMER

This report has been reviewed by the Environmental Research Laboratory, U.S. Environmental Protection Agency, and approved for publication. Approval does not signify that the contents necessarily reflect the views and policies of the U.S. Environmental Protection Agency, nor does mention of trade names or commercial products constitute endorsement or recommendation for use.

FOREWORD

Man and his environment must be protected from the adverse effects of trace metals and other forms of pollution, and the unwise management of solid waste. Efforts to protect the environment require a focus that recognizes the interplay between the components of our physical environment--air, water, and land. The University of Rhode Island contributes to this multidisciplinary focus through programs engaged in

- studies on the effects of environmental contaminants on the biosphere, and
- a search for ways to prevent contamination and to recycle valuable resources.

This report helps us understand the consequences of various forms of solid waste disposal for marine trace metal pollution.

John A. Knauss

John A. Knauss, Dean
Graduate School of Oceanography

SECTION 1

INTRODUCTION

The disposal of wastes at a nearshore site may affect the environment by introducing heavy metals (among other pollutants) at subtoxic or toxic levels. Since certain wastes (notably sewage plant effluent, sewage sludge, and dredge spoils) have high metal concentrations, pollution of the affected environment is likely, and it is important to assess the impact of this pollution on the ecosystem. There are three steps to such an assessment: determining the fate of a pollutant metal, determining which metal species (i.e., free ionic, organically bound, particulate, etc.) have deleterious biological effects, and determining the deleterious effects of different metal concentrations.

This study has been concerned with understanding the fate of manganese, iron, nickel, copper, cadmium and zinc in the estuarine and nearshore environment. In particular, we have addressed three central questions: 1) how are these metals partitioned between the dissolved and particulate phases, 2) to what extent are they removed from the water column into sediments, in the nearshore environment? and 3) under what conditions are these metals released from sediments.

We have also addressed a related problem. Benthic nutrient regeneration is a major source of nutrients to nearshore waters. The dumping of polluted solids into these waters may, by impacting the benthic community, decrease the benthic fluxes of nutrients and lower the fertility of the overlying waters. Our results give insights into the question of whether nearshore dumping is likely to be a problem in this respect.

SECTION 2

CONCLUSIONS

Estuarine conditions vary greatly as a function of season, fertility (i.e., bloom vs. non-bloom conditions), and river runoff; and certainly there are major variations from one estuary to another. Hence caution must be used in extrapolating results from our study of two estuaries, concentrating on summer conditions, to other seasons and systems.

Our results reveal that about half of the dissolved copper, and more than half of the dissolved nickel, cadmium and zinc, entering the Hudson River at the harbor remain in the dissolved form until removed from the estuary by advection (water flow). Thus it is clear that adsorption, salting out, and other processes do not purify the water of these elements; they remain largely dissolved, presumably the state most toxic to organisms. On the other hand, we cannot do the mass balance well enough to rule out the possibility that up to half of the dissolved nickel, cadmium, and zinc entering the Hudson accumulate in sediments. In the case of copper, our data show that about this fraction is removed from solution into sediments. Manganese is apparently slowly removed from nearshore waters by oxidation onto particulates. Where estuarine residence times are on the order of a month and temperatures are warm, most of the dissolved manganese will be removed into sediments.

The benthic flux of iron, manganese, nickel, copper and cadmium out of anoxic nearshore sediments is consistent with the relative solubility of these metals in oxic and anoxic environments. Apparently as a result of insoluble sulfide formation, nickel, copper and cadmium have low pore water concentrations and are released at low rates to the overlying waters. Manganese and iron have high concentrations in anoxic pore waters; they are rapidly released although iron, which is very quickly oxidized in bottom water, shows a low net flux. These results suggest that release of nickel, copper, cadmium and other metals from dumped dredge spoils can be minimized by disposal of spoils under low energy, high productivity waters.

Nutrient benthic fluxes at highly polluted and a relatively clean Narragansett Bay sites are similar, indicating that pollution does not inhibit benthic bacterial decomposition and nutrient regeneration.

SECTION 3

RECOMMENDATIONS

With regard to preventing toxic metal release, the best type of nearshore environment for dumping dredge spoils and metal rich wastes are low energy environments underlying productive waters. The low energy will obviate sediment dispersal, and the high productivity will supply biogenic debris and insure maintenance of a reducing environment in which most heavy metals are sequestered within sediments. Polluted sediments are likely to be at least as highly reducing as clean sediments at a potential dump site. Thus a site where sediments are currently anoxic very near the interface (certainly within the top centimeter) would appear to be suitable for dumping.

These conclusions are based on very limited sampling and must be tested by more field work on pore water chemistry and metal benthic fluxes.

The effect of pollutants on benthic nutrient regeneration has not been adequately considered. While our results do not indicate that this is a problem, the possibility should be evaluated by more extensive work.

SECTION 4

OVERVIEW OF EXPERIMENTAL WORK AND DISCUSSION OF INTERRELATIONSHIPS

If we are to formulate a way of dumping dredge spoils and sewage sludge while minimizing release of toxic heavy metals from these wastes, we must understand the conditions under which dissolved metals are released from solid wastes, and their subsequent behavior in the nearshore and estuarine environments. To meet these needs we formulated and carried out a series of field and laboratory esperiments. These can be divided into four general studies. In the first, we separated pore waters from cores at three different locations in Narragansett Bay. The pore water samples were analyzed for nutrients, sulfate, sulfide, total CO_2 (TCO_2), major cations, and heavy metals in order to gain an appreciation of factors controlling the heavy metal content of pore waters. Such an appreciation is crucial to our objectives because the presence of metals in pore waters heralds their eventual release to the overlying water column.

Our second study was a laboratory experiment in which a total of six Narragansett Bay box cores, with about 10 cm of supernatant water, were spiked with γ-ray emitting isotopes of sodium and heavy metals. After 1-13 days the distribution of metals in the supernate, pore waters, and solids were assayed. These experiments give us insights into metal behavior in the Bay, and also allow us to estimate the rate at which interstitial water (and its contained metals and nutrients) is pumped across the sediment-water interface by organisms.

Our third study involved the experimental measurement of nutrient and metal fluxes across the sediment-water interface. These measurements allowed us to check the fluxes predicted from pore water data, thereby testing our working model for sediment-water exchange. They also provided prima-facia data on fluxes, which themselves are very valuable for determining conditions under which toxic heavy metals will be sequestered in the sediment.

Our fourth study was a two-pronged effort to understand the fate of dissolved heavy metals once they have been released into estuarine waters. We completed a synoptic study of the distribution of dissolved and particulate manganese in Narragansett Bay. We also carried out two studies of the distribution of dissolved and particulate heavy metals in the Hudson River estuary. These results provide the basis for a first order answer to the question of whether individual heavy metals, once released to the water column, will remain in the dissolved state or will rapidly sediment out.

SECTION 5

PORE WATER WORK

STATION LOCATIONS

Pore water chemistry and benthic fluxes were studied at three locations in Narragansett Bay - Jamestown North (JN), Rumstick Neck (RN), and Sabin Point (SP) (figure 5-1). The Jamestown North site has an active macrobenthic community and is regarded as a relatively unpolluted site. The Sabin Point site has a relatively small community of macrobenthos and high level of hydrocarbons; it is regarded as a highly polluted site where the benthos has been impacted. Rumstick Neck is intermediate both in location and in the degree to which it has been affected by pollution.

ANALYTICAL TECHNIQUES

Pore Water Sampling

Standard pore water sampling methods used in this work employed two coring devices. The first was a hand inserted box core (30 x 9 x 25 cm), which allowed specific separation of the surface layers of sediment down to 15-20 cm. This was placed into the sediment by a diver, sealed under water, and returned to the laboratory. Once in the lab the core was separated as soon as possible, usually within 12 hours of sampling. Separation was carried out in a He-inflated glove bag in the refrigerator at 4°C. Fractions of 1/2 to 1 cm in depth were scraped from the box core into large centrifuge bottles. These were then centrifuged in a refrigerated centrifuge at 4000 G for 10 minutes. The resulting supernatant pore waters were siphoned into large syringes, and filtered through a 0.45 micron Nucleopore filter before chemical analysis. An average of 40-60 cc of pore water were extracted from each 1 cm fraction in this manner. The second coring method used was diver-assisted large gravity core. A 4 1/2 in diameter plastic sewage pipe was adapted for the normal 2 1/2 inch gravity corer. Sampling was achieved down to 100 cm in the sediment. This was extruded, in air, in fractions of 2 cm at 5 or 10 cm intervals. Again the samples were placed in large centrifuge bottles and the pore water extracted as before. Transfer of exposed sample to sealed centrifuge bottle was accomplished in less than one minute.

Porosity

Sediment porosity (ϕ), as measured by the volume of saturated sediment occupied by interstitial water, is estimated from the formula

Fig. 1: Narragansett Bay core locations.

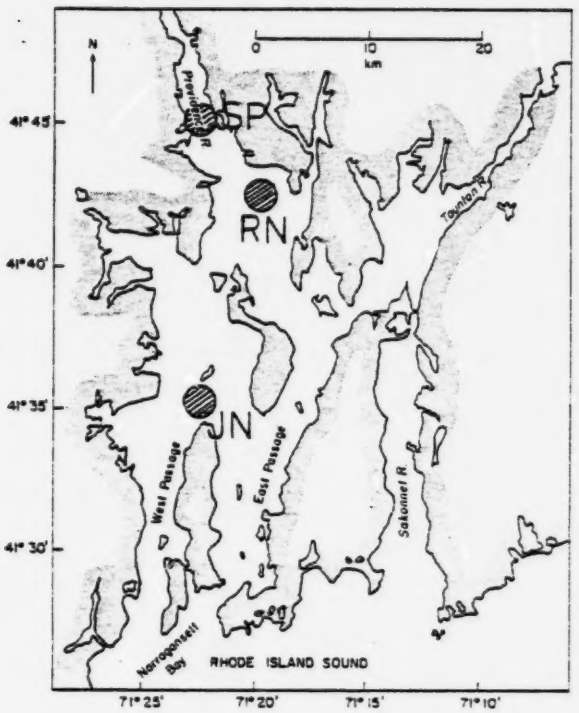

Station Locations

SP - This is the Sabin Point station located in the Providence River (71°23' W, 41°45'N). It lies just south of the intersection of Bullock Point Reach and Sabin Point Reach in the river channel.

RN - This is the Rumstick Neck station located at the mouth of the Providence River (71°20'W, 41°42'N). Situated along the Rumstick Neck Reach of the shipping channel it lies between buoys R"14" and N"16" (1975).

JN - The Jamestown North station is in a central location between Conanicut and Hope Islands (71°23'W, 41°35'N).

$$= \frac{V_{pw}}{V_{pw} + V_{solids}}$$

where V_{pw} is the volume of interstitial water (pore water) and V_{solids} is the volume of solids. In this work,

$$V_{pw} = v_i = \frac{m}{\rho}/\text{supernat} + \frac{m}{\rho} / \text{evap.}$$

where m is the mass of fluid removed and ρ is the density ($\rho_{supernate}$ is taken to be 1.02 and $\rho_{evap.}$ is 1.00 g/cm^3). From 1/3 - 1/2 of the interstitial water is removed by centrifugation and siphoning off the supernate, the remainder by evaporation.

In this work the masses of both the inorganic and organic fractions of the total solids are available, so that the contribution of both fractions to the total volume of solids may be estimated as follows:

$$V_{solids} = v_i = \frac{m}{\rho}/\text{inorganic} + \frac{m}{\rho}/\text{organic}$$

where m is the dry mass of the solid phases and ρ-inorganic is taken as 2.5 and ρ-organic arbitrarily as 1.0. Most of the volume of sediment is inorganic inorganic, however, explicit inclusion of the organic phase does reduce the calculated porosity by about 4%. Sediment weights have been corrected for evaporated salts.

Organic Matter Content

Organic matter content is estimated by determining weight loss on ignition (475°C) of dry sediment samples and is expressed as a percentage of oven-dry weight (90°C). Possible losses of bound water or CO_2 are ignored but are considered relatively small.

pH

A variety of pH measurement techniques have been used on pore water samples, both filtered and unfiltered. The most reliable resutls appear to be obtained using unfiltered pore water, which was the procedure employed in cores SP-7 and JN-11 and later (higher number) cores. In these cases, a small (5 ml) sample of unfiltered pore water was injected directly into a 10 ml syringe body, fitted closely around a combination pH electrode, previously calibrated against standard buffers and equilibrated with seawater for at least 1/2 hour. When sufficient sample was available, the apparatus was filled to overflowing. Exchange with the atmosphere, kept to a minimum, occurred several cm away from the active portion of the glass electrode. Readings were taken after initial rapid change had become stable or drifted slowly, normally about 10 minutes after injection.

Total CO_2

The implementation of low molecular weight gas chromatographic techniques (Davey and Curl 1967) allowed determination of the total carbon dioxide (TCO_2) content of the pore water samples. A filtered sample of 0.5 ml was introduced into an in-line HCl reaction chamber by a sample loop injection system. Released gases were then passed with the Helium carrier through an indicating Drierite column to remove water vapor. It is believed that H_2S released by some of the samples was also removed by the Drierite. Separation of the CO_2 peak was accomplished using a Porpak QS molecular sieve column following the Drierite column. The gases were monitored by a thermistor detector and read out on a Hewlett Packard integrator unit in addition to a strip chart recorder. Specific retention time of the CO_2 peak varied relative to the length of the different columns employed from day to day.

Standards run were a concentration series of Na_2CO_3 solutions ranging from 1 mM to 100 mM and in a NaCl matrix approximating Bay water chlorinity. Within this range standard peak areas varied linearly with concentration. The precision for both samples and the 2 mM standard was ±4%.

It was also determined, with the use of sequential analysis, that cold storage of samples in capped glass vials caused no significant loss of TCO_2 over a 2-3 day period.

$SO_4^=$

Analysis of the sulfate ion was obtained through a $BaSO_4$ precipitation method employing a radioactive Ba tracer. Similar analysis had previously been used by Goode (1968) to determine microgram quantities of sulphur in petroleum, and by Dimitt and Graham (1976) in the analysis of microgram amounts of sulfate in solution.

To 1 ml of each filtered pore water sample was added 1 ml of a 135 mM $Ba(NO_3)_2$ solution spiked with ^{133}Ba. The resulting precipitate was then quantitatively transferred and filtered through a 0.45 μm Nucleopore filter to collect the filtrate. Subsequently the filter was transferred to a counting vial for ^{133}Ba determination.

The 81 Kev and 356 Kev γ -rays of the ^{133}Ba tracer, with a 10.4 year half-life, were monitored for 4000-8000 sec. with a GeLi detector linked to a Nuclear Data 2200 Analyzer, and the spectra were read out to a magnetic tape unit. These peaks were then quantified using the program GAMNL by the IBM-370 computer system of the University of Rhode Island. The $SO_4^=$ concentration is proportional to the ^{133}Ba peak area. Analysis of standards confirmed that the ^{133}Ba activity precipitated is proportional to the $SO_4^=$ concentration. The precision is ±5% for sea water.

The speed of preparation allows the sample to be fixed within minutes after separation from the sediment. Subsequent analysis by -ray counting can then be accomplished at any time due to the long half-life of the tracer.

$S^{=}$ & NH_3

The ammonia and sulphide methods are the standardized colorimetric techniques of Solorzano (1969) and Cline (1969) respectively. The only modifications made are concerned with the sample volume, owing to the quantity of pore water available as well as the high concentration of these nutrients in the pore water.

Ammonia samples have a final total volume (after dilution) of 10 mls, and the reagents are added in proportion to this volume. The phenol-blue color produced in the reaction adheres to Beers Law from 0-40 μM NH_3. All samples are diluted to fit within this range of the standard curve.

Sulphide samples also require dilution prior to the addition of the reagent (N, N-dimethyl-p-phenylenediamine sulfate and ferric chloride in 50% (v/v) HCl). This determination has three reagent concentrations corresponding to three sulphide ranges, 3-40 $\mu MS^{=}$, and 250-1000 $\mu MS^{=}$; all have proved to be linear when absorbance is compared to concentration. A 5 ml final sample volume has been used in all instances and a proportionate amount of the reagent added.

It should be noted that ΣCO_2 concentrations are used as an index of nutrient quantity, taking some of the guess work out of dilution factors.

Phosphates

Reactive phosphate concentrations were determined by molybdate blue colorimetry (Murphy and Riley, 1962) with a Technicon AutoAnalyzer (Industrial Method 155-71 W). 880 nm interference filters were used with red sensitive (s-1) phototubes and 50 mm flow cells. The technique is linear over at least 0-10 μM-P. We diluted standards and samples identically with deionized water to obtain sample absorbance in this range. Undiluted working standards (0-1000 μM) were prepared in deionized water, which was also used to measure reagent blanks (baseline), and for intersample wash. Working phosphate standards were always prepared from the same 1000 μM primary standard, which has shown no drift over a three year period. Standards and deionized water blanks were checked several times during the duration of the experiments by the manual phosphate technique to ensure high precision.

The Technicon recommended wetting agent (Levor IV) forms an insoluble Ca^{2+} and Mg^{2+} salt in seawater. In order to avoid this, and yet maintain good bubble flow, we preconditioned the tubing by first pumping a dilute Levor IV solution, followed by pumping distilled water and then reagents for 15 minutes each prior to sample runs. This technique effectively conditions the inside walls of the AutoAnalyzer tubing for about eight hours and allows elimination of a wetting agent from the reagents.

Dissolved silicate interference is negligible. Sulfide interference is eliminated by bubbling air through those samples which, after dilution, still exhibited a sulfide odor. Removal of sulfide below the "nasal detection limit" eliminated sulfide interference. No attempt was made to eliminate interferences from dissolved iron III, arsenic IV, or tannins.

Analytical precision of the phosphate data is estimated to be within 5%. All samples were determined in duplicate.

Silicates

Dissolved silica was determined by molybdate blue colorimetry using ascorbic acid as a reducing reagent with a Technicon AutoAnalyzer (Industrial Method 186-72 W). 815 nm interference filteres were used with red-sensitive (s-1) phototubes and 25 mm flow cells.

The technique is linear over the range 0-50 µm. We diluted samples and standards identically with deionized water to obtain sample absorbances in this range. Standards (0-1000 µ) were prepared in deionized water, which was also used as reagent blanks (baseline) and intersample wash. Working silicate standards were always prepared from the same primary silica standard (20,000 µm), which has shown no drift for many years. Silicate standards and blanks were checked with the manual technique (Mullin and Riley, 1955) to ensure high precision. Since all samples and standards after dilution were of about the same salinity, no attempt was made to correct for salinity effects on absorbance (salt factor: Fanning and Pilson, 1973).

Acetone was omitted from the Technicon method reagents. Acetone increases sensitivity but introduces irreproducibility. Reagent concentrations were modified slightly to obtain maximum sensitivity. Wetting agents (Levor IV) were also omitted (see discussion in phosphate technique).

Phosphate interference at the 1000 µm-P level is insignificant. Sulfide interference was eliminated by degassing (see phosphate technique).

Analytical precision of the silicate data is estimated to be ±5%. All samples were determined in duplicate.

Na^{+}, Ca^{++}, Mg^{++}

Major cation analysis of Na, Ca, and Mg was accomplished by atomic absorption spectroscopy using the method of E.V. Hoffman (1975). A Perkin-Elmer model 360 atomic absorption spectrophotometer with flame attachments and digital readout enabled rapid and simplified analysis.

A 0.5 ml aliquot of each filtered sample, which had been previously acidified for storage, was diluted 200 times in a 0.1 N HNO_3 solution containing 1000 ug/gm LaO and 1000 ug/gm CsCl. Dilutions of Copenhagen standard sea water were used to establish standard curves. Flame atomic absorption techniques as outlined in the standard methods manuals of Perkin Elmer were used.

Atom ratios of Ca/Na and Mg/Na were determined by a direct relationship to those determined in the standard Copenhagen water. The precision of the ratio determinations is ±1%.

Metals

Iron, manganese, cadmium, copper and nickel concentrations have been determined by flameless atomic absorption spectrophotometry, using either the Perkin Elmer model 503 or the 360 spectrophotometers. Both are equipped with the HGA 2100 graphite furnace.

Iron and manganese are in sufficient quantity in pore waters such that they are analyzed by a direct injection procedure. If dilutions of these pore water samples is required, Sargasso Sea water of known concentration is used. To each one ml. sample, 5 µl of G. Fredrick Smith ultra pure concentrated sulfuric acid is added to maintain the metals in solution.

Cadmium, copper and nickel are analuzed by flameless atomic absorption after concentrating the sample by a modified cobalt APDC (ammonium pyrillodine dithiocarbonate) copreciation method (Boyle and Edmond, 1975). An 8-12 gram pore water sample is weighed into a 20 ml scintillation vial; to this is added 0.2 mls of the cobalt chloride solution, followed by the addition of 0.4 mls of the APDC. The sample is shaken vigorously, and the reaction is allowed to proceed for no less than one half hour. The sample is then filtered onto a 2.5 cm diameter, .45 µm pore size, Nucleopore filter. The filter is removed from a millipore filtration unit and placed in a 215 dram ultra clean polyvial containing 1.0 ml of 3N G. Fredrick Smith redistilled nitric acid, and is sonicated for a period of no less than one hour. After sonication the filter is removed, the sample is now ready for analysis.

Because these trace metals exist in very minute quantity, i.e. Cd < 0.10 ppb, Cu < 3 ppb, it is necessary to clean the reagents and containers used in this method. All polyvials and 20 ml scintillation vials are soaked in a 50% HCl bath overnight. These are then removed to a one liter container, and rinsed several times with double deionized water (DDI). Another 50% HCl solution is added to the container, and the vials are sonicated for three hours. The containers are then rinsed at least three times with DDI water. The containers are sonicated for another three hours in DDI water. The vials are rinsed six times with DDI water and placed in a clean bench to dry.

Cobalt chloride is cleaned in the following manner: 0.425 grams of $CoCl_2$ $CoCo_2 \cdot 6H_2O$ is made to 150 mls with 9 M HCl and passed through a column of Dowex 1 - X8 anion exchange resin (4 grams No - 200 Cl^-) Co, Cu, Zn, and Fe^{3+} are retained while Ni and Mn pass through. The column is eluted with 40 mls of 4 M HCl. The color sequence of eluent will change from a blue violet, to rose and pink (the Co-containing fraction, which is saved), to clear (stop). The cofraction is made up to 500 ml with DDI water.

4 g ammonium pyrillodine dithiocarbomate (APDC) is dissolved in 200 mls Double DeIonized water. The slurry produced is filtered through a 0.45 µm Nucleopore filter and dispensed into a separatory funnel. The APDC is then extracted 5 times with 20 mls of Methyl Isobutyl Ketone (MIBK), and each organic fraction is thrown away.

DISCUSSION OF RESULTS

Pore water chemistry for 9 Jamestown North cores, one Rumstick Neck core, and eight Sabin Point cores are given in tables 5-1 to 5-18, and plotted in figures 5-2 to 5-12.

Before discussing the results, it is appropriate to review two simple models of organic matter diagenesis. The second model, which will be adopted in the ensuing discussion, provides a very useful framework for the interpretation of our results.

Consider an enclosed volume with sea water and organic matter. Assuming the organic matter has the Redfield stoichiometry it will be decomposed according to the following reaction:

$$5(CH_2O)_{106}(NH_3)_{16}(H_3PO_4) + 690\ O_2 \longrightarrow 530\ CO_2 + 80\ HNO_3 + 5\ H_3PO_4 + 610\ H_2O$$

This reaction will continue until all oxygen is consumed. Narragansett Bay water has a summertime total CO_2 (TCO_2) content of about 2,000 $\mu M\ kg^{-1}$ and O_2 content of 150 $\mu M\ kg^{-1}$. If it were encapsulated, the total CO_2 content would rise to 2,115 $\mu M\ kg^{-1}$ when all O_2 is consumed. In a system in which O_2 diffuses in and CO_2 diffuses out the maximum TCO_2 content present under anaerobic conditions is marginally higher as a result of the fact that O_2 diffuses faster than CO_2. The TCO_2 content of virtually all pore waters sampled as part of this work is greater than 2150 μM, reflecting metabolic CO_2 production by a pathway other than oxygen reduction.

When all oxygen has been consumed, oxidation by nitrate commences according to the general reaction:

$$5(CH_2O)_{106}(NH_3)_{16}(H_3PO_4) + 472\ HNO_3 \longrightarrow 530\ CO_2 + 276\ N_2 + 886\ H_2O + 5\ H_3PO_4$$

Model nitrate concentrations at the end of O_2 reduction (which are variable because they depend on initial nitrate concentrations in the encapsulated water) are about 30 μM. Complete reduction of this much nitrate would produce about 34 μM of CO_2, about 25% of that produced by O_2 reduction or about 0.05% of that produced by complete reduction of all encapsulated sulfate. Hence nitrate reduction is not important in the total metabolism, although it may be extremely important in the nitrogen balance itself.

When all nitrate has been consumed, oxidation proceeds by sulfate according to the reaction:

$$(CH_2O)_{106}(NH_3)_{16}(H_3PO_4) + 53\ SO_4^{=} \longrightarrow 106\ HCO_3^{-} + 16\ NH_3 + H_3PO_4 + 53\ H_2S.$$

Table 1: Pore water data for Jamestown North Core #3 (7/3/75)
Trace metal concentrations in ppb.

Depth (cm)	Porosity	Organic matter	pH	CO_2 (mM)	$SO_4^=$ (mM)	$S^=$ (mM)	NH_3 (mM)	$PO_4^=$ (mM)	Si (mM)	Ca/Na atom ratio X 10^{-2}	Mg/Na atom ratio X 10^{-1}	Mn	Fe	Cd	Cu	Ni
Supernatant-A				2.17	26.3	-	7.9	4.2	60			510	140	0.31	3.5	1.6
Supernatant-B				-	-	-	16.3	4.1	59			510	70	0.04	1.3	0.8
0 - 1				3.16	22.3	-	160	25	240			2100	4100	0.11	6.6	8.1
1 - 2				2.80	26.5	-	143	41	280			2200	5700	<0.05	3.8	4.1
2 - 3				2.93	25.0	-	105	41	300			1510	6000	<0.03	3.1	1.6
3 - 4				3.03	25.5	-	121	27	290			1660	4500	<0.05	2.8	1.6
4 - 5				3.07	24.4	-	121	36	300			1060	4800	<0.03	2.6	1.2
5 - 6				2.99	23.0	-	117	52	320			1060	6200	<0.03	8.6	6.3
6 - 7				3.34	23.6	-	280	60	340			630	4300	<0.05	7.9	7.8
7 - 8				2.56	22.0	-	125	55	310			630	4900	<0.05	4.0	1.2
8 - 9				3.06	24.9	-	126	34	300			850	3700	<0.05	7.7	1.9
9 - 10				2.90	26.0	-	117	28	290			1080	3200	<0.03	2.8	1.0
10- 11				2.67	24.2	-	97	33	280			690	3400	<0.03	4.1	1.2

Table 2: Pore water data for Jamestown North Core #5 (7/15/75)
Trace metal concentrations in ppb.

Depth (cm)	Porosity	Organic matter	pH	CO_2 (mM)	$SiO_4^{=}$ (mM)	$S^{=}$ (mM)	NH_3 (mM)	$PO_4^{=}$ (mM)	Si (mM)	Ca/Na atom ratio $\times 10^{-2}$	Mg/Na atom ratio $\times 10^{-1}$	Mn	Fe	Cd	Cu	Ni
Supernatant-A			7.68	2.15	26.7	-	135	4.1	82	2.16	1.10	380	74	1.50	3.4	3.1
Supernatant-B			7.67	2.15	25.6	-	28	4.4	83	2.15	1.10	390	106	0.21	5.4	1.9
0 - 1			7.58	2.88	27.4	-	91	23	350	2.16	1.11	1810	3800	0.15	5.6	3.0
1 - 2			-	3.20	25.5	0.05	154	43	420	2.12	1.09	1090	5300	<0.05	7.2	3.1
2 - 3			7.62	3.11	26.8	-	145	71	460	2.17	1.08	820	6400	<0.05	9.5	3.8
3 - 4			7.52	3.50	27.0	-	155	67	470	1.80	1.12	860	4700	<0.05	6.1	2.0
4 - 5			7.54	3.25	26.4	-	153	65	480	2.00	1.12	890	4400	<0.05	7.3	2.6
5 - 6			7.56	5.33	25.1	0.05	165	150	500	-	-	1160	3600	0.15	30	7.6
6 - 7			7.61	3.30	23.2	-	157	73	520	2.17	1.09	1310	3900	<0.05	9.0	3.3
7 - 8			7.61	3.48	23.4	0.05	152	56	500	2.25	1.11	1010	3100	<0.05	7.9	2.7
8 - 9			7.56	3.14	25.5	-	144	48	460	-	-	1000	1400	<0.05	4.4	1.4
9 - 10			7.60	2.93	26.3	-	136	44	450	2.19	1.09	900	2300	0.15	21	5.8
10 - 11			7.74	3.28	23.2	-	151	41	420	-	-	670	610	<0.05	5.1	1.4
11 - 12			-	-	-	-	-	-	-	-	-	-	-	-	-	-
12 - 13			7.62	2.98	25.5	-	106	13.8	370	2.16	1.08	300	200	0.10	4.0	1.5
13 - 14			-	-	-	-	-	-	-	-	-	-	-	-	-	-
14 - 15			-	-	-	-	-	-	-	-	-	-	-	-	-	-
15 - 16			7.68	2.81	24.6	0.05	90	9.3	360	2.24	1.09	200	90	<0.05	3.1	0.6
16 - 17			7.77	3.04	23.7	-	210	2.0	340	2.15	1.08	200	190	<0.05	4.7	3.0

Table 3: Pore water data for Jamestown North Core #6 (7/22/75)
Trace metal concentrations in ppb.

Depth (cm)	Porosity	Organic matter	pH	CO_2 (mM)	$SO_4^=$ (mM)	$S^=$ (mM)	NH_3 (uM)	$PO_4^=$ (uM)	Si (uM)	Ca/Na atom ratio X 10	Mg/Na atom ratio X 10	Mn	Fe	Cd	Cu	Ni
Supernatant-A			7.59	2.00	25.4	-	2.6	2.70	63	2.19	1.14	260	22	0.50	4.9	2.8
Supernatant-B			7.80	2.05	26.5	-	2.6	2.72	65	2.17	1.06	250	21	0.28	5.4	1.6
0 - 1			7.69	2.35	26.9	-	74	15	290	2.20	1.07	1680	2000	0.09	15	4.3
1 - 2			7.70	2.55	26.9	<0.05	90	25	380	2.22	1.12	960	2600	<0.05	6.2	3.5
2 - 3			7.77	3.00	26.6	-	93	36	420	2.27	1.09	710	2900	<0.05	4.8	2.0
3 - 4			7.72	2.57	23.7	<0.05	106	50	480	2.16	1.12	580	3700	<0.05	10	3.9
4 - 5			7.75	2.54	25.4	-	99	38	430	2.19	1.12	570	2500	<0.05	4.9	2.9
5 - 6			7.82	2.65	26.5	<0.05	125	62	460	-	-	640	3500	<0.05	7.7	7.0
6 - 7			7.80	2.92	26.9	-	152	82	490	2.21	1.11	620	3600	<0.05	8.8	6.0
7 - 8			7.88	3.00	25.0	<0.05	112	68	480	2.24	1.10	680	2600	<0.05	1.8	5.3
8 - 9			7.64	3.02	25.7	-	122	64	470	2.20	1.09	630	2400	<0.05	7.0	5.5
9 - 10			7.83	2.85	27.3	<0.05	99	55	420	2.20	1.10	640	1910	<0.05	6.4	3.2
10 - 11			7.88	2.75	-	-	109	44	390	2.23	1.09	550	1490	<0.05	5.3	2.6
11 - 12			7.90	2.70	-	<0.05	91	39	350	-	-	510	1490	<0.05	5.2	2.4
12 - 13			7.90	2.40	25.5	-	79	30	310	2.25	1.10	420	800	<0.05	3.4	2.6
13 - 14			7.96	2.30	25.2	<0.05	69	24	290	-	-	330	350	<0.05	4.2	1.4
14 - 15			7.98	2.98	24.1	-	67	16	240	2.20	1.10	260	230	<0.05	2.1	2.2
15 - 16			7.92	2.16	23.5	<0.05	70	13	210	2.21	1.11	210	123	0.07	5.2	5.9

Table 4: Pore water data for Jamestown North Short Core #7 (9/23/75)
Trace metal concentrations in ppb.

Depth (cm)	Poros-ity	Organic matter	pH	CO_2 (mM)	$SO_4^=$ (mM)	$S^=$ (mM)	NH_3 (uM)	$PO_4^=$ (uM)	Si (uM)	Ca/Na atom ratio $\times 10^{-2}$	Mg/Na atom ratio $\times 10^{-1}$
Supernatant-A				2.55	25.7	0.004	63	5.1	180	2.17	1.12
Supernatant-B				2.45	23.2	-	65	5.1	180	2.17	1.12
0 - 1	0.75	4.3		2.75	25.4	0.027	107	35	330	2.19	1.09
1 - 2	0.67	3.8		2.85	24.9	-	115	24	340	2.17	1.10
2 - 3	0.67	4.0		2.75	25.4	0.007	119	38	350	2.17	1.10
3 - 4	0.67	5.0		2.73	-	-	122	51	370	2.17	1.11
4 - 5	0.70	4.7		3.00	23.4	0.010	115	52	340	2.16	1.13
5 - 6	0.65	4.2		2.85	-	-	128	67	370	2.15	1.12
6 - 7	0.70	5.0		2.75	26.2	0.010	113	53	340	2.16	1.12
7 - 8	0.69	4.8		2.75	25.0	0.011	106	50	320	2.17	1.13
8 - 9	0.71	4.6		2.75	26.8	-	102	38	300	2.17	1.14
9 - 10	0.67	4.2		2.70	-	0.010	103	35	310	2.16	1.12
10 - 11	0.69	4.8		3.10	24.9	-	108	38	300	2.17	1.13
11 - 12	0.67	4.1		3.00	-	0.006	95	31	300	2.16	1.12
12 - 13	0.67	4.1		2.45	22.7	-	97	30	300	2.16	1.13
13 - 14	0.66	4.0		2.73	-	-	97	36	300	2.16	1.10
14 - 15	0.80	4.0		2.45	23.6	-	100	33	310	2.17	1.10
15 - 16	0.69	4.6		2.55	-	0.008	102	27	300	2.18	1.10
16 - 17	0.66	3.8		2.95	24.6	-	103	24	310	2.17	1.11
17 - 18	0.66	4.0		3.00	-	0.045	140	32	340	2.19	1.10
18 - 19	0.68	4.1		3.25	23.2	0.007	128	22	350	2.19	1.11

Table 5: Pore water data for **Jamestown North Long Core #8 (9/23/76)**
Trace metal concentrations in ppb.

Depth (cm)	Poros-ity	Organic matter	pH	CO_2 (mm)	$SO_4^=$ (mm)	$S^=$ (mm)	NH_3 (um)	$PO_4^=$ (um)	Si (um)	Ca/Na atom ratio$_2$ X 10^{-2}	Mg/Na atom ratio$_1$ X 10^{-1}
5	0.69	4.5	7.54	2.6	25.7	0.006	-	25	300	2.20	1.14
10	0.67	4.3	7.82	2.2	25.2	-	-	29	270	2.19	1.14
15	0.70	4.7	7.63	2.1	25.4	0.014	-	16	270	2.20	1.13
20	0.72	4.4	7.64	2.3	23.2	0.017	157	18	360	2.19	1.13
30	0.71	4.2	7.70	3.8	24.3	0.100	330	36	520	2.16	1.12
40	0.74	4.6	7.68	6.7	23.4	0.38	510	59	670	2.15	1.12
45	0.73	4.2	7.78	8.3	22.3	0.29	580	63	700	2.15	1.11
50	0.74	4.6	7.73	8.7	21.5	1.11	730	66	690	2.15	1.12
60	0.72	4.1	7.74	10.5	21.8	1.77	940	73	750	2.16	1.11
70	0.75	4.7	7.63	12.1	22.4	2.20	1190	77	760	2.16	1.11
80	0.76	4.5	7.61	13.1	19.1	2.30	1010	81	730	2.12	1.13
90	0.72	4.1	7.60	15.0	19.9	3.20	1790	85	780	2.11	1.12
100	0.64	3.8	7.75	16.0	19.9	2.20	1230	88	740	2.09	1.14
110	0.72	4.8	7.74	17.3	18.7	3.60	1360	92	740	2.09	1.12

Table 6: Pore water data for Jamestown North Short Core #9 (1/20/76)
Trace metal concentrations in ppb.

Depth (cm)	Porosity	Organic matter	pH	CO_2 (mm)	$SO_4^=$ (mm)	$S^=$ (mm)	NH_3 (um)	$PO_4^=$ (um)	Si (um)	Ca/Na atom ratio $\times 10^{-2}$	Mg/Na atom ratio $\times 10^{-1}$
Supernatant-A				1.90	23.0	<0.003	3.0	1.1	15		
Supernatant-B				1.86	23.5	<0.003	3.3	1.1	15		
0 - ½	0.76	5.1		2.33	23.9	<0.003	-	3.1	100		
½ - 1	0.70	5.7		2.32	22.2	-	18.4	4.1	140		
1 - 2	0.68	5.3		2.41	21.6	-	48	5.0	150		
2 - 3	0.65	5.0		2.49	20.7	<0.003	69	12.3	180		
3 - 4	0.66	5.0		2.48	23.6	-	76	14.5	180		
4 - 5	0.69	5.2	7.42	2.41	25.6	<0.003	60	17.0	200		
5 - 6	0.68	5.3		2.36	22.3	-	63	20	220		
6 - 7	0.71	6.0	7.49	2.33	22.9	<0.003	68	16.0	210		
7 - 8	0.69	5.6		2.31	23.6	<0.003	-	20	220		
8 - 9	0.69	5.5		2.38	23.5	-	67	16.0	220		
9 - 10	0.69	5.6	7.58	2.33	24.8	-	71	17.0	220		
10 - 11	0.67	5.3		2.31	24.6	<0.003	65	17.0	210		
11 - 12	0.65	4.6		2.25	23.5	-	63	15.1	190		
12 - 13	0.65	4.9		2.25	22.3	-	63	16.0	190		
13 - 14	0.66	5.0	7.58	2.25	23.7	-	58	14.2	180		
14 - 15	0.66	4.8	7.74	2.06	24.3	-	54	10.6	160		

Table 7: Pore water data for Jamestown North Long Core #10 (2/12/76)
Trace metal concentrations in ppb.

Depth (cm)	Porosity	Organic matter	pH	CO_2 (mm)	$SO_4^=$ (mm)	$S^=$ (mm)	NH_3 (um)	$PO_4^=$ (um)	Si (um)	Ca/Na atom ratio X 10^{-2}	Mg/Na atom ratio X 10^{-1}
5	0.72	7.1	-	2.72	24.4	-	77.0				
10	0.66	4.2	7.77	2.44	22.8	-	91				
15	0.65	4.3	-	2.30	22.0	0.017	47				
20	0.65	10.2	7.82	2.26	23.0	0.017	36				
25	0.70	4.9	7.68	2.50	23.6	0.017	75				
30	0.72	4.8	-	3.03	22.5	0.022	141				
35	0.71	4.4	7.66	4.09	21.3	0.072	220				
40	0.72	3.9	7.82	4.60	22.3	0.150	610				
45	0.72	4.4	7.93	5.16	22.6	0.184	320				
50	0.69	4.4	-	6.29	21.6	0.093	480				
55	0.71	4.3	7.87	7.29	22.0	0.191	630				
65	0.69	4.0	7.82	11.6	19.5	0.470	1050				
75	0.66	3.8	-	11.6	19.4	0.102	930				
85	0.67	3.9	7.98	12.9	19.0	0.300	930				
90	0.66	4.1	-	13.8	17.5	0.710	1020				

Table 8: Pore water data for Jamestown North Core #11 (7/13/76)
Trace metal concentrations in ppb.

Depth (cm)	Porosity	Organic matter	pH	CO_2 (mM)	$SO_4^=$ (mM)	$S^=$ (mM)	NH_3 (uM)	$PO_4^=$ (uM)	Si (uM)	Ca/Na atom ratio X 10^{-2}	Mg/Na atom ratio X 10^{-1}	Mn (ppb)	Fe (ppb)	Cd (ppb)	Cu (ppb)	Ni (ppb)
0 - ½				2.83	26.2	<0.003	75	13.0				2500	2000	<.10	2.6	5.8
½ - 1				2.73	25.7	-	82	31				1580	5700	<.10	<1	3.4
1 - 2				2.89	-	<0.003	101	50				890	5700	<.10	1.6	3.1
2 - 3				2.98	25.8	-	104	61				700	5500	<.10	1.8	1.6
3 - 4				2.75	25.2	<0.003	90	35				290	3200	.19	7.0	2.2
4 - 5				2.56	26.0	<0.003	88	35				230	3100	<.10	3.2	1.8
5 - 6				2.58	24.7	<0.003	82	27				240	2400	<.10	2.6	1.8
6 - 7				2.71	25.8	<0.003	71	22				240	1800	<.10	2.2	2.0
7 - 8				2.94	25.1	<0.003	72	22				230	1440	<.10	1.8	3.0
8 - 9				2.52	26.0	<0.003	68	18.8				195	800	<.10	<1	1.6
9 - 10				2.47	25.4	<0.003	62	13.0				220	250	<.10	<1	1.9
10 - 11				2.40	26.2	<0.003	58	15.0				170	-	<.10	<1	2.3
11 - 12				2.75	26.3	<0.003	57	12.1				160	85	.16	1.4	4.1
12 - 13				2.35	26.5	<0.003	51	11.1				155	42	.16	<1	2.6
13 - 14				2.50	26.2	<0.003	45	10.1				148	44	<.10	8.4	13.4
14 - 15				2.50	24.3	0.003	41	8.7				122	101	.10	<1	2.6

Table 9: Pore water data for Jamestown North Core #12 (7/13/76)
Trace metal concentrations in ppb.

Depth (cm)	Porosity	Organic matter	pH	CO_2 (mm)	$SO_4^=$ (mm)	$S^=$ (mm)	$HPO_4^=$ (um)	$PO_4^=$ (um)	Si (um)	Ca/Na atom ratio X 10^{-2}	Mg/Na atom ratio X 10^{-1}	Mn	Fe	Cd	Cu
4 - 6				3.17	26.0	<0.003	120	15.5				210	155	<.10	<1
10 - 12				2.58	25.5	<0.003	64	10.1				135	50	.34	<1
16 - 18				2.76	25.3	<0.003	97	9.7				114	80	<.10	<1
22 - 24				3.11	24.9	0.011	161	20				83	60	<.10	<1
28 - 30				4.23	24.4	0.036	250	29				28	45	<.10	<1
34 - 36				5.41	24.8	0.030	240	41				11	42	<.10	<1
40 - 42				6.33	25.8	0.102	410	47				9	62	<.10	<1
46 - 48				7.16	23.3	0.39	460	58				11	67	<.10	<1
52 - 54				8.29	21.6	0.32	590	65				26	56	<.10	<1
58 - 60				9.12	20.1	0.38	640	75				52	101	2.29	<1
67 - 70				10.4	22.8	0.51	740	80				8	47	<.10	<1
77 - 80				11.0	20.7	0.74	810	85				6	58	<.10	<1
87 - 90				12.3	22.5	0.60	860	94				1	42	<.10	<1
96 - 99				12.4	21.2	0.67	950	92				10	55	<.10	<1

Table 10: Pore water data for Rumstick Neck #1 - Short Core (8/26/75)
Trace metal concentrations in ppb.

Depth (cm)	Porosity	Organic matter	pH	CO_2 (mM)	$SO_4^=$ (mM)	$S^=$ (mM)	NH_3 (mM)	$PO_4^=$ (mM)	Si (mM)	Ca/Na atom ratio X 10^{-2}	Mg/Na atom ratio X 10^{-1}	Mn (ppb)	Fe (ppb)	Cd (ppb)
Supernatant-A				2.23	23.1	-	.041	.007	.078					
Supernatant-B				2.15	25.2	-	.041	.007	.078					
0 - 1				3.40	25.2	-	.161	.130	.400			460	11200	<.26
1 - 2				3.87	25.4	<0.05	.198	.190	-			320	10700	<.60
2 - 3				4.80	23.9	-	.24	.188	.460			250	5160	<.28
3 - 4				4.55	25.0	<0.05	.27	.140	.470			149	740	<.17
4 - 5				4.90	24.0	-	.29	.180	.490			105	990	<.11
5 - 6				4.75	24.6	<0.05	.32	.180	.510			94	800	<.31
6 - 7				5.55	22.6	-	.37	.180	.530			55	490	<.25
7 - 8				5.80	23.1	<0.05	.44	.190	.560			46	410	<.10
8 - 9				6.60	23.0	0.08	.46	.200	.610			30	600	<.14
9 - 10				6.85	22.8	0.16	.52	.210	.640			21	820	<.20
10 - 11				8.85	19.9	0.20	.61	.260	.670			39	450	<.30
11 - 12				8.45	21.7	0.39	.66	.240	.700			22	760	<.19
12 - 13				9.30	21.7	0.28	.71	.250	.700			37	560	<.40
13 - 14				9.75	21.5	-	.78	.240	.730			17.7	1190	<.10
14 - 15				11.5	21.4	0.34	.88	.240	.730			12.0	760	<.21
15 - 16				11.1	21.2	-	.89	.230	.770			23	1590	<.84
16 - 17				11.8	21.4	0.52	1.01	.210	.750			4.1	800	<.24
17 - 18				11.6	20.1	-	0.99	.230	.780			5.7	1320	
18 - 19				13.4	21.3	0.99	1.05	.230	.750			2.6	1380	

Table II: Pore water data for Sabin Point Core #1 - (8/4/75)
Trace metal concentrations in ppb.

Depth (cm)	Porosity	Organic matter	pH	CO_2 (mm)	$SO_4^=$ (mm)	$S^=$ (mm)	NH_3 (mm)	$PO_4^=$ (mm)	Si (mm)	Ca/Na atom ratio X 10^{-2}	Mg/Na atom ratio X 10^{-1}	Mn	Fe	Cd (ppb)
Supernatant-A				2.19	23.0	0.05	.093	.027	.064			85		
Supernatant-B				2.14	24.3	-	.067	.020	.057			84		<.10
0 - 1	0.87	9.8		5.30	24.2	0.05	.370	.430	.440			241		<.10
1 - 2	0.85	10.5		7.40	20.5	0.06	.580	.570	.540			154		.15
2 - 3	0.83	9.9		8.80	22.4	0.09	.660	.580	.530			119		<.10
3 - 4	0.82	9.5		10.6	19.6	0.60	.760	.570	.560			67		<.10
4 - 5	0.85	10.0		12.0	18.5	1.00	.830	.570	.600			40		.20
5 - 6	0.82	10.1		13.2	19.0	1.01	.870	.580	.630			34		<.10
6 - 7	0.84	12.6		14.8	17.2	1.18	.930	.550	.670			17		<.10
7 - 8	0.85	12.0		16.2	15.7	1.10	1.030	.540	.710			10		<.10
8 - 9	0.85	11.7		17.8	15.5	1.29	1.020	.510	.790			3		<.10
9 - 10	0.86	13.4		18.6	16.1	1.23	1.080	.510	.810			3		.30
10 - 11	0.87	13.1		19.1	13.0	1.51	1.180	.510	.85			3		<.10
11 - 12	0.84	11.8		19.4	14.7	1.32	1.230	.500	.840			3		<.10
12 - 13	0.84	11.2		20.6	14.1	-	1.230	.500	.840			3		<.10
13 - 14	0.80	9.9		22.3	13.3	1.30	1.200	.500	.830			3		.15
14 - 15	0.84	12.7		-	13.1	1.30	1.270	.490	.820			3		<.10

Table 12: Pore water data for Sabin Point Core #2 - (8/11/75)
Trace metal concentrations in ppb.

Depth (cm)	Porosity	Organic matter	pH	CO_2 (mm)	$SO_4^=$ (mm)	$S^=$ (mm)	NH (mm)	$PO_4^{\equiv}$ (mm)	Si (mm)	Ca/Na atom ratio X 10^{-2}	Mg/Na atom ratio X 10^{-1}	Mn (ppb)
Supernatant-A			-	-	-	-	-	.016	.065	2.15	1.07	261
Supernatant-B			-	-	-	-	-	.018	.066	2.20	1.07	
0 - 1			-	-	22.5	0.05	.430	.360	.570	2.19	1.07	261
1 - 2			7.60	7.30	23.0	0.05	.560	.510	.620	2.18	1.08	226
2 - 3			-	8.45	19.9	-	.800	.610	.660	2.20	1.07	127
3 - 4			-	10.2	17.2	0.05	.830	.590	.660	2.29	1.09	63
4 - 5			7.79	11.3	17.6	0.09	.850	.540	.700	2.19	1.02	36
5 - 6			7.73	13.5	17.0	-	1.000	.500	.700	2.19	1.10	26
6 - 7			-	-	-	-	-	-	-	-	-	--
7 - 8			7.88	16.5	17.1	-	1.130	.470	.690	2.14	1.00	5
8 - 9			7.83	16.0	15.8	0.72	1.280	.470	.760	2.19	1.05	10
9 - 10			7.78	16.1	13.6	1.08	1.460	.480	.750	2.19	1.04	30
10 - 11			7.79	-	14.9	1.63	1.420	.460	.730	2.18	1.02	6
11 - 12			7.80	17.5	-	0.85	1.600	.440	.730	2.15	1.02	5
12 - 13			7.95	18.8	-	-	1.540	.450	.710	2.14	1.04	23
13 - 14			7.93	17.2	12.9	-	1.480	.440	.670	2.16	1.05	4
14 - 15			7.92	19.7	12.8	1.16	1.570	.440	.740	2.15	1.04	4
15 - 16			8.01	-	12.6	-	1.630	.430	.720	2.13	1.04	8
16 - 17			7.99	-	12.7	-	1.640	.430	.710	2.16	1.13	8

Table 13: Pore water data for Sabin Point Core #3 (10/7/75)
Trace metal concentrations in ppb.

Depth (cm)	Poros-ity	Organic matter	pH	CO_2 (mm)	$SO_4^=$ (mm)	$S^=$ (mm)	NH_3 (mm)	$PO_4^=$ (mm)	Si (mm)	Ca/Na atom ratio X 10^{-2}	Mg/Na atom ratio X 10^{-1}
5	0.82	6.7	7.83	9.36	20.7	0.77	.68	.370	.530	2.30	1.11
10	0.82	7.6	7.68	14.3	17.5	-	.99	.400	.580	2.20	1.07
15	0.78	6.4	8.04	17.6	15.3	1.44	1.24	.400	.600	2.19	1.06
20	0.67	3.4	-	-	-	-	-	-	-	-	-
25	0.73	4.1	7.83	25.2	11.1	2.3	1.73	.330	.650	2.15	1.08
30	0.70	3.2	7.66	27.8	10.7	3.4	1.79	.310	.650	2.13	1.07
35	0.71	2.9	7.70	30.7	9.7	4.9	1.94	.290	.660	2.14	1.07
40	0.71	3.2	7.57	32.9	-	6.5	1.91	.280	.680	2.16	1.08
45	0.70	3.2	7.68	33.3	8.3	5.4	2.10	.270	.740	2.16	1.04
50	0.72	3.3	8.03	32.7	8.0	5.3	2.21	.270	.760	2.13	1.04
55	0.72	3.2	7.87	33.8	8.2	5.9	2.20	.260	.780	2.17	1.04
60	0.72	3.2	-	34.9	7.6	4.7	2.10	.240	.750	-	-

Table 14: Pore water data for **Sabin Point Core #4 (10/7/75)**
Trace metal concentrations in ppb.

Depth (cm)	Porosity	Organic matter	pH	CO_2 (mm)	$SO_4^=$ (mm)	$S^=$ (mm)	NH_3 (mm)	$PO_4^=$ (mm)	Si (mm)	Ca/Na atom ratio X 10^{-2}	Mg/Na atom ratio X 10^{-1}
Supernatant-A				2.33	22.8	<0.004	>.150	.022	.073	2.21	1.11
Supernatant-B				2.46	22.0	<0.004	>.150	.020	.072	2.24	1.10
0 - ½	0.92	14.2		5.27	21.7	<0.004	>.150	.210	.360	2.27	1.09
½ - 1	0.91	14.5		8.51	19.9	0.004	>.150	.460	.470	2.32	1.09
1 - 2	0.92	17.1		13.9	17.7	0.015	>.150	.850	.590	2.38	1.08
2 - 3	0.91	18.0		20.3	14.5	-	>.150	1.200	.760	2.36	1.10
3 - 4	0.91	17.2		25.8	13.0	1.94	2.500	1.300	.850	2.36	1.10
4 - 5	0.89	15.1		32.0	9.8	2.00	3.100	1.400	.920	2.30	1.08
5 - 6	0.87	13.4		36.5	7.4	2.4	3.400	1.400	.920	2.34	1.09
6 - 7	0.86	11.9		40.2	5.1	3.3	3.700	1.400	.960	2.28	1.09
7 - 8	0.86	12.1		52.3	0.5	4.9	4.100	1.300	.940	2.24	1.08
8 - 9	0.86	13.7		41.0	0.5	5.5	4.300	1.300	.950	2.23	1.08
9 - 10	0.86	12.6		41.1	0.5	6.5	4.400	1.200	.940	2.20	1.07
10 - 11	0.86	12.5		39.7	0.5	4.9	4.200	1.100	.960	2.22	1.04
11 - 12	0.87	13.5		42.3	4.3	5.8	3.900	1.000	.920	2.18	1.06
12 - 13	0.89	15.4		36.6	6.0	6.4	3.500	.900	.840	2.16	1.06
13 - 14	0.83	11.2		33.6		6.2	3.200	.700	.800	2.11	1.04
14 - 15	0.86	13.9		29.4	11.2	4.8	2.700	.560	.750	2.10	1.06
15 - 16	0.83	12.2		26.3	13.3	5.2	2.600	.510	.670		

Table 15: Pore water data for Sabin Point Core #5 (1/27/76)
Trace metal concentrations in ppb.

Depth (cm)	Porosity	Organic matter	pH	CO_2 (mm)	$SO_4^=$ (mm)	$S^=$ (mm)	NH_3 (mm)	$PO_4^=$ (mm)	Si (mm)	Ca/Na atom ratio $\times 10^{-2}$	Mg/Na atom ratio $\times 10^{-1}$
Supernatant-A				1.68	19.4	0.003	0.30	.003	.034		
Supernatant-B				1.73	19.6	0.003	0.29	.004	.036		
0 - ½	0.88	10.2		3.42	21.1	0.003	-	.032	.170		
½ - 1	0.85	10.0		3.43	23.9	0.003	-	.100	.230		
1 - 2	0.82	9.0		4.67	22.0	0.003	0.35	.190	.300		
2 - 3	0.80	9.3	7.62	8.27	22.6	0.003	0.38	.230	.310		
3 - 4	0.80	9.0	7.60	6.27	22.0	0.018	0.52	.290	.380		
4 - 5	0.82	10.4	7.70	6.95	22.1	0.144	1.04	.330	.390		
5 - 6	0.80	9.6	7.52	7.54	20.7	-	-	.340	.390		
6 - 7	0.83	11.5	7.54	8.90	-	0.149	1.07	.370	.440		
7 - 8	0.82	10.7	7.54	11.0	19.3	0.31	0.97	.380	.460		
8 - 9	0.80	10.4	7.55	11.4	-	0.45	0.91	.400	.480		
9 - 10	0.80	10.3	7.76	12.8	17.3	0.69	1.00	.390	.440		
10 - 11	0.81	11.8	7.58	13.4	16.8	0.87	1.18	.390	.440		
11 - 12	0.82	10.3	7.54	14.7	15.7	-	1.09	.420	.510		
12 - 13	0.80	9.9	7.64	15.4	16.1	0.92	1.11	.400	.500		
13 - 14	0.79	9.2	7.60	16.5	16.0	1.21	1.20	.400	.500		
14 - 15	0.78	8.9	7.73	17.8	14.2	1.21	1.07	.380	.520		
15 - 16	0.75	8.0	7.79	17.9	14.4	1.11	1.18	.380	.520		
16 - 17	0.77	9.0	7.56	18.3	14.4	1.51	1.34	.380	.580		

Table 16: Pore water data for Sabin Point Long Core #6 (1/27/76)
Trace metal concentrations in ppb.

Depth (cm)	Poros-ity	Organic matter	pH	CO_2 (mm)	$SO_4^=$ (mm)	$S^=$ (mm)	NH_3 (mm)	$PO_4^=$ (mm)	Si (mm)	Ca/Na atom ratio X 10^{-2}	Mg/Na atom ratio X 10^{-1}
5			7.56	8.16	20.8	-	.93	.790	.510		
10			7.60	13.4	17.7	0.78	1.000	.710	.450		
15			7.65	15.7	15.2	0.83	2.0	.590	.480		
20			7.80	20.7	13.5	1.48	1.750	.460	.540		
25			7.72	20.5	11.6	1.05	3.2	.370	.510		
30			7.75	23.4	9.0	1.56	1.760	.340	.550		
35			7.95	27.1	9.3	1.90	1.960	.300	.540		
40			7.63	28.1	8.4	1.82	1.950	.300	.620		
45			-	29.0	6.8	2.3	1.900	.280	.560		
50			-	-	6.5	2.1	2.1	.280	.650		
55			-	30.5	-	2.2	1.880	.270	.610		
60			-	31.3	6.9	1.9	2.0	.270	.630		

Table 17: Pore water data for Sabin Point Core #7 - (7/6/76)
Trace metal concentrations in ppb.

Sabin Point Core #7 (7/6/76)

Depth (cm)	Porosity	Organic matter	pH	CO_2 (mM)	$SO_4^=$ (mM)	$S^=$ (mM)	NH_3 (mM)	$PO_4^=$ (mM)	Si (mM)	Ca/Na atom ratio $\times 10^{-2}$	Mg/Na atom ratio $\times 10^{-1}$	Mn	Fe	Cd	Cu	Ni (ppb)
Initial flux				2.26			.020	.007								
Supernatant				2.85	22.4	0.003	-	.044								
0 - 1			7.73	5.09	24.7	0.003	.380	.230				157	7000		1.8	6.5
1 - 2			7.52	5.35	21.6	0.005	.410	.380				123	2400			7.0
2 - 3			7.59	6.36	21.3	0.005	.530	.450				140	600		1.8	5.5
3 - 4			7.61	6.99	21.1	-	.620	.490				149	760			9.0
4 - 5			7.52	8.79	20.1	0.20	.750	.500				81	88		1.8	5.1
5 - 6			7.47	10.3	18.5	0.67	.850	.520				54	48		<1	2.3
6 - 7			7.48	11.1	-	0.83	.960	.510				31	50		<1	2.8
7 - 8			7.51	11.9	18.4	1.05	1.120	.500				18	270			4.9
8 - 9			7.51	14.0	17.5	1.34	1.560	.480				7	45		<1	2.3
9 - 10			7.46	16.2	16.2	1.83	1.280	.480				8	480			4.4
10 - 11			7.50	15.7	15.5	1.59	1.410	.480				7	410			5.5
11 - 12			7.58	16.6	15.1	1.76	1.440	.490				2	182			3.7
12 - 13			7.55	18.0	14.5	2.2	1.440	.420				2	126			2.3
13 - 14			7.66	20.6	14.1	1.34	1.420	.480				<2	51			2.7
14 - 15			7.53	20.3	13.5	2.4	1.510	.490				3	300			4.9
15 - 16			7.49	23.5	12.5	2.5	1.620	.470				3	270			4.9

Table 18: Pore water data for Sabin Point Core #8 - (7/6/76)
Trace metal concentrations in ppb.

Sabin Point Core #8 (7/6/76)

Depth (cm)	Porosity	Organic matter	pH	CO_2 (mM)	$SO_4^=$ (mM)	$S^=$ (mM)	NH_3 (mM)	$PO_4^=$ (mM)	Si (mM)	Ca/Na atom ratio $\times 10^{-2}$	Mg/Na atom ratio $\times 10^{-1}$	Mn	Fe	Cd	Cu
5 - 7			7.2	12.0	19.2	0.34	.90	.520				46	59	.20	<1
11 - 13			7.5	17.7	15.6	1.01	1.15	.410				2	97	<.10	<1
17 - 19			7.6	21.4	13.1	1.18	1.54	.390				2	113	<.10	1.6
23 - 25			7.7	25.6	9.6	1.54	1.79	.390				<1	80	<.10	2.6
29 - 31			7.6	29.1	7.8	2.3	2.1	.430				<1	102	<.10	2.8
35 - 37			7.7	32.8	4.7	1.83	2.3	.400				<1	109	<.10	1.4
41 - 43			7.7	30.8	1.8	2.2	2.4	.390				<1	46		
47 - 49			7.7	36.5	0.9	2.4	2.6	.380				4.7	410	.26	11.9
53 - 55			7.68	35.5	<0.5	2.9	2.6	.380				<1	113	<.10	2.7
59 - 61			7.80	38.9	<0.5	2.4	2.7	.360				<1	133	<.10	<1
65 - 68			7.77	40.0	<0.5	2.7	2.7	.380				<1	100	<.10	<1
72 - 75			7.67	39.3	<0.5	3.7	2.7	.320				<1	102	<.10	<1

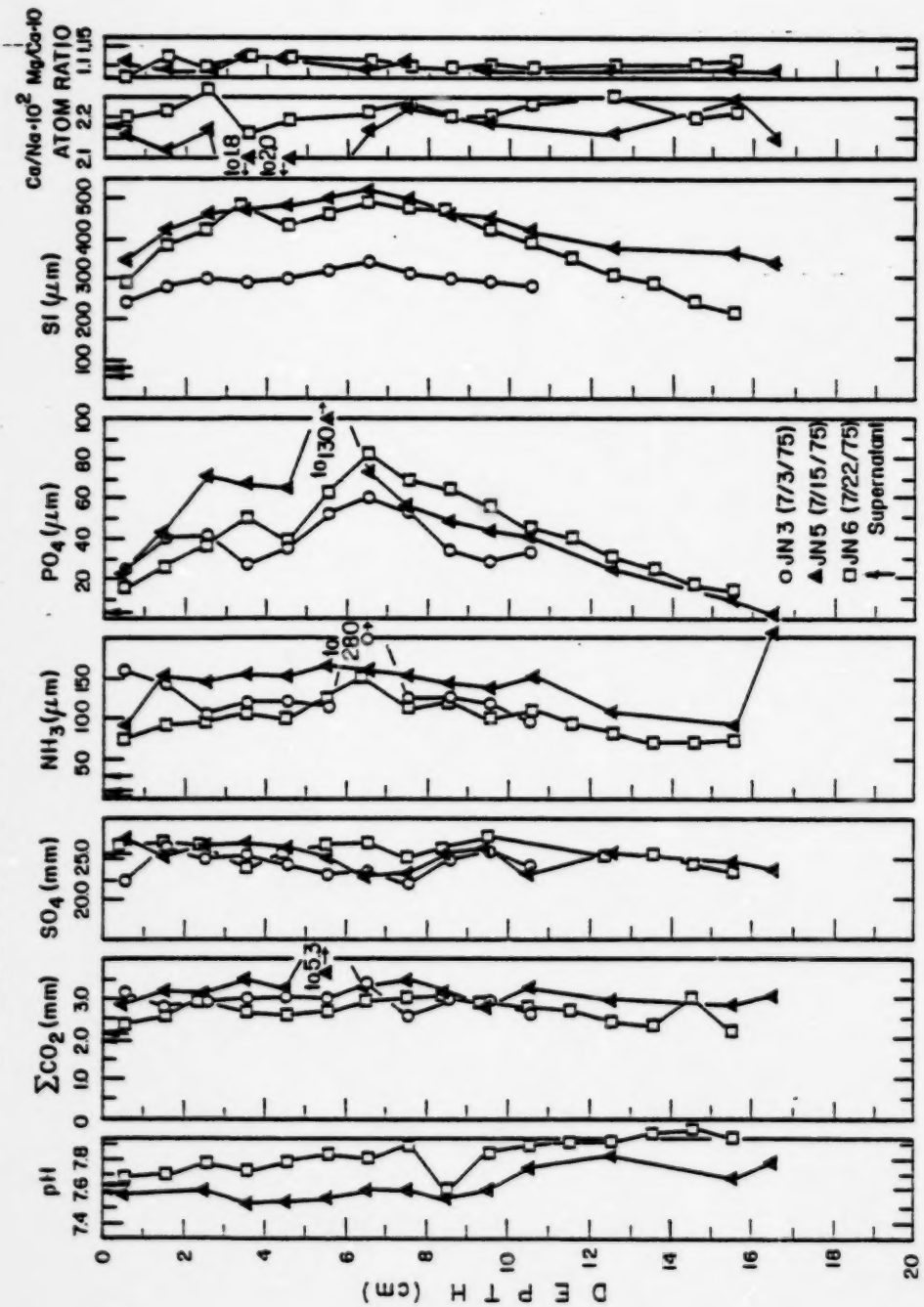

Fig. 2: Pore water chemistry of Narragansett Bay cores.
JN - Jamestown North, RN-Rumstick Neck, SP - Sabin Point

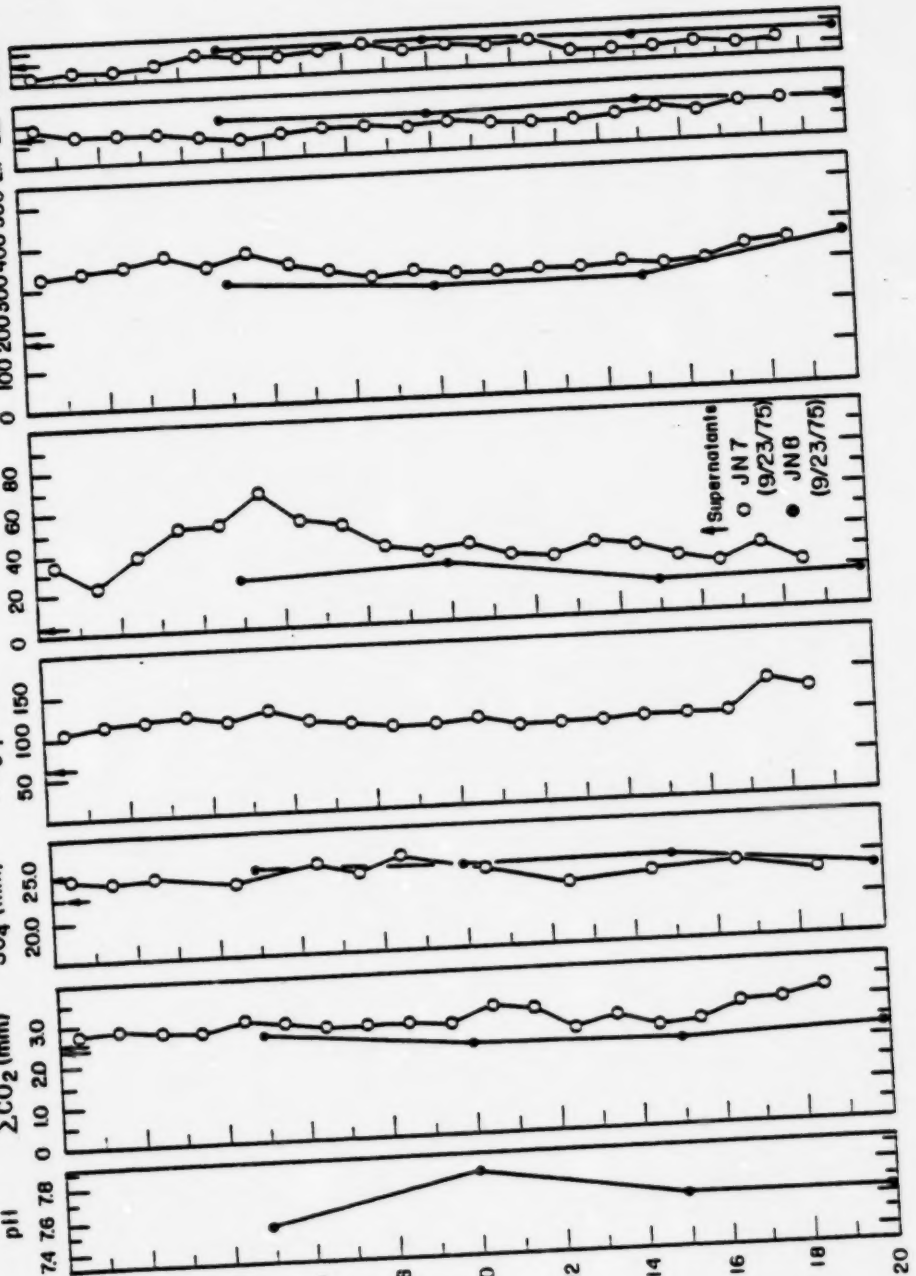

Fig. 3: Pore water chemistry of Narragansett Bay cores.
JN - Jamestown North, RN - Rumstick Neck, SP - Sabin Point

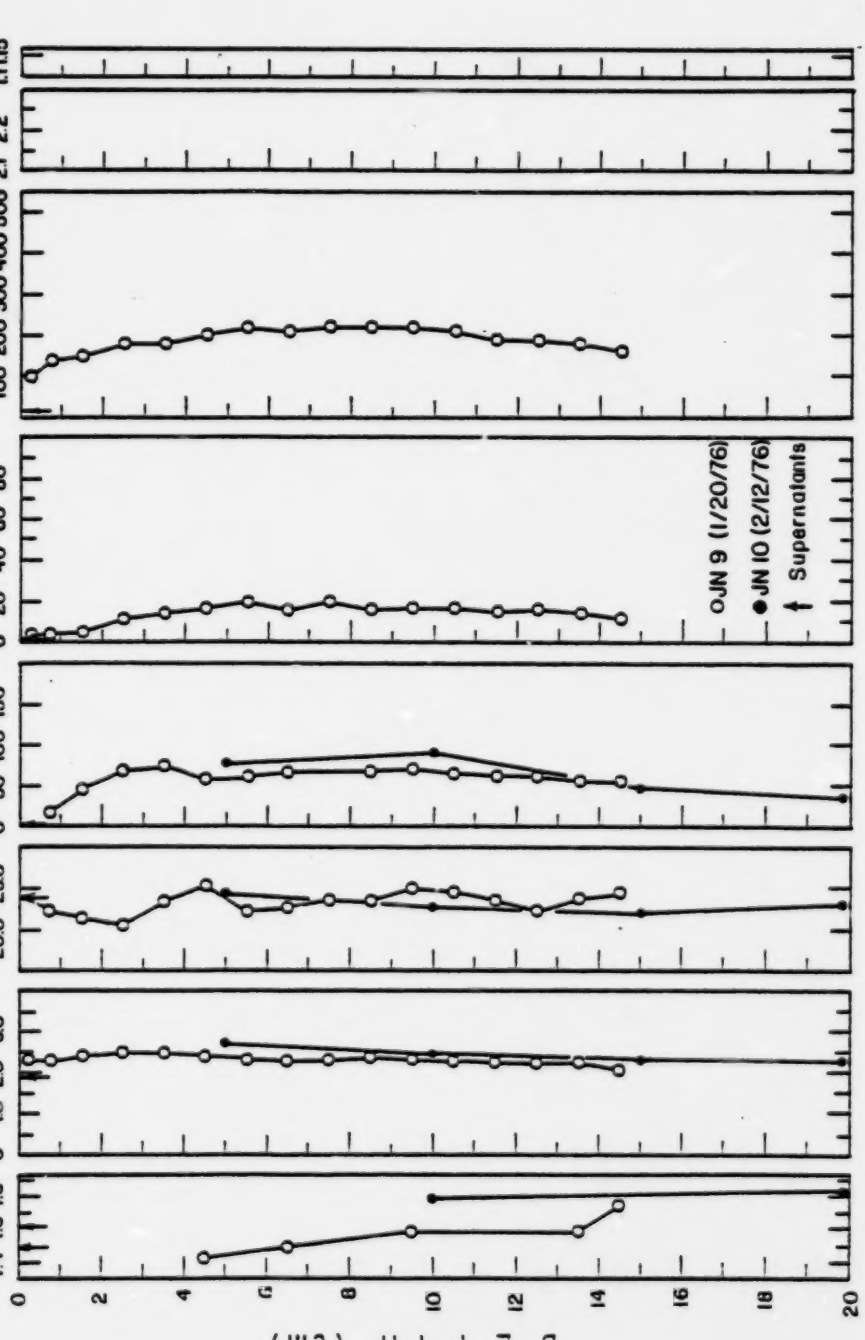

Fig. 4: Pore water chemistry of Narragansett Bay cores.
JN - Jamestown North, RN - Rumstick Neck, SP - Sabin Point

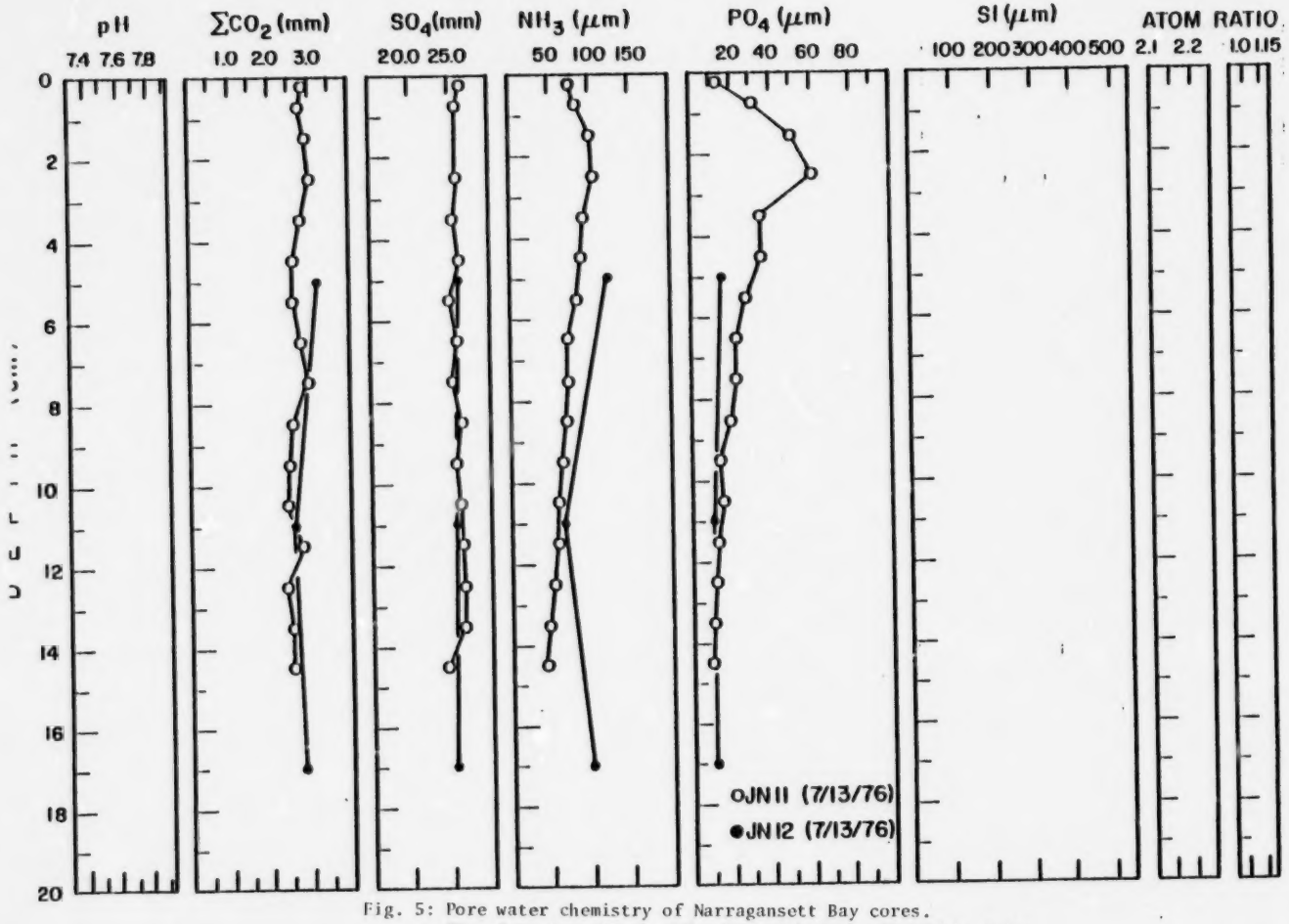

Fig. 5: Pore water chemistry of Narragansett Bay cores.
JN - Jamestown North, RN - Rumstick Neck, SP -Sabin Point

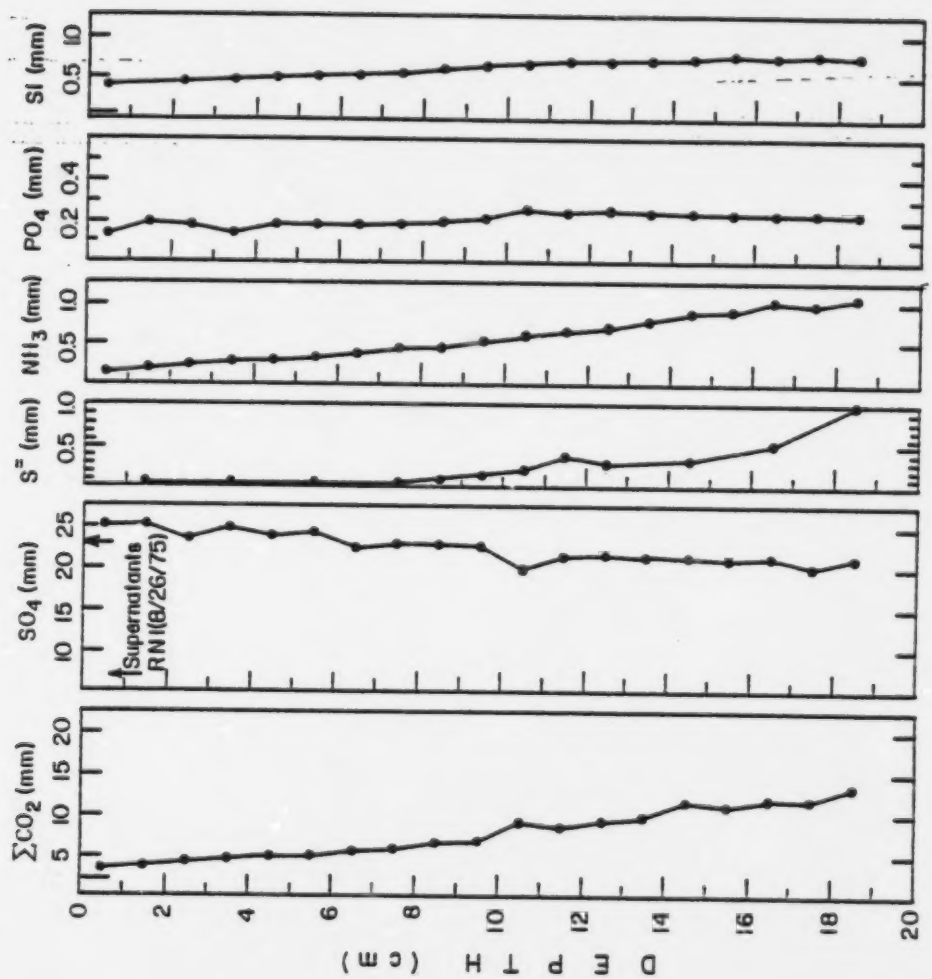

Fig. 7: Pore water chemistry of Narragansett Bay cores.
JN - Jamestown North, RN - Ruanstick Neck, SP - Sabin Point.

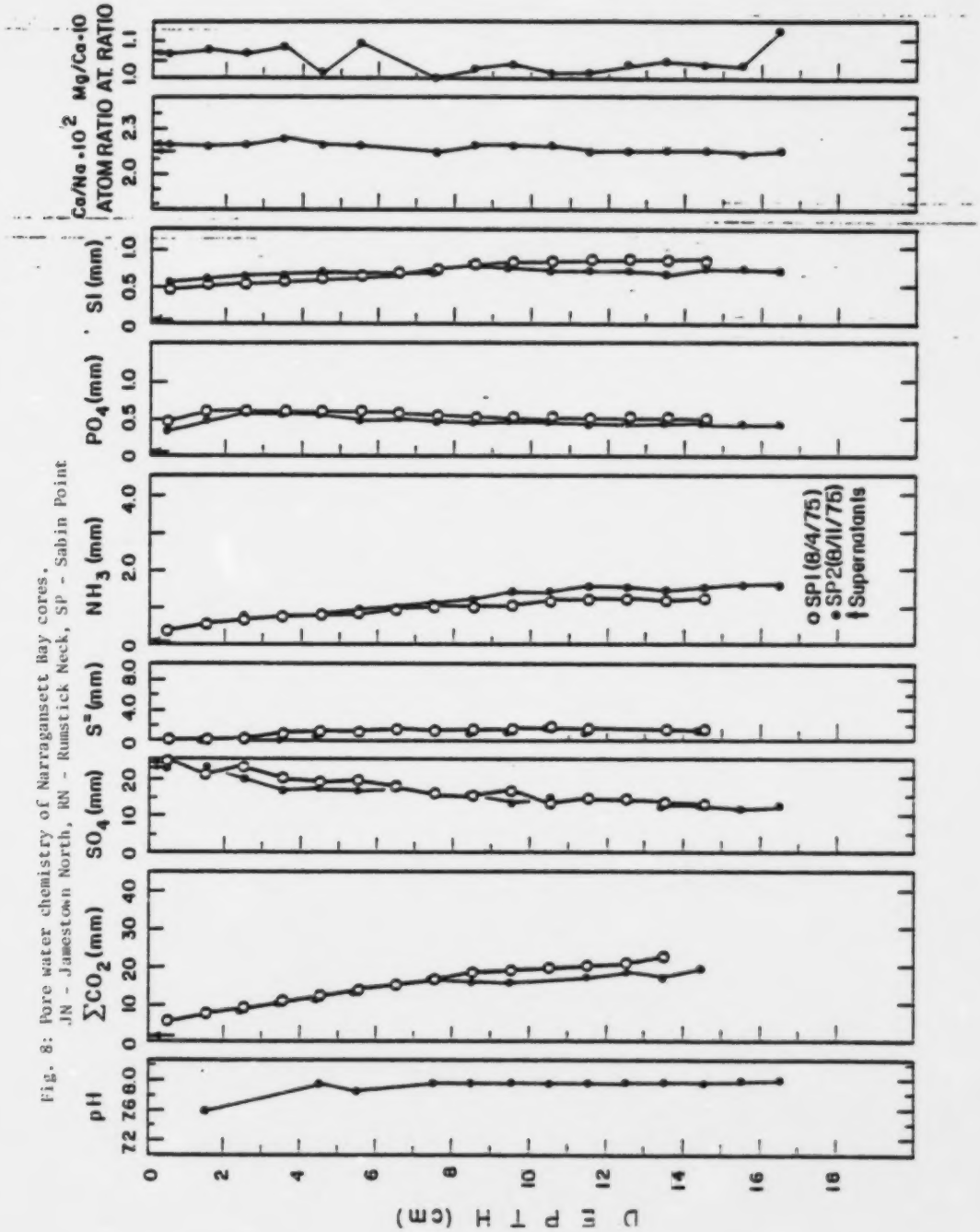

Fig. 8: Pore water chemistry of Narragansett Bay cores.
JN - Jamestown North, RN - Rumstick Neck, SP - Sabin Point

Fig. 9: Pore water chemistry of Narragansett Bay cores.
JN - Jamestown North, RN - Rumstick Neck, SP - Sabin Point

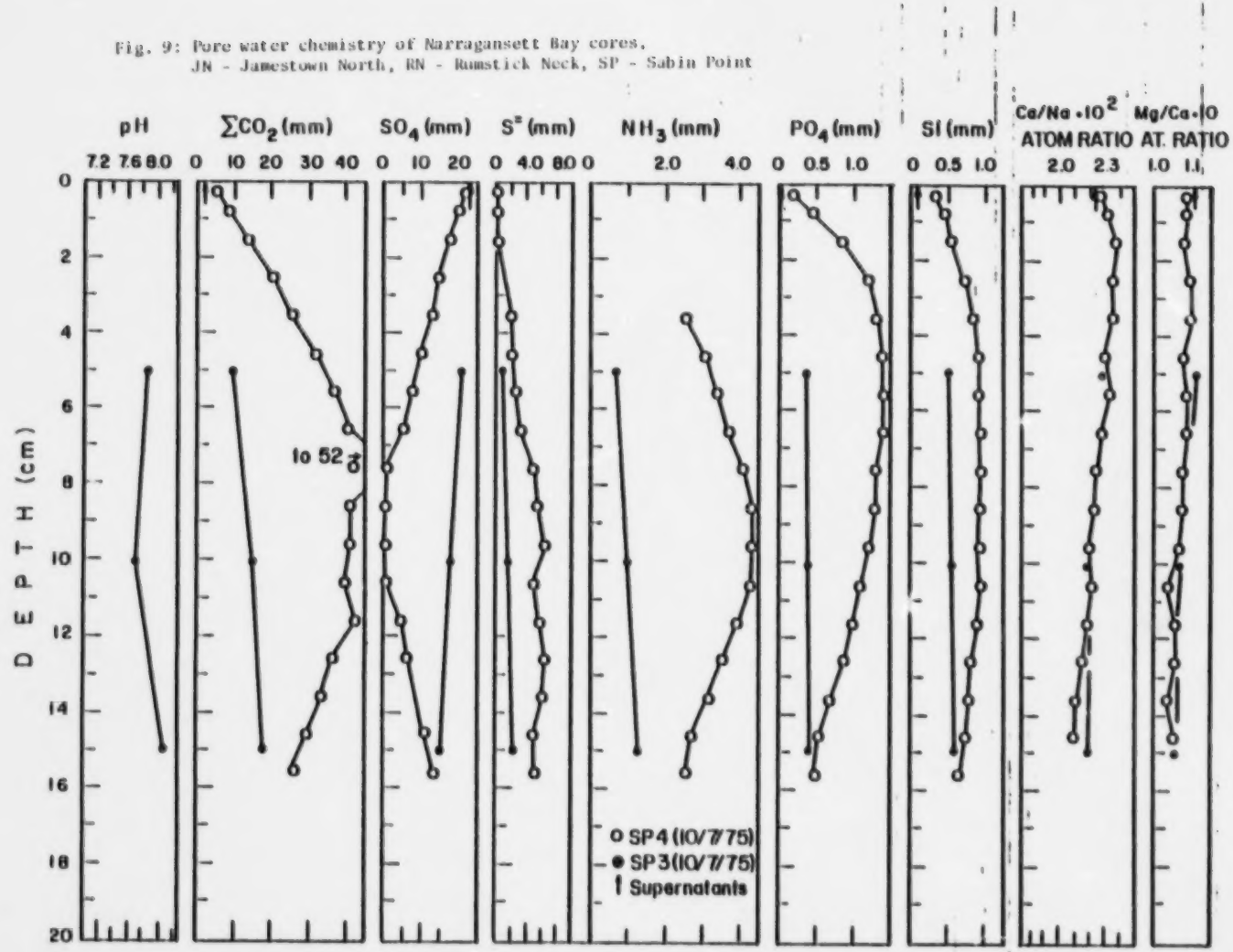

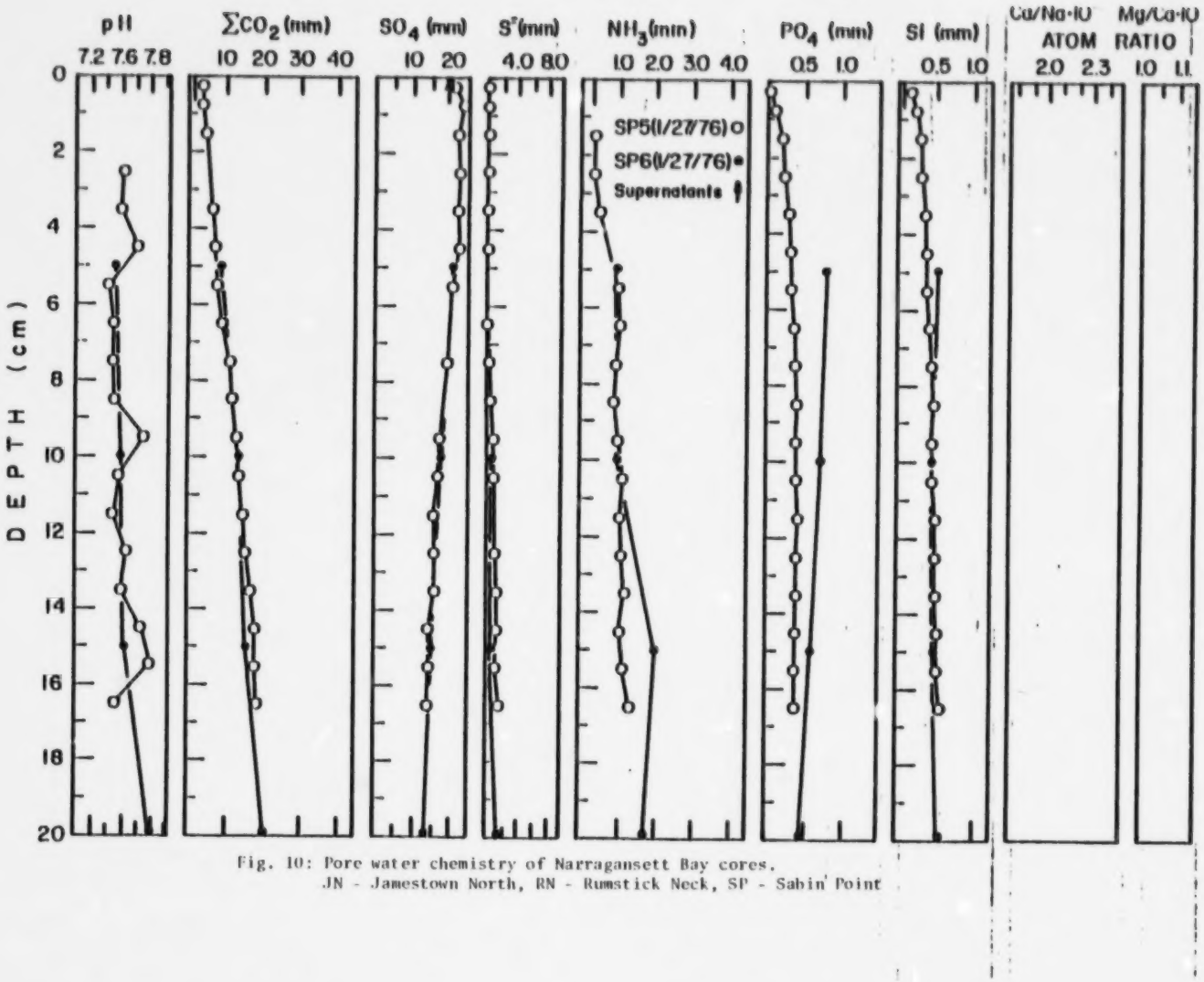

Fig. 10: Pore water chemistry of Narragansett Bay cores.
JN - Jamestown North, RN - Rumstick Neck, SP - Sabin Point

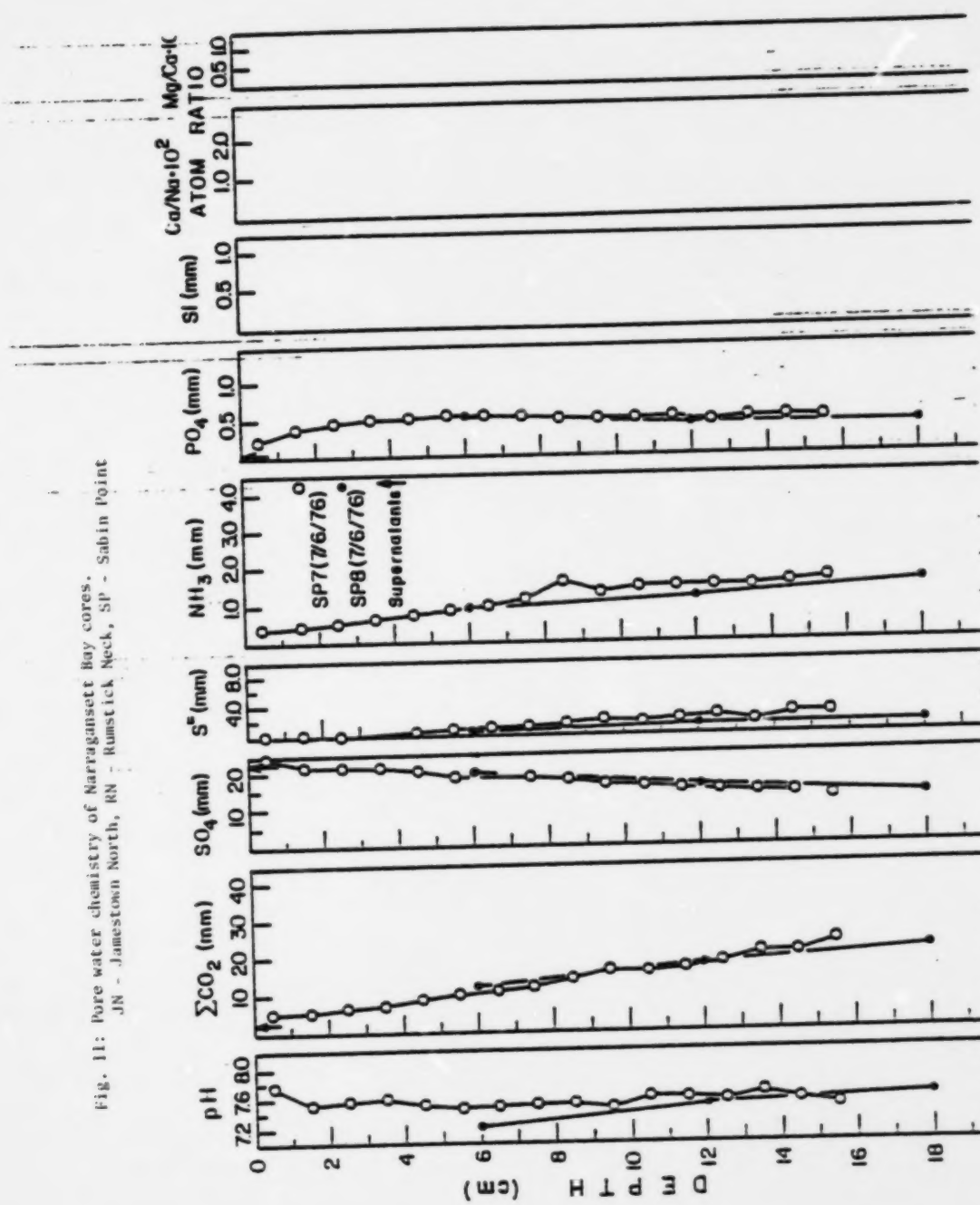

Fig. 11: Pore water chemistry of Narragansett Bay cores.
JN - Jamestown North, RN - Rumstick Neck, SP - Sabin Point

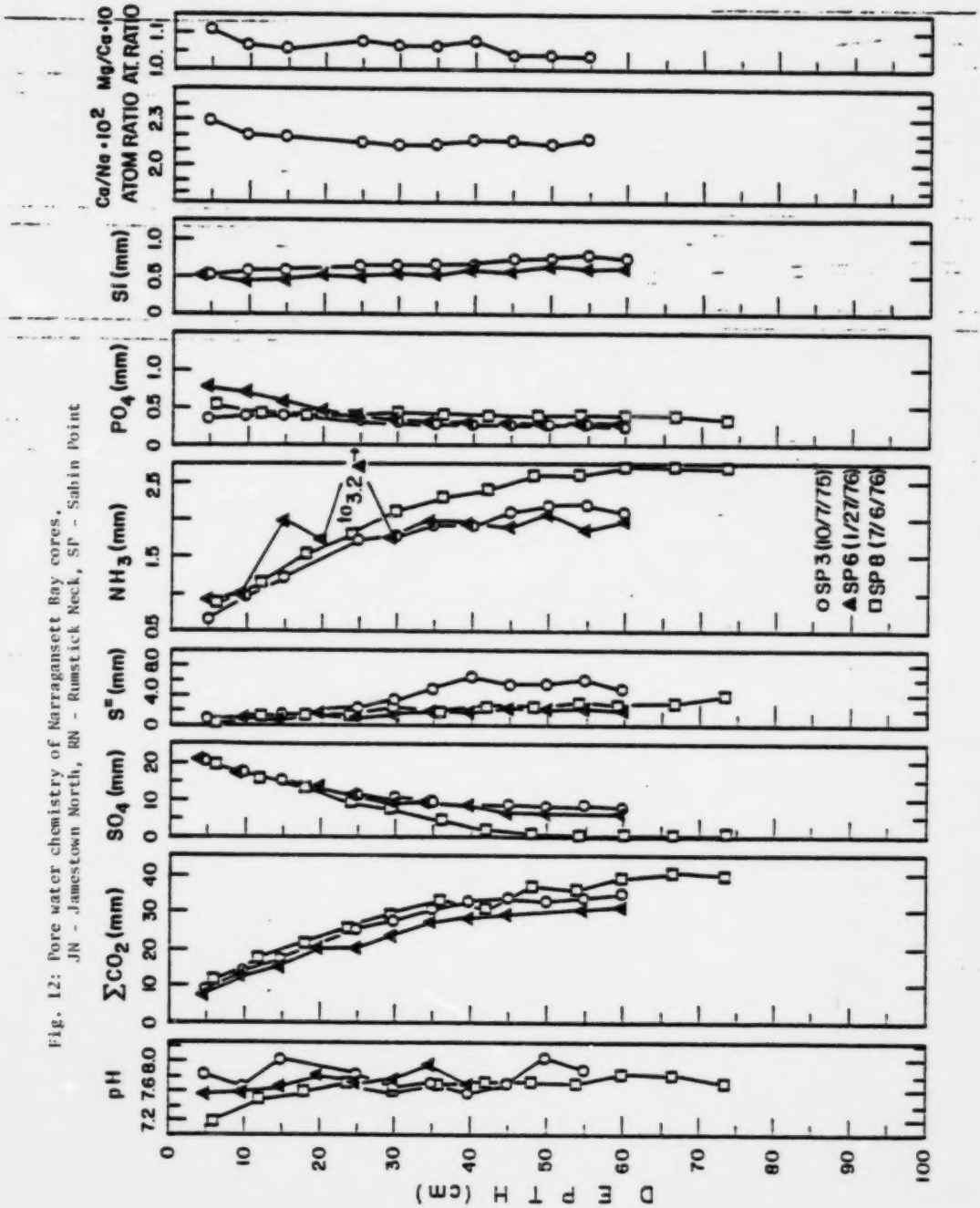

Fig. 12: Pore water chemistry of Narragansett Bay cores.
JN - Jamestown North, RN - Rumstick Neck, SP - Sabin Point

The $SO_4^=$ content of Bay water is about 28,000 $\mu M\ kg^{-1}$; hence complete reduction of $SO_4^=$ produces 56,000 $\mu M\ kg^{-1}$ of TCO_2.

An alternative scheme can be considered in which, during oxygen reduction, organic nitrogen is released as ammonia (not NO_3^-):

$$(CH_2O)_{106}\ (NH_3)_{16}\ (H_3PO_4) + 106\ O_2 \longrightarrow 106\ CO_2 + H_3PO_4 + 106\ H_2O.$$

In this case, the TCO_2 content at the end of oxygen reduction will be 2,150 $\mu M\ kg^{-1}$. If the NH_3 content of the initial bottom water is zero, at the end of O_2 reduction will be 67 $\mu M\ kg^{-1}$. Throughout diagenesis, the NH_3/TCO_2 and $PO_4^=/TCO_2$ ratios will be 16/106 and 1/106, respectively.

In virtually all our pore water samples, the TCO_2 content exceeds the value of 2150 μM reached at the end of O_2 reduction. Hence it is apparent that, throughout our cores, metabolic CO_2 has been produced by $SO_4^=$ reduction. This is true even for the top centimeter of the sediments at the Jamestown North study site.

As predicted for sulfate reduction, TCO_2 increases at about 1/2 the rate at which $SO_4^=$ decreases (fig. 5-13). The only exception is for core SP-4, in which $SO_4^=$ goes to zero and CH_4 formation is apparently significant.

The second model above (no NO_3^- formation) predicts that NH_3 and TCO_3 should increase in the ratio of 16/106. A plot of NH_3 vs. TCO_2 for five cores (fig. 5-14) reveals that, to a first approximation, this relationship is obeyed; in the worst case the $[NH_3]$ is half the predicted value. Phosphorus, however, which is predicted to increase 1/106 times as fast as TCO_2, always shows concentrations much greater than the predicted values (fig. 5-15). This almost certainly reflects the fact that, in anoxic sediments, ferric hydroxides dissolve and release the phosphorus they had previously sequestered (Bricker and Troup, 1975).

In pore waters from the top few centimeters of cores from Jamestown North, Rumstick Neck and Sabin Point, H_2S concentrations are generally at or below the detection limit (3 μM). This indicates that at these sites the $S^=$ produced by $SO_4^=$ reduction rapidly reacts with iron in the sediments to form insoluble iron sulfides. Deeper within the sedimentary column the $S^=$ concentration rises, reflecting a lag in formation of iron sulfides.

The metal concentrations in the pore water samples are extremely interesting. As has been observed for the pore waters of other anoxic sediments, Mn and Fe concentrations are very high. They reach a maximum near the sediment-water interface and decrease with depth in the sediment. Cadmium concentrations at all three sites are generally below the detection limit of .03-.10 ppb. Copper concentrations are similar to or less than estimated ambient bottom water values of 1-3 ppb. Profiles sometimes have a few very high values. This is believed to reflect copper contamination by "leakage" of particulates around membrane filters and into the "filtered" sample. Coupled high iron and copper concentrations (e.g. for the 5-6 cm sample of JN-3, the 3-4 cm sample of JN-6, and the 47-49 cm sample of SP-8) are evidence

for this. Copper concentrations decreased during the sampling period; we interpret this as reflecting better and better procedures as the work progressed, and regard the latest, lowest concentrations as the most reliable values. Nickel concentrations were generally comparable to bottom water values. Results again were somewhat variable, and it is not clear if we were measuring true concentrations or only upper limits.

The high concentrations of Fe and Mn and low concentrations of Cu, Cd and Ni undoubtedly reflect the relative solubilities of these metals in the presence of $S^{=}$, as discussed by Thompson et al (1975) and Elderfield and Hepworth (1975).

The shape of the TCO_2 - depth profiles (fig. 5-2 to 5-12) give considerable insight into mechanisms by which metabolites and metals, once released to the pore water, are transported out of the sediment. In sediments undisturbed by the feeding and burrowing activity of organisms, TCO_2 is expected to increase rapidly near the interface; under such conditions in a diffusion-controlled system, the first derivative of concentration with respect to depth is positive and the second derivative is negative. This expectation is in fact followed at Sabin Point. At Jamestown North, however, TCO_2 profiles are flat or even show shallow maxima (at 5 cm) and shallow minima (at 15 cm) before increasing monatonically below 2-25 cm. Such profile shapes (characteristic of NH_3, Si and $PO_4^{\equiv}$ as well as TCO_2) can only be explained by assuming an advective transport of water (resulting from the activity of organisms) across the sediment-water interface. In the absence of concentration gradients, diffusion cannot transport metabolites. Pumping transports metabolites by exchanging metabolite-rich pore waters and bottom waters. Steady state metabolite concentrations in the pore waters are equal to the ratio of the metabolic production rate and the water exchange rate. Below 20 cm at the Jamestown site, the activity of the macrobenthos is very small; the system is diffusion-controlled and pore water concentrations increase with depth.

SECTION 6

LABORATORY TRACER EXPERIMENTS

During the summer of 1975 and again during the summer of 1976, three box cores were collected in the field and returned to the laboratory. About 10 cm of supernatant Bay water was placed on the cores and spiked with radioisotopes of Na, Sr, Ba, Hg, Fe, Mn, Zn, Cd, and (in 1975 only) Ce in glass microspheres. The distribution of activity in the supernatant was monitored for up to two weeks. At the end of the monitoring period the cores were sliced, and the distribution of activity in both pore waters and sediment were determined as a function of depth.

The rate of disappearance of Na^{22} from the supernate afforded a basis for calculating the rate at which organisms pump water between sediments and overlying water. The distribution of highly insoluble tracers with depth gave an estimate of the bulk rate of mixing of the solid phase of the sediments. Finally, the distribution of metals between oxidizing supernate, reducing pore water, and sediments gave an index of the solubility of the metals under reducing and oxdizing conditions.

The decrease with time of radioisotope concentrations in the supernate is shown in figure 6-1. The Na decrease is entirely due to transport into the pore waters: there is no uptake of Na into the solid phase. The rate of decrease is far more rapid than can be accounted for by diffusion alone; the discrepancy is ascribed to the pumping activity of organisms. We have calculated a "biopumping rate" from a simple model in which we assume that pore water and supernate each are well-mixed reservoirs. This assumption for pore waters is undoubtedly violated, but our system is undetermined and our data will not constrain a more sophisticated model. The biopumping rate thus calculated is 0.7 $cm^3\ cm^{-2}\ day^{-1}$. This result is used elsewhere to calculate the pumping contribution to the flux of chemicals across the sediment-water interface.

Fe is removed very rapidly from the supernate and is absent from the pore waters. The iron radioisotope "tags" the surface sediment particles. The distribution of these particles as a function of depth in the sediment, as measured by counting the Fe activity in the bulk sediment (fig. 6-2), allows us to model the movement of particles in terms of diffusion coefficient. Similarly, we can calculate a particle diffusion coefficient for the 1975 experiment from the distribution of Ce-tagged microspheres. Diffusion coefficients calculated for four cores are about $3 \times 10^{-7}\ cm^2\ sec^{-1}$; this compares favorably with the value of $2 \times 10^{-6}\ cm^2\ sec^{-1}$ measured by Aller and Cochran (1974) in Long Island Sound. The difference may reflect real variability or may be due to the fact that we injured the benthos by taking the cores from the environ-

Figure 1.

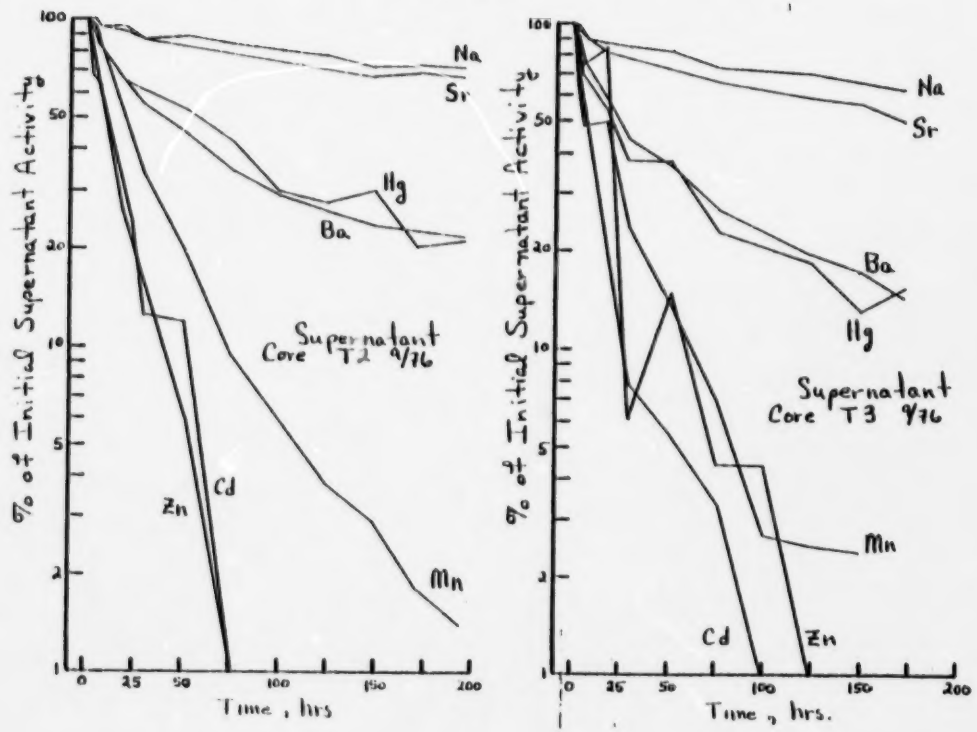
% of Initial Supernatant Activity
100
50
20
10
5
2
1
Na
Sr
Hg
Ba
Mn
Zn
Cd
Supernatant
Core T2 9/76
0
25
50
100
150
200
Time, hrs
% of Initial Supernatant Activity
Na
Sr
Ba
Hg
Supernatant
Core T3 9/76
Mn
Cd
Zn
Time, hrs.

Figure 2a

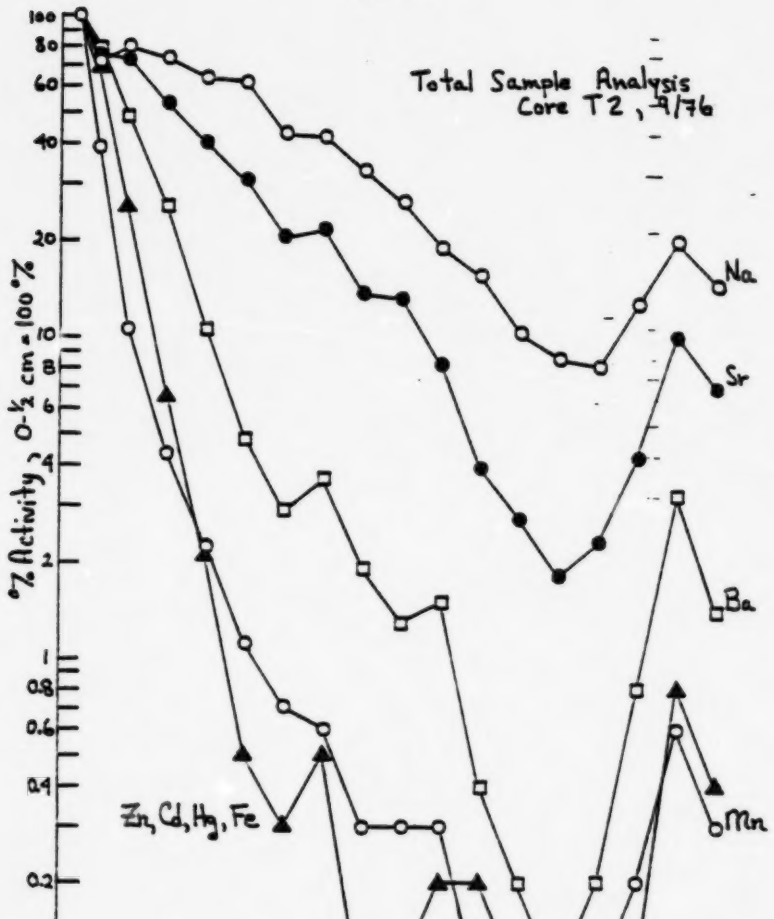
Total Sample Analysis
Core T2, 9/76
% Activity, 0-½ cm = 100%
Depth, cm
Na
Sr
Ba
Mn
Zn, Cd, Hg, Fe
100
80
60
40
20
10
8
6
4
2
1
0.8
0.6
0.4
0.2
0.1
0
2
4
6
8
10
12
14
16

ment.

The distribution of tracers in the pore waters at the end of the experiment is shown in figure 6-3, for two cores. From these results and tracer experiment results shown in the previous two figures, we can back calculate the tracer content of the solid phase. Our calculations show that essentially none of the sodium, 52% of theSr, 95% of the Ba, 93% of the Mn, 96% of the Hg, and virtually all of the Cd, Zn and Fe are in the solid phase. The result for Na was used in the preceeding exchange calculation. Sr and Ba presumably occupy exchange sites in the solid phase. The Mn radioisotope apparently equilibrates rapidly with stable manganese and mimics its distribution: at the end of the experiment the supernate concentration shows a maximum in the top centimeter and decreases with depth. Fe is quantitatively removed from solution within an hour after the start of the experiment. Surprisingly, it does not dissolve in the pore waters, despite the fact that the pore water Fe concentration near the sediment surface is about 5000 ppb. We speculate that the low pore water Fe content reflects a large sedimentary Fe reservoir with which pore waters are in contact. Zn and Cd are also absnet from the pore waters. They disappear from the supernate rapidly, with a "half life" of about 10 hours. Within the sediment they apparently form highly insoluble sulfides and are thus sequestered in the solid. In the case of cadmium, this interpretation is consistent with the very low pore water concentrations.

Figure 2b

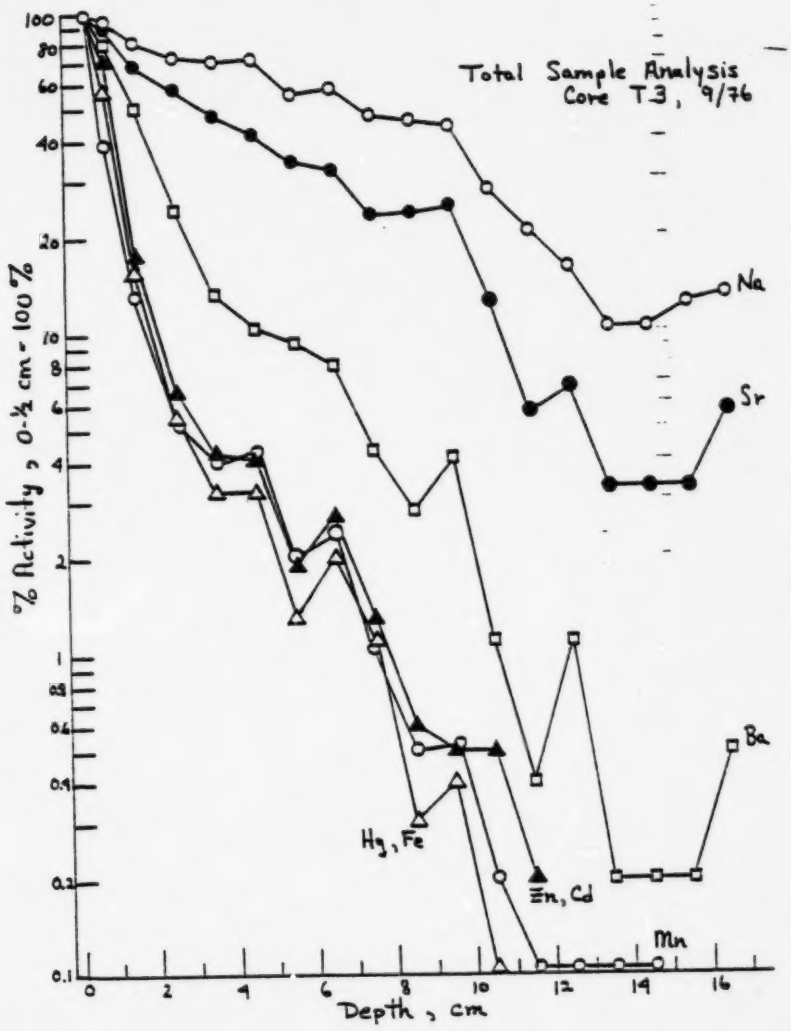
Total Sample Analysis
Core T3, 9/76
% Activity, 0-½ cm = 100%
Depth, cm
Na
Sr
Ba
Hg, Fe
Zn, Cd
Mn

Figure 3a

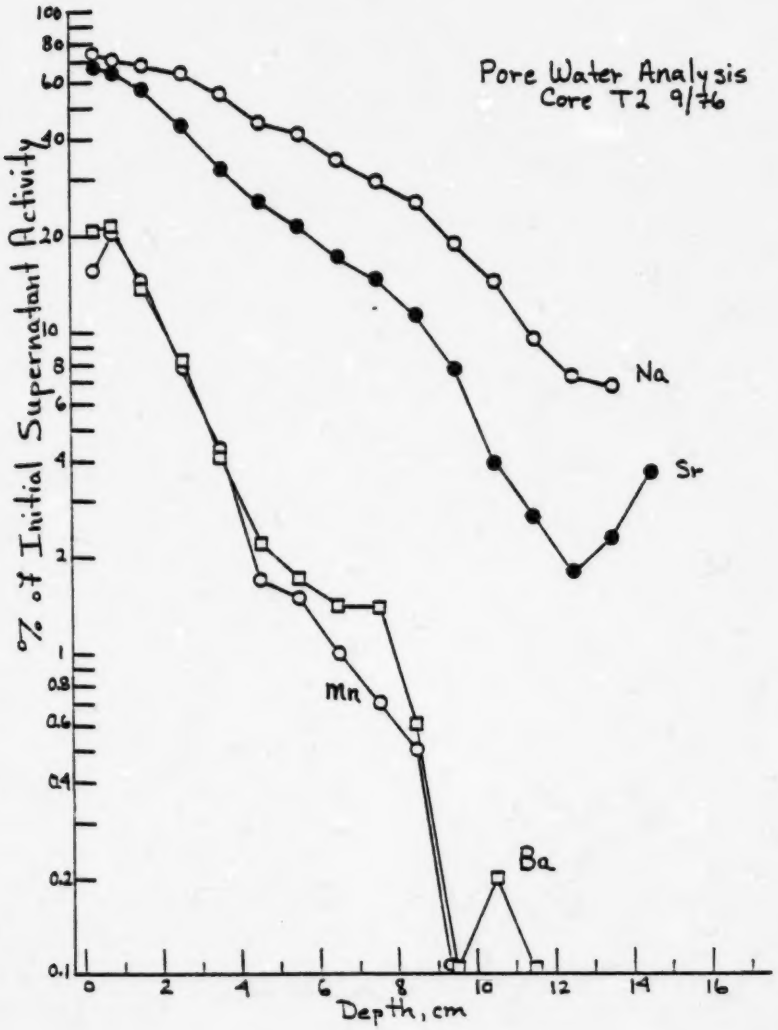
Pore Water Analysis
Core T2 9/76
% of Initial Supernatant Activity
100
80
60
40
20
10
8
6
4
2
1
0.8
0.6
0.4
0.2
0.1
Na
Sr
Mn
Ba
0
2
4
6
8
10
12
14
16
Depth, cm

Figure 3b

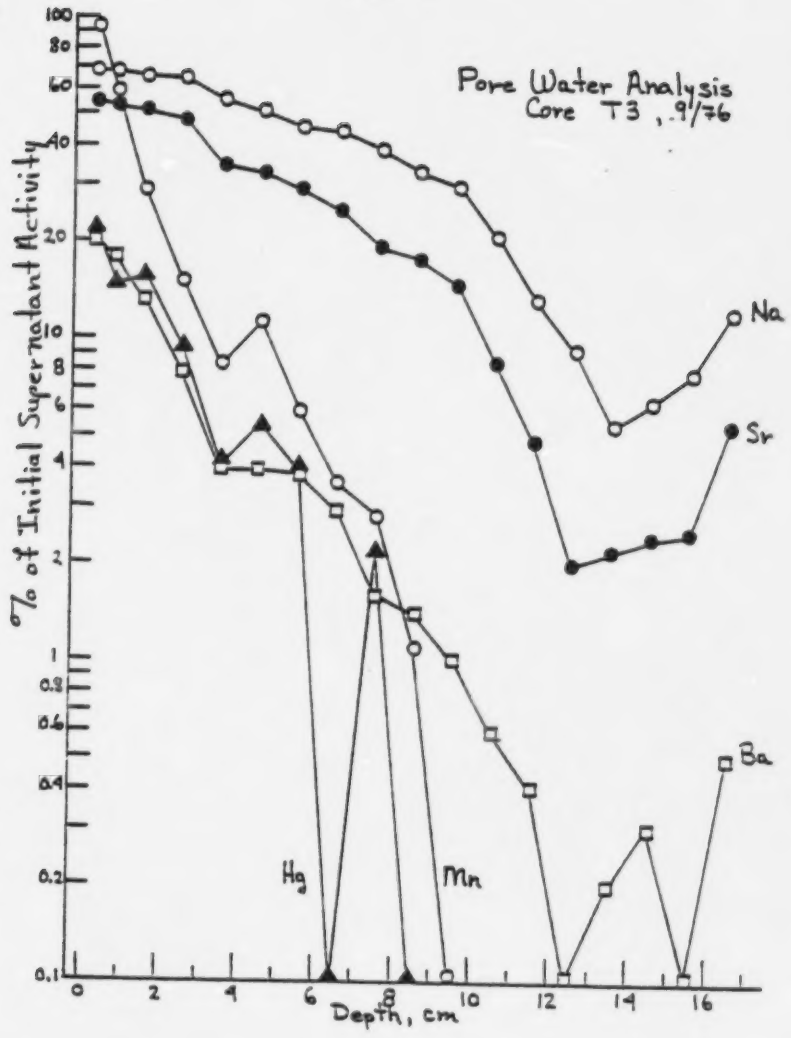
Pore Water Analysis
Core T3, 9/76
% of Initial Supernatant Activity
100
80
60
40
20
10
8
6
4
2
1
0.8
0.6
0.4
0.2
0.1
0
2
4
6
8
10
12
14
16
Depth, cm
Na
Sr
Ba
Hg
Mn

SECTION 7

BENTHIC FLUX EXPERIMENTS

BENTHIC FLUX SAMPLING

Fluxes from the sediment were monitored using two methods. The first was a large chamber device, from which approximately 1 l samples could be withdrawn (Hale, 1974). This chamber isolated a portion of the water column, approximately 11 cm high over the sediment interface. An initial sample was taken and the chamber was sealed. At the end of a three hour period the final sample was withdrawn. Along with initial and final samples a series of ambient samples were also taken, returned to the lab, and analysis completed.

The second device utilized an adaptation of the box coring equipment. The core was fitted with a flexible impermeable membrane at one port. At a second port a sampling tube with a valve was attached. The box was placed on the bottom and inserted leaving 10 cm of overlying water in the box. Along with an initial sample, ambients were collected. The membrane permitted both an intermediate 1 1/2 hour sample and a final 3 hour sample to be extracted from the box. Sample size was limited to 50 ml, but the convenient size of equipment and ease of proceedure enabled increased precision on the part of the divers. Samples were returned for analysis within 6 hours of being taken.

Samples were filtered through a 0.4 Nuclepore filter and analyzed for nutrients and metals.

BENTHIC FLUX MEASUREMENTS IN NARRAGANSETT BAY

The results of the trace metal and nutrient flux measurements are listed in tables 7-1 and 7-2, and figures 7-1, 2, 3. Listing is chronological by site and the devices employed in the measurements are specified, although the results do not seem to depend on the apparatus employed. Most measurements are for the Jamestown site but a few trace metal results are included for Sabin Point and, in the case of nutrient fluxes, a substantial number of results are given for Sabin Point and Rumstick Neck (intermediate site). Most measurements were made in the warm water months, but fall and winter resutls are reported for nutrients. The device labelled "c-o" is actually a plastic dark bottle used as a control. Also note that the units used in each table differ: Metal fluxes are reported on a per square meter basis while nutrient fluxes are on a per square centimeter basis.

To facilitate interpretation of the results, histograms of the metal flux, metal flux control, and nutrient flux measurements have been prepared and are

Table I

Narragansett Bay Metal Flux[1]

($\mu M\ cm^{-2}\ day^{-1}$)

		Cd	Cu	Ni	Mn	Fe
				Jamestown North		
24 Jun 75	C-0	-1.9	11.	9.2	1300.	-580.
	C-2	-1.5	7.1	-32.	570.	1800.
	C-3	0.4	5.7	0.0	330.	480.
26 Jun 75	C-0	0.24	24.	3.1	33.	280.
	C-2	-0.48	0.0	-14.	720.	1400.
	C-3	-0.32	2.8	-6.1	560.	1300.
1 Jly 75	C-0	0.72	18.	38.	-23.	0.
	C-2	-0.08	9.9	16.	7000.	100.
	C-3	-0.16	-2.8	-0.5	850.	-560.
8 Jly 75	C-0	-0.16	-2.8	-15.	-13.	-40.
	C-2	-1.0	1.4	-24.	230.	-56.
	C-3	0.24	7.1	4.6	490.	26.
	C-3(48h)	0.10	1.2	1.7	520.	410.
10 Jly 75	C-0	-0.16	-4.2	0.0	-18.	-3.2
	C-2	-0.64	7.1	4.6	190.	44.
	C-3	-0.48	-1.4	-3.1	3800.	110.
15 Jly 75	C-0	-0.40	-1.4	92.	0.	0.1
	C-2	-0.64	-1.4	-7.7	460.	13.
	C-3	-0.08	1.4	-1.5	560.	92.
22 Jly 75	C-0	0.08	-2.8	-11.	0.	-11.
	C-2	0.08	8.5	1.5	410.	54.
	C-3	-0.24	-11.	-4.6	390.	21.
29 Jly 75	C-0	-2.7	-7.1	-6.1	16.	-15.
	C-2	-0.08	-4.2	-1.5	560.	11.
	C-3	-0.08	-2.8	-1.5	480.	9.7
31 Jly 75	C-0	-0.24	-7.1	-9.2	130.	-32.
	C-2	0.24	-8.5	-7.7	110.	15.
	C-3	-0.48	-13.	-31.	380.	29.
	C-3(48h)	-0.01	0.0	0.19	530.	39.
13 Jly 76	B-1	-	-	-	461.	-
	B-2	-	-	-	180.	-
				Sabin Point		
6 Jly 76	B-1	-	-5.8	-	-	181.
	B-2	-	-8.5	-	-	15.

1) Experiments of 3h duration unless noted otherwise. Code "C" designates PVC chamber (27L, 0.25m^2 area); "B" designates box core (~2.3L, 0.023m^2 area); "C-0" refers to simultaneous dark bottle experiment.

Table 2

Narragansett Bay Nutrient Flux

($\mu M\ cm^{-2}\ d24$)

		NH_3	PO_4	SiO_2
			Sabin Point	
19 Aug 75	C-1	>1.4	0.44	>-0.05
	C-2	>0.8	0.71	>0.5
	C-3	>0.7	0.77	>0.3
	B-2	1.8	0.31	1.7
27 Jan 76	B-1	.18	0.05	0.0
	B-2	-0.24	0.12	0.0
6 Jly 76	B-1	0.46	0.05	-
	B-2	>-0.4	0.12	-
			Rumstick Neck	
26 Aug 75	C-0	0.30	0.06	0.27
	C-2	0.76	0.04	0.90
	C-3	0.98	0.17	1.7
	B-1	0.56	0.08	0.89
			Jamestown North	
24 Jun 75	C-0	0.01	0.01	0.18
	C-1	0.30	0.07	0.91
	C-2	0.29	-	-
	C-3	0.15	-	-
26 Jun 75	C-0	0.00	-0.01	0.05
	C-1	0.24	0.07	1.0
	C-2	0.26	-	-
	C-3	0.26	-	-
1 Jly 75	C-0	0.00	-0.01	-0.24
	C-1	0.37	0.09	1.3
	C-2	0.41	-	-
	C-3	0.39	-	-
8 Jly 75	C-0	0.00	-0.01	0.24
	C-1	0.32	0.08	1.3
	C-2	0.19	-	-
	C-3	0.15	-	-
	C-3(48h)	0.19	-	-
15 Jly 75	C-0	0.02	0.01	0.01
	C-1	0.25	0.04	0.83
	C-2	0.24	-	-
	C-3	0.28	-	-
23 Sep 75	C-2	0.24	0.07	1.1
	C-3	0.56	0.08	1.0
	B-4	0.22	0.06	1.4
	B-5	0.06	0.04	1.1
20 Jan 76	B-1	0.028	0.01	0.0
	B-2	0.027	0.00	0.0
13 Jly 76	B-1	0.14	0.04	-
	B-2	0.44	0.06	-

Figure 1

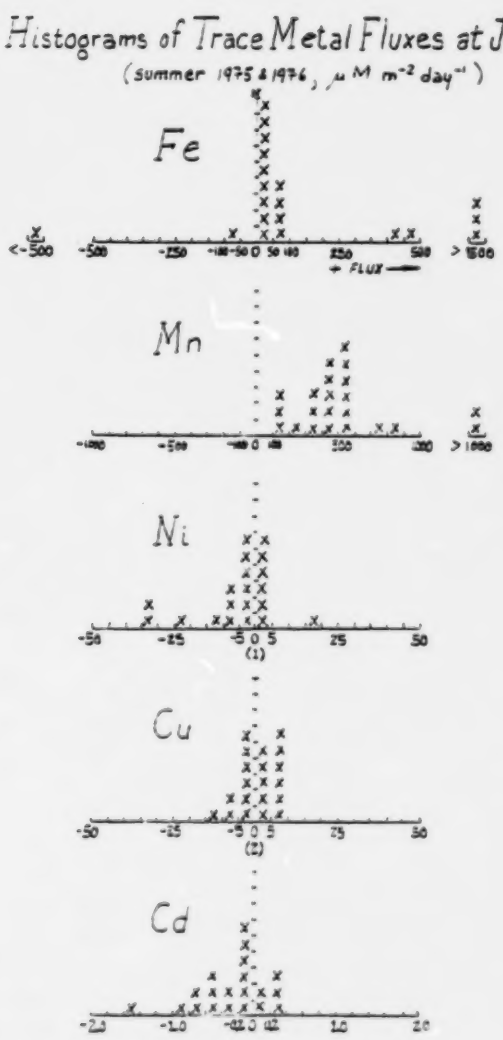
Histograms of Trace Metal Fluxes at Jamestown
(summer 1975 & 1976, μM m⁻² day⁻¹)
Fe
<-500
-500
-250
-100 -50 0 50 100
250
500
>1500
+ FLUX —
Mn
-1000
-500
-100 0 100
300
>1000
Ni
-50
-25
-5 0 5
25
50
(1)
Cu
-50
-25
-5 0 5
25
50
(2)
Cd
-2.0
-1.0
-0.2 0 0.2
1.0
2.0

Figure 2

Histograms of Nutrient Fluxes in Narragansett Bay[1]

($\mu M\ cm^{-2} day^{-1}$)

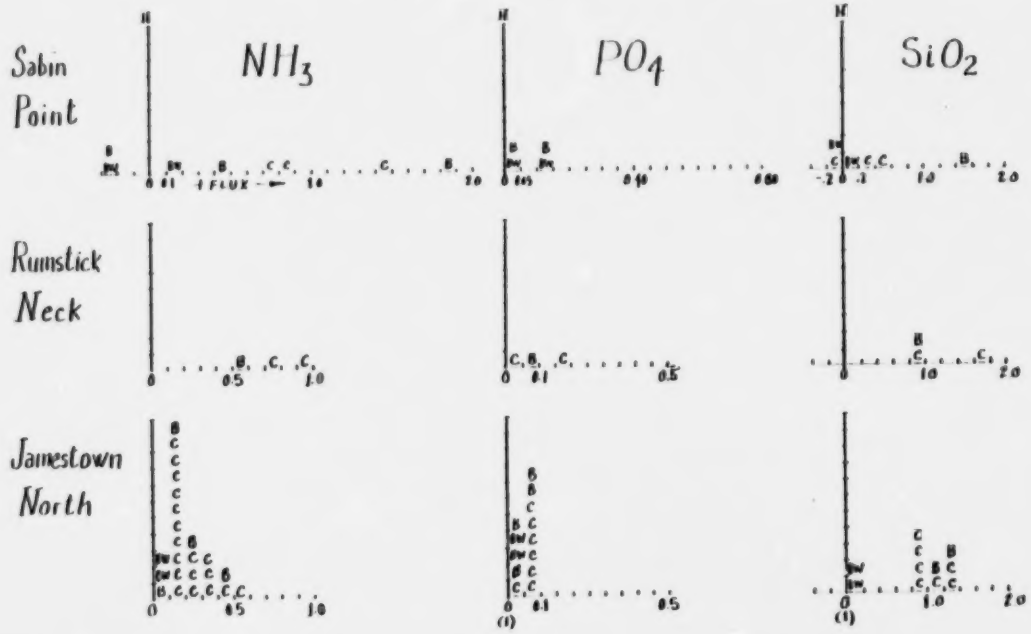

1) "B" = boxcore; "C" = chamber; trailing "W" indicates winter measurement
Zero results are alternately placed in lowest increments, positive first, and no of such results shown in parenthesis

Figure 3

Histograms of Dark Bottle Results at Jamestown
($\mu M\ m^{-2}\ day^{-1}$)

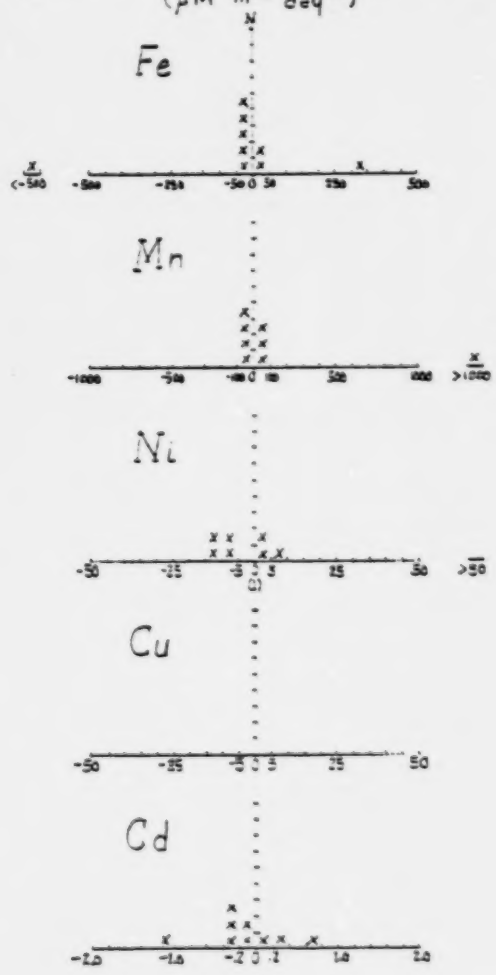

presented below. Flux measurements have been divided into arbitrary intervals and the number of results found within each interval is indicated. A positive flux means transfer from sediment to overlying water.

First consider the trace metal histograms. There is no consistent bias in the results of the control experiments. However, the results of the in situ flux measurements do show significant differences for some metals. Outlying values are easily identified in the figures. The central tendency for each metal is usually quite evident from the histograms. Nickel and Copper show no clear evidence of flux while cadmium is perhaps slightly negative. For manganese and iron, however, the data show a definite flux. In the case of manganese, the flux is clearly large and positive, centering about 400-500 $\mu M\ m^{-2}\ day^{-1}$. No negative fluxes were obtained for manganese but occasionally much higher fluxes were encountered, the reality of which is difficult to assess.

Although the evidence is less clear for iron, because of occasional large negative as well as positive results, there appears to be an unmistakable tendency for clustering of results on the positive side of zero. On the basis of this evidence, the flux of iron is expected to be somewhat less than that of manganese. The present results suggest values of a few tens of $\mu M\ m^{-2}$ day-1 or about 1/10 the manganese flux at Jamestown, a relatively pristine site.

The few data available for sabin point suggest a similar positive flux of Fe from the sediment, but, on the basis of two recent results, sediment at that site may be acting as a sink for copper, consistent with the organic-rich, reducing nature of the material found there.

Histograms of nutrient fluxes at three sites in Narragansett Bay are present in the attached figures. Several observations can be made about these data. It is evident that nutrient fluxes at Sabin Point vary widely whereas at Jamestown the results are relatively consistent. Few data are available for Rumstick Neck, but those that are available are compatible with its intermediate geographical location. One of the clearest generalizations may be made about the winter (BW) and summer fluxes; in almost every case the winter results are as low or lower than the warm water results. Thus a clear seasonal pattern in nutrient flux is evident, with fluxes approaching low or zero during mid-winter. The seasonality is most clearly seen for SiO_2 flux measured at Jamestown, where winter fluxes are barely measureable (0.1 $\mu M\ cm^{-2}$ day) while summer and fall fluxes average greater than 1.0, at least an order of magnitude higher. These conclusions are generally consistent with earlier and nutrient flux results of Hale (1974) and Nixon et al (1976).

MODELLING NUTRIENT AND METAL FLUXES FROM PORE WATER GRADIENTS AT THE JAMESTOWN NORTH STUDY SITE

The flux across the sediment water interface is equal to the sum of the diffusive and advective fluxes (the latter being the transport due to the pumping activity of organisms). The diffusive flux is estimated from the concentration gradient (dC/dZ) at the sediment-water interface and the apparent diffusion coefficient of ions and molecules (Da). The biopumping flux, which is a model estimate of the advective flux, is taken as the product of the

biopumping rate (estimated above as 0.7 cm^3 cm^{-2} day^{-1}) and the average concentration of a constituent in the top 20 cm of a core. Calculated values of diffusive and biopumping fluxes of H_4SiO_4, NH_3, $PO_4^{\equiv}$, TCO_2 and Mn^{++} are tabulated in table 7-3, along with averages of fluxes measured using two different apparatuses. "Deep diffusive fluxes" (fluxes of metabolites from below 25 cm into the zone of bioturbation) and "biodiffusion fluxes" (advective fluxes calculated from a model in which the advection of water is assumed to be random and described by a diffusion coefficient estimated from the Na data in the tracer experiment, as 4×10^{-5} cm^2 sec^{-1}). All models and calculations are described in detail in the appendix entitled, Benthic fluxes of nutrients and metals in Narragansett Bay, Rhode Island.

This table points up two significant conclusions. Firstly, the sum of the diffusive flux and biopumping flux are, for all constituents, in fair agreement with the measured benthic fluxes, indicating that the system is well described. Secondly, diffusive and biopumping fluxes are comparable. Thus even at this station, where there is an active benthic community transporting metabolites between sediments and bottom water, degradation of metabolites near the sediment-water interface and diffusion into the overlying water is responsible for about half the benthic flux.

SABIN POINT AND RUMSTICK NECK NUTRIENT FLUXES

Only a few preliminary data are available on Sabin Point and Rumstick Neck nutrient fluxes (tables 7, 1-2). The available results suggest that nutrient fluxes at these locations are comparable to, or perhaps greater than, Jamestown North values.

This result, if borne out by additional data, would be quite significant. There are two reasons pollution of Sabin Point sediments could lower the nutrient fluxes. Firstly, polution impacts the benthic community and thereby decreases release of nutrients by biopumping. Secondly, pollution may lower the total metabolism of the bacteria which, presumably, are responsible for most of the organic matter degradation and nutrient regeneration. The equality of Sabin Point and Jamestown North fluxes would imply that, in the event, neither of these considerations act to lower nutrient fluxes. This is a reasonable result. The model calculations for Jamestown North reveal that about half of all nutrient release results from decay and diffusion within the top centimeter of the sediment. In the absence of biopumping, we would expect bacterially mediated decay and regeneration to continue, with the establishment of nutrient concentration gradients steep enough to drive all nutrients out of the sediments by diffusion alone.

DISCUSSION OF RESULTS ON BENTHIC FLUXES OF METALS AT JAMESTOWN NORTH

The Mn flux at Jamestown North is 0.05 μM cm^{-2} day^{-1}. As discussed below and by Graham et al (1976) this flux is large enough to significantly influence the Mn distribution in Narragansett Bay. The Fe flux is about an order of magnitude less than the manganese flux. At first glance this appears surprising: since the iron and manganese concentrations in pore waters are similar, we would predict similar fluxes. Undoubtedly the discrepancy reflects rapid oxidation of Fe^{II} to Fe^{III} following migration out of sediments into the water

column.

Benthic fluxes of Ni, Cu, and Cd are very small, perhaps even negative. This undoubtedly reflects the low concentrations of these elements in the interstitial waters.

In a qualitative sense, the flux results reflect the solubility of metals in different oxidation states. Sediments at JN are reducing and the bottom water is oxidizing. The Ni, Cu and Cd concentrations in pore waters are very low; consequently so are the benthic fluxes. Pore water Fe and Mn concentrations are high; the manganese flux is high as a result, and the iron is small because of rapid bottom water oxidation.

SECTION 8

TRACE METALS IN THE HUDSON ESTUARY

INTRODUCTION

In the simplest sense estuaries can be thought of as channels where fresh river waters are mixed with seawater. The fact that these end-members have such distinct chemical properties makes these zones of mixing likely sites of reaction with respect to many elements including trace metals.

Some of these metals have been shown to have drastically different concentrations in seawater and estuaries. Table 1 shows that, of the four metals we have measured in Sargasso Sea water, all had much lower concentrations than in either estuarine environment. Nevertheless, the estuarine metal concentrations are relatively low and may therefore be affected by any source within an estuary such as anthropogenic input.

Because metals within estuaries should be reactive as well as sensitive to perturbations, detailed studies of their distributions should provide much useful information. In fact many such investigations have been undertaken in recent years. Windom et al., 1971; Helz et al., 1974; Gardiner 1974; Boyle et al., 1974; Martin et al., 1970; Fubai et al., 1975; Sholkovitz 1976; and many others have proposed and demonstrated such phenomenon as desorption, adsorption, complexation and flocculation of metals in estuarine environments.

Our original objective in the Hudson Estuary was to place limits on the importance of such processes in controlling the distributions of a series of trace metals (Cu, Mn, Ni, Fe, Cd, Zn) across the mixing zone. To some extent this was possible, but we've also shown that the predominant factor controlling many of these distributions in the Hudson is not a chemical response but any essentially point source anthropogenic input.

Perhaps this should not be too surprising since the Hudson Estuary flows through one of the most populated areas in the world (Figure 1). Some 15 million people live in the New York City/New Jersey area alone. These centers discharge about 2 billion gallons of sewage into the Hudson per day. This equals an input of 60 m^3/sec of sewage in various degrees of treatment (Figure 2). Freshwater flows are monitored at the dam on Green Island. The average high flow is 1200 m^3/sec while the low riverine value is about 250 m^3/sec. Thus, during some low flow periods, the sewage input into the Lower Hudson River Estuary can be as much as 30% of the riverine flow.

Table 1

Comparison between Ranges of 'Soluble' Metal Concentrations Found in the Hudson Estuary, Narragansett Bay, Rhode Island and the Sargasso Sea

Metal	Hudson Estuary (µg/kg)	[1]Narragansett Bay (µg/kg)	[2]Sargasso Sea (µg/kg)
Cd	.10 - .50	.05 - 1.0	.005 - .025
Zn	2.5 - 35	5.0 - 30	---------
Cu	2.0 - 7.0	1.0 - 7.0	.10 - .12
Mn	15 - 70	10 - 30	.01 - .15
Ni	1.0 - 10	3.0 - 10	.12 - .17

[1]unpublished data of the author

[2]Cd, Cu, and Ni values were taken from Bender and Gagner (1976). Mn data was taken from Bender, et al. (1976).

Figure 1. Map of the Hudson River Estuary

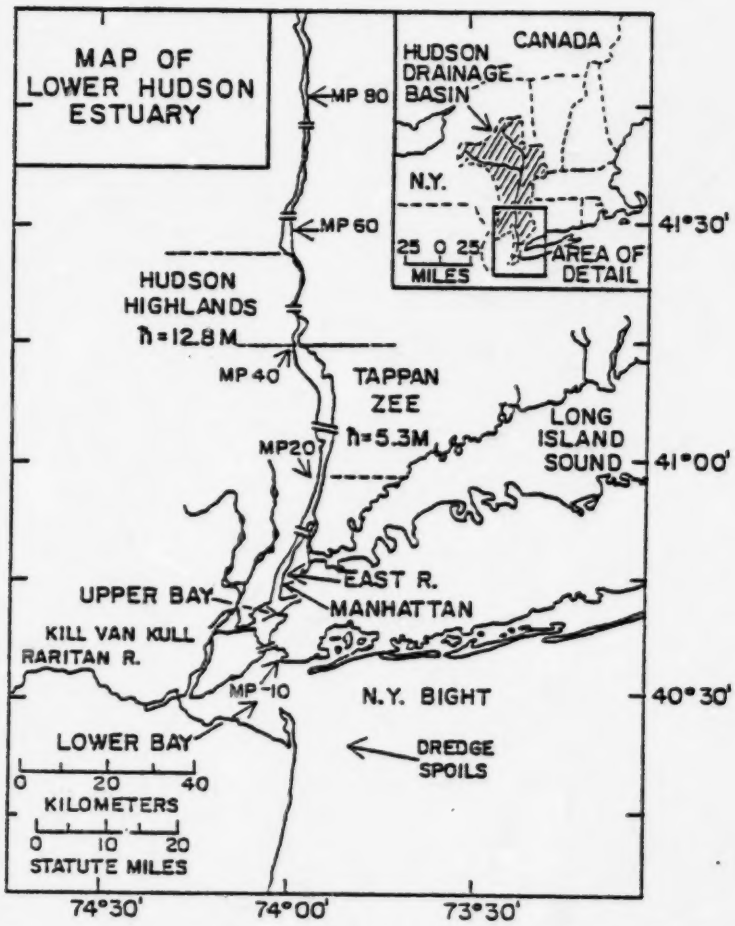

Figure 2. Map showing major points of sewage discharge to the Lower Hudson Estuary indicating the magnitude and degree of treatment as of 1975

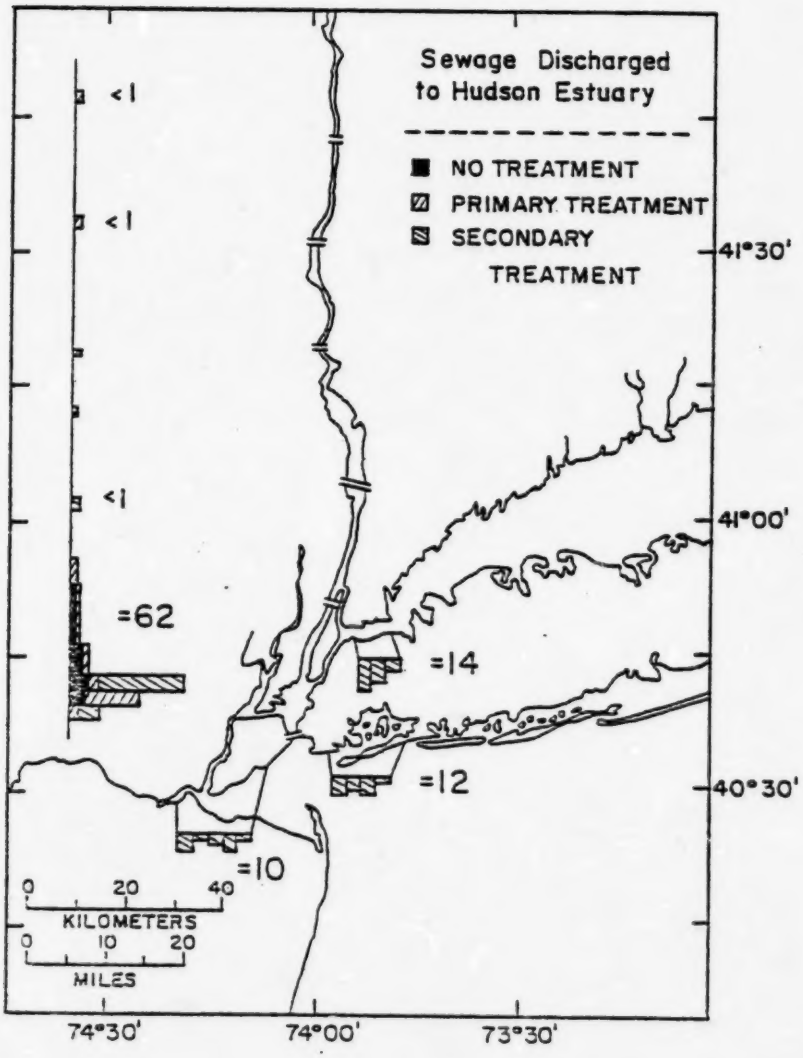

ANALYTICAL

The samples for this study were collected from the Lower Hudson River Estuary over two periods: April, 1974, during a spring runoff and in October, 1975, during an unused fall flooding period. As soon as possible after collection (< 12 hrs), aliquots of these samples were filtered through pre-washed, pre-weighed 0.4 micron Millipore filters, transferred to acid-cleaned linear polyethylene bottles and acidified to pH 2 with ultra-pure 6 N HCl.

Additional samples were stored on ice in the dark and analyzed for reactive-phosphate within 3 days after collection. These samples were also used to determine chlorinities using a AIC Chloride Titrator.

A more detailed description of the analytical procedures used to do the metal analyses is given elsewhere (Klinkhammer, 1977). Briefly, concentrations of soluble cadmium, zinc, copper, manganese and nickel were determined employing an ion-exchange preconcentration technique followed by quantitative analyses with a Perkin-Elmer 503 Atomic Absorption Spectrophotometer in conjunction with their Deuterium Arc Background Corrector. Zinc was done by flame while the other metals were analyzed by flameless, graphite-furnace atomic absorption. Efficiencies of metal elutions with 3 N HNO_3 from columns of Chelex-100 cation exchange resin were followed by adding a tracer solution to each sample. This spike contained the gamma-emitting, isotopically-pure isotopes listed in Table 2. The eluates were counted with a Nuclear Data 4000 Channel Analyzer at the Rhode Island Nuclear Science Center. The yields were calculated by comparison with an appropriate standard counted in the same manner as the samples.

Blanks were generally less than 10% at any sample concentration and are summarized in Table 3. The overall precision of these analyses was determined by analyzing duplicates (Table 4) and was better than ±8% for all metals. Standard addition experiments performed on the eluates of five samples selected to cover the salinity range in the estuary did not reveal any matrix interference greater than this level of uncertainty.

Soluble iron concentrations for samples collected in October, 1975, were also determined by flameless atomic absorption after pre-concentration using a APDC coprecipitation procedure which is a modified version of that technique developed by Boyle and Edmond (1975). The technique employed here was the same as that used by Bender and Gagner (1976) for preconcentrating Cu, Ni and Cd from Sargasso Sea water, except that 250 ml samples were used for these analyses. The average efficiency of these coprecipitations was 86% as determined by addition of a ^{59}Fe tracer. The precision from duplicate analyses was generally better than ±10%.

The results of the soluble analyses are listed in table 5 along with the salinity and mile point designation of each sample. The mile point is the distance in nautical miles from the tip of Manhattan, the Battery, with upstream positions being given positive numbers.

The size of 'soluble' manganese (<0.4 microns) was further constrained by the results of a series of dialysis experiments. Ten 25 ml aliquots of samples

Table 2

Relevant Data Concerning Tracer Used
during Chelex Preconcentration

Stable, isotopically pure species (> 99%)	Gamma-emitting isotope produced	KeV	Half-life (hours)
^{106}Cd	^{107}Cd	093	6.7
^{68}Zn	^{69m}Zn	439	13.8
^{63}Cu	^{64}Cu	511	12.0
^{55}Mn	^{56}Mn	847	2.58
^{64}Ni	^{65}Ni	1481	2.56

Table 5

Summary of Total Blanks Found
during Chelex Preconcentration

Metal	Absolute range of blanks in ppb	Mean blank and standard deviation in ppb	Mean blank as ±% of sample concentration
Cd	-.037 to +.019	-.001 ± .018	3.3
Zn	-.070 to +2.76	0.40 ± 1.05	5.1
Cu	-o.15 to +0.25	0.15 ± 0.15	5.5
Mn	-1.31 to +1.55	0.49 ± 0.95	2.6
Ni	-0.28 to +0.30	0.10 ± 0.18	3.9

Statistics were calculated from a total of 29 sample-blank pairs.

Table 4

Results of Duplicate Analyses of Metal Concentrations Found by AA after Preconcentration with Chelex Resin

Metal	Number of pairs	Percent standard deviation from the mean
Cd	19	6.4
Zn	19	7.5
Cu	19	2.5
Mn	19	6.0
Ni	19	4.4

Table 5-1

Mile Point Locations, Depths, Salinities and the Soluble Concentrations of Six Metals (Cd, Fe, Zn, Cu, Mn, and Ni) for Samples Collected from the Hudson Estuary

Mile Point	Depth *	Salinity o/oo	pH	** Cd	Ni	APRIL, 1974 Zn	Cu	Mn
34	S	0.60	7.65	.32	3.7	24	3.2	21
	M	0.60	7.63	.31	2.9	7.5	3.2	21
	B	0.62	7.64	.29	2.5	8.0	3.3	16.7
24.5	S	1.99	7.62	.23	5.1	15.4	4.0	34
	B	2.00	7.64	.37	2.2	7.7	3.1	31
14	S	3.59	7.55	.194	2.4	8.0	3.0	44
	M	3.62	7.60	.27	3.8	14.5	3.2	45
	B	3.65	7.69	.40	5.3	23	6.5	---
SALIN-	S	1.73	---	.27	9.3	28	4.1	27
ITY	S	1.74	---	.23	1.51	7.6	4.2	31
GRAD-	M	3.62	---	.28	3.2	11.0	3.4	42
IENT	S	1.95	---	.152	1.12	15.6	3.3	34
	S	2.20	---	.26	1.93	15.0	3.5	29
	S	2.38	---	.28	2.7	16.6	3.5	36
	S	2.63	---	.32	2.4	11.0	3.5	39
	S	3.20	---	.28	2.5	8.6	3.3	33
	S	3.06	---	.187	1.95	11.2	3.3	32
	S	3.59	---	.24	3.1	11.3	2.9	48
	S	5.09	---	.50	4.1	17.7	5.9	59
	S	5.96	---	.30	4.5	16.0	4.0	53
	S	5.85	---	.23	3.4	11.0	3.1	51
	S	6.68	---	---	4.0	16.3	2.9	52
0.5	S	7.71	7.55	.30	3.4	13.6	2.7	60
	M	12.00	7.60	.33	4.8	25	3.7	50
	B	15.90	7.69	.34	---	29	2.9	39
-8	B	22.33	7.85	.34	6.6	31	2.3	35
-15	S	21.59	7.89	.50	10.8	33	6.3	46
	B	21.79	7.93	.36	6.4	22	4.5	40
-18.5	S	29.71	7.98	.30	4.7	14.9	2.8	9.8
	M	30.33	8.06	.091	4.8	9.0	1.29	8.4
	B	32.26	8.01	.187	1.82	6.1	5.5	2.1

* S = surface; M = mid-column; B = bottom

** All soluble concentrations are in $\mu g/kg$.

Table 3-2

Mile Point	Depth *	Salinity o/oo	Cd	** Ni	OCTOBER, 1975 Zn	Cu	Mn	Fe
33	S	.07	.162	1.49	3.5	2.9	1.9	92
31	S	.07	.142	1.80	7.3	3.0	1.5	21
29	S	.07	.134	1.60	4.4	3.2	1.2	16.2
27	S	.89	.139	1.26	2.4	3.2	1.2	38
26	S	1.03	.34	2.6	6.0	3.4	2.1	23
25	S	.31	.20	2.1	3.3	3.5	1.2	31
	B	1.49	.157	1.21	4.0	2.9	2.1	14.2
23	S	.48	.129	2.0	3.0	3.0	1.1	26
	B	1.25	.198	2.4	3.0	3.5	1.1	33
21	S	.83	.39	2.5	8.6	3.6	2.0	21
	B	1.25	.093	1.25	4.1	3.5	2.1	26
20	S	.89	.29	2.3	4.4	3.3	1.8	14
	B	4.90	.194	2.5	6.7	3.0	19.6	44
18	S	1.10	.25	2.0	4.8	3.1	2.2	10.0
	B	6.29	.22	2.9	3.6	3.0	23	58
16	S	1.68	.44	2.7	5.9	3.3	4.5	22
	B	4.31	.25	2.9	5.2	3.2	15.3	23
14	S	1.98	.196	2.6	5.9	3.2	6.7	33
	B	4.06	.177	3.0	4.7	3.3	17.1	26
12	S	2.66	.145	2.2	3.6	3.0	9.4	18.2
	B	8.22	.20	2.7	6.7	2.7	28	52
10	S	3.33	.175	2.6	6.9	3.2	14.8	16.9
	B	8.17	.39	3.2	7.6	2.8	41	31
8	S	4.19	.184	1.6	9.6	3.2	20	16.9
	B	12.40	.21	3.8	9.3	2.5	43	22
6	S	4.48	.20	2.4	6.8	3.0	21	24
	B	17.63	.26	4.5	14.5	2.3	46	13
4	S	6.83	.179	2.5	6.4	2.6	28	10.0
3	S	8.11	.34	3.4	9.6	3.1	34	15.9
1	S	11.47	.28	3.8	9.3	2.6	41	13.3
	M	18.46	----	4.0	14.3	2.6	44	51
0.5	S	12.40	.26	4.8	14.7	3.8	40	15.9
0	S	13.76	.63	4.7	11.8	3.0	42	12.3

Table 3-3

Mile Point	Depth *	Salinity o/oo	** OCTOBER, 1975 Cd	Ni	Zn	Cu	Mn	Fe
-1	S	13.72	.36	4.7	14.3	3.2	41	14.9
	S	13.87	----	5.3	30	3.6	44	39
-2	S	15.43	.27	4.4	10.3	2.5	40	13.6
-4	S	16.67	.157	4.8	11.6	3.1	43	13.1
	S	16.70	.61	4.8	14.4	3.1	47	12.3
	S	16.72	.26	4.3	11.8	2.6	45	14.6
	B	20.69	.136	4.2	10.3	2.3	39	10.6
-6	S	18.13	.170	4.0	10.8	2.3	40	10.6
-8	S	20.52	.167	3.2	9.8	2.4	34	8.3
-9	S	21.16	.22	4.1	10.2	2.4	41	4.7
-10	S	22.52	.23	4.2	8.8	2.3	28	7.0
	B	30.70	.100	2.1	3.6	1.08	5.8	20

* S = surface; M = mid-column; B = bottom
** All soluble concentrations are in $\mu g/kg$.

collected in October, 1975, were dispenses into small plastic bottles. These samples had been previously filtered through 0.4 micron Millipore filters. Half of these aliquots were acidified and half were left unacifified. A dialysis bag filled with deionized water was placed in each bottle. Manganese concentrations in and out of each bag were measured after 3 and 6 days. In all cases agreement was quite good as shown in Figure 3. These resutls show convincingly that soluble manganese as defined by 0.4 micron filtration also passed through dialysis tubing having an effective pore size of 20 Angstroms.

Preweighed, acid-washed 0.45 micron Millipore filters were used to collect particulate samples. After filtration, the filters were rinsed to remove sea salt and equilibrated in a clean bench before reweighing to determine total particulate loading (Table 6).

These samples were then oxidized using a LFE Corporation Model 505 Low Temperature Asher. Most samples required ashing for 12 hours to successfully destroy all organic matrices. The ash was then quantitatively transferred to a polyethylene vial using 200 microliters of ultra-pure HF. This digestion was allowed to proceed at least one week before 100 microliters of ultra-pure HNO_3 were added after which the solutions were allowed to stand an additional week. After complete digestion the samples were quenched with doubly-deionized H_2O obtaining a final volume of 1 ml.

A 100 microliter aliquot of each quenched sample was dispenses onto a small filter pad and evaporated to dryness in a clean bench. Each filter was irradiated for 5 minutes in a flux of 4 $(10)^{12}$ neutrons/cm^2/sec, allowed to cool, and counted on a Ge(Li) detector tied into a Nuclear Data 4000 Channel Analyzer. By comparison with a standard, these spectra were used to calculate concentrations of particulate manganese and aluminium.

Dilutions of the original quenched solutions were used to determine concentrations of particulate Cd, Zn, Cu, Mn, Ni, and Fe by flameless AA (Tables 7 and 8). Since these solutions were diluted at least a factor of five with 3 $\underline{N}$ HNO_3 before determining concentrations by AA, it was felt that any matrix interferences would be minimal. Subsequent standard addition experiments performed on samples selected to cover the range of major ion concentrations expected in this sample group, showed that any such effect was insignificant within the limits of AA reproducibility (about ±5%).

DISCUSSION

Jim Simpson at Lamont-Doherty has done much work in trying to understand the geochemistry of the Hudson Estuary. He was the first to point out that reactive-phosphate is an essentially conservative tracer for the sewage being discharged into the Lower Hudson (Simpson, et al., 1975). This fact proved to be extremely useful to us in formulating a budget for trace metals in the same system (Klinkhammer, 1977). This is most easily demonstrated by Figure 4, which shows that the distributions of reactive-phosphate are very similar to those of soluble manganese, zinc and nickel. This suggests that the distributions of these three metals are strongly affected by an anthropogenic source. Copper is anomalous in this respect and its distribution approaches that predicted by conservative mixing (Figure 5).

Table 6-1

Mile Point Locations, Depths, Salinities, and the Particulate Concentrations of Six Metals for Samples Collected from the Hudson Estuary

Mile Point	Depth *	Salinity o/oo	Suspended load mg/kg	** Cd	Ni	Zn	APRIL, 1974 Cu	Mn	Fe
34	S	0.60	8.4	.050	0.8	---	1.65	13.8	810
	M	0.60	7.0	.121	1.2	4.7	1.61	6.9	850
	B	0.62	14.3	.072	0.8	4.2	1.21	5.8	740
24.5	S	1.99	26.8	.112	6.4	6.7	2.8	11.5	1290
	B	2.00	30.0	.092	1.2	8.5	3.2	17.1	1360
14	S	3.59	27.7	.074	0.7	4.2	2.5	9.7	1080
	M	3.62	28.5	.201	8.0	7.7	4.8	14.9	1750
	B	3.65	15.6	.073	1.2	4.0	2.7	6.0	810
SALIN-	S	1.73	17.5	.112	1.5	6.0	2.9	7.0	1180
ITY	S	1.74	10.9	.057	0.7	3.3	1.19	5.6	650
GRAD-	M	3.62	11.4	.048	1.1	3.7	2.1	6.1	730
IENT	S	1.95	20.3	.077	1.2	5.8	3.3	10.5	1240
	S	2.20	21.6	.103	1.3	6.4	3.9	11.8	1302
	S	2.38	20.6	.106	1.1	5.7	3.7	12.0	1280
	S	2.63	30.9	.111	1.6	7.9	4.5	14.1	1570
	S	3.20	16.5	.030	0.2	2.0	3.6	3.5	430
	S	3.06	20.3	.060	0.7	5.2	2.3	8.2	941
	S	3.59	11.9	---	---	---	---	---	---
	S	5.09	0.6	.016	0.1	0.79	und	1.30	138
	S	5.96	13.9	.068	2.8	1.84	0.82	2.0	260
	S	5.85	11.0	.030	und	0.48	und	0.81	90
	S	6.68	11.8	.070	0.9	3.9	1.56	3.5	610
	S	7.71	13.5	.068	0.6	4.1	2.8	5.9	881
	M	12.00	8.8	.154	0.6	3.8	3.6	5.0	640
	B	15.90	28.9	---	---	---	---	---	---
	B	22.33	10.9	.049	0.4	1.77	1.89	3.4	350
	S	21.59	3.8	.044	0.4	4.1	3.2	3.1	300
	B	21.79	7.7	.027	und	3.00	1.98	2.7	260
	S	29.71	---	.013	und	0.20	und	0.91	40
	M	30.33	---	.006	und	0.04	und	0.22	7
	B	32.26	0.9	.010	und	0.29	2.5	0.40	30

* S = surface; M = mid-column; B = bottom

** All soluble concentrations are in μg/kg.

und = undetectable

Table 6-2

Mile Point	Depth *	Salinity o/oo	Suspended load mg/kg	Cd	** Ni	Zn	Cu	Mn	Fe
					OCTOBER, 1975				
33	S	.07	8.8	.055	0.75	4.2	1.52	11.7	690
31	S	.07	9.2	.072	0.72	4.6	1.83	12.0	690
29	S	.07	9.0	.062	1.03	7.1	1.34	19.9	1100
27	S	.89	8.2	.136	0.84	4.8	2.2	15.1	850
26	S	1.03	16.4	---	---	---	---	23	---
25	S	.31	7.0	.037	0.63	4.1	1.28	14.5	600
	B	1.49	30.3	.090	1.56	9.0	3.5	27	1420
23	S	.48	36.2	.079	1.42	7.6	3.4	26	1350
	B	1.25	31.2	.271	1.36	9.1	3.8	33	1400
21	S	.83	15.3	.051	0.91	5.3	2.4	22	970
	B	1.25	52.2	.132	2.23	13.9	5.7	40	2200
20	S	.89	6.6	.038	1.00	4.7	2.0	17.1	740
	B	4.90	19.0	.101	1.02	7.5	2.8	18.7	2200
18	S	1.10	11.8	.035	0.47	3.1	0.81	14.1	690
	B	6.29	13.2	.034	0.85	4.6	2.7	16.4	810
16	S	1.68	8.6	.029	0.68	4.5	1.63	11.6	530
	B	4.31	29.0	.058	1.27	9.3	4.3	18.7	1230
14	S	1.98	8.6	.024	0.40	2.7	1.08	10.6	430
	B	4.06	40.9	.066	0.26	8.1	5.0	15.7	1360
12	S	2.66	9.6	.025	0.68	4.6	1.50	16.9	530
	B	8.22	23.5	.066	1.09	7.4	4.7	12.8	1070
10	S	3.33	14.3	.039	0.82	4.9	2.6	13.1	770
	B	8.17	23.8	---	1.04	8.0	4.4	13.6	1070
8	S	4.19	11.5	.034	0.60	4.5	2.3	9.2	---
	B	12.40	12.5	.048	0.55	3.4	2.5	8.3	570
6	S	4.48	2.9	.030	0.45	3.9	2.6	6.1	390
	B	12.63	8.6	.035	0.50	3.1	2.6	4.4	500
4	S	6.83	7.0	.023	0.41	2.8	1.29	8.4	470
3	S	8.11	1.7	.022	0.33	2.9	0.98	3.0	290
1	S	11.47	2.6	.022	0.33	2.3	1.27	5.5	280
	M	18.46	0.8	.021	0.17	1.50	0.99	3.2	160
0.5	S	12.40	2.5	.012	0.17	1.31	0.48	2.2	160
0	S	13.67	2.8	.024	0.18	1.38	0.48	2.3	130

Table 6-3

Mile Point	Depth *	Salinity o/oo	Suspended load mg/kg	Cd **	Ni **	Zn **	Cu **	Mn **	Fe **
				OCTOBER, 1975					
-1	S	13.72	0.7	.030	0.25	1.62	0.83	2.2	150
	S	13.87	0.7	.011	0.24	1.71	0.98	2.4	40
-2	S	15.43	2.6	.014	0.28	1.64	1.01	2.1	130
-4	S	16.67	5.5	.009	0.17	1.12	0.32	3.5	100
	S	16.70	2.1	.095	0.14	1.13	0.54	2.1	120
	S	16.72	2.2	.030	0.17	1.57	0.60	4.1	125
	B	20.69	4.4	.012	0.21	1.38	0.58	4.8	100
-6	S	18.13	2.5	.011	0.24	1.99	1.04	2.5	110
-8	S	20.52	1.4	.005	1.55	0.73	und	2.5	50
-9	S	21.16	1.8	.006	0.08	0.83	und	1.84	45
-10	S	22.52	1.4	.007	0.49	1.07	0.23	2.7	80
	B	30.70	2.9	.012	0.21	1.71	0.80	5.4	200

* S = surface; M = mid-column; B = bottom
** All soluble concentrations are in μg/kg.
und = undetectable

Figure 3. Plot of soluble manganese concentrations found inside and outside dialysis bags

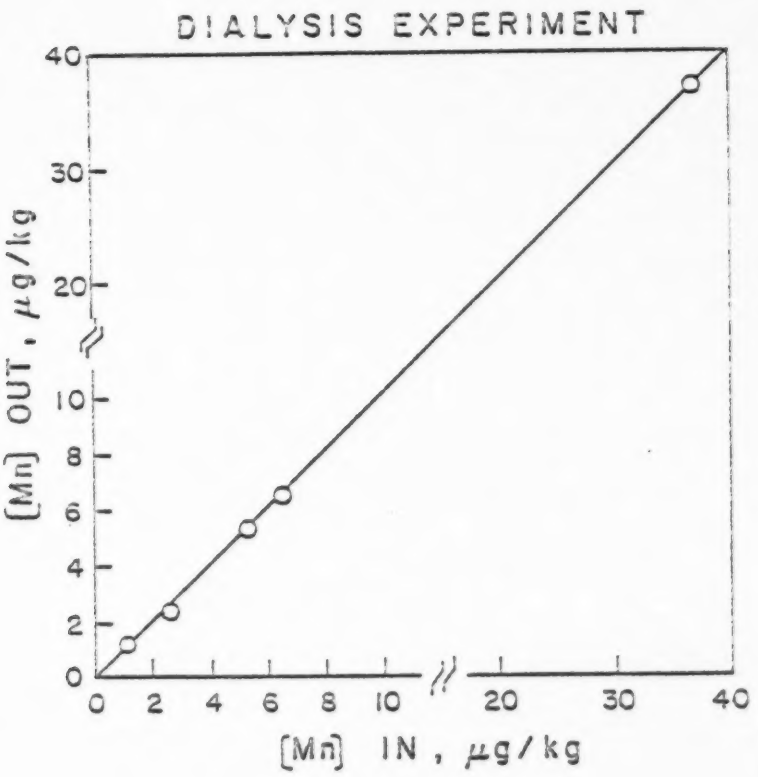

Figure 4. Plots of soluble zinc, copper, manganese, nickel, and molybdate-reactive phosphate concentrations versus salinity for samples collected in April, 1974, and October, 1975

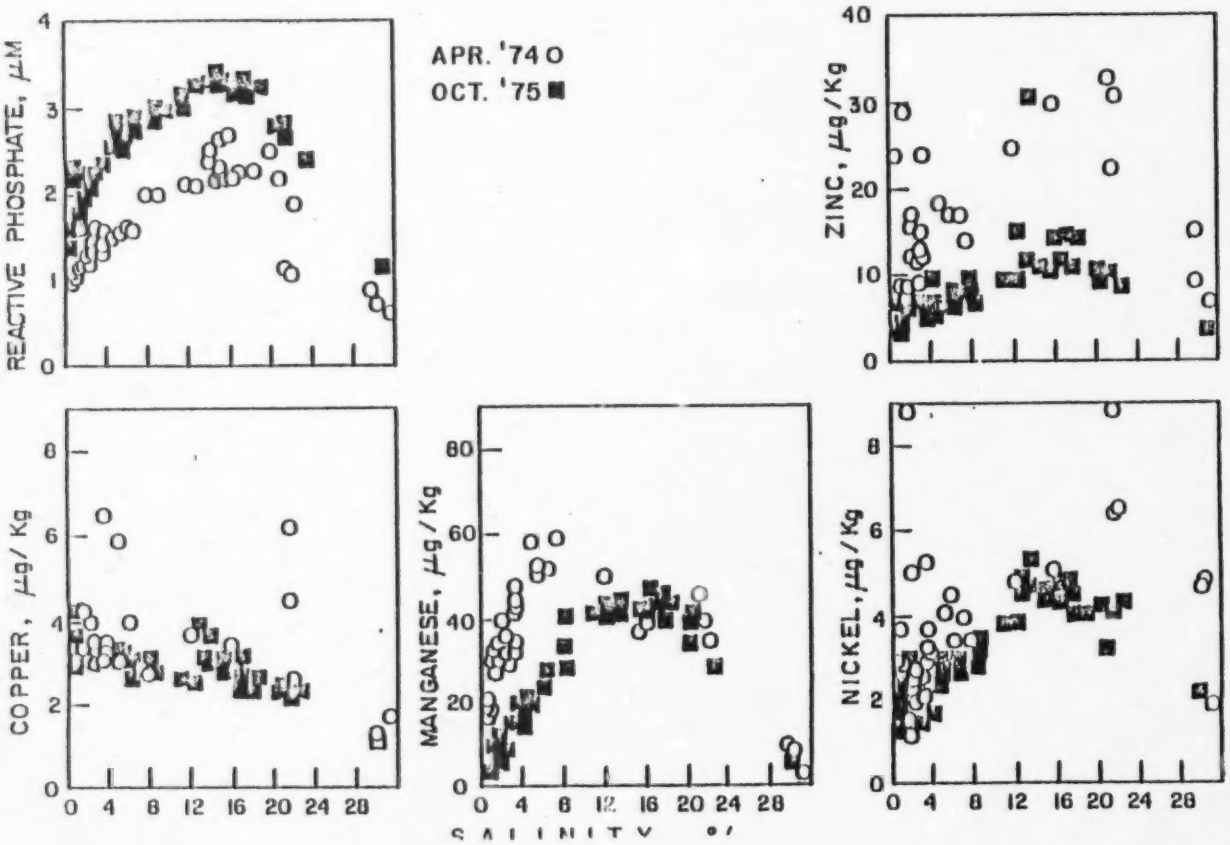

Figure 5. Examples of conservative and non-conservative behavior of a dissolved species as revealed by plots of concentration versus salinity

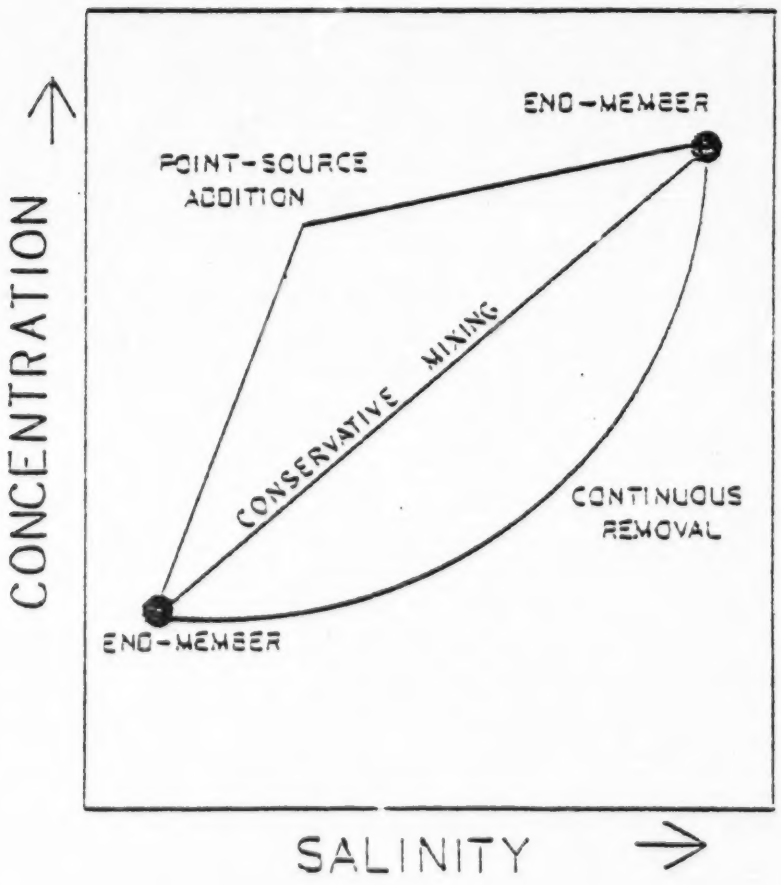

Our results for soluble Cd and Fe are shown in Figure 6. The noise in these measuremtns was such that it precluded any hard condlusions; although the range of values are consistent with those found by other workers in similar systems (Windom et al., 1971; Hunt, 1973). The solid phase data proved to be more enlightening with respect to these two metals. Figure 7 is a plot of the suspended load versus the percent of total Cd as solids. The boundaries were drawn from the experimental considerations of cadmium adsorption developed by Gardiner (1974). Eighty-five percent of our cadmium data from the Hudson fall within the limited dictated by Gardiner's adsorption-controlled distribution coefficients. Although this model puts only limited constraints on the system, the agreement is encouraging and at least suggests that adsorption may be affecting the mass-transport of cadmium in the Hudson Estuary.

This hypothesis is further supported by the cadmium to aluminum weight-ratios (Table 8) plotted in Figure 8. All of these particulates had Cd/Al ratios well above those predicted by crustal models (Turekian and Wedepohl, 1961). This was not true for iron which had ratios close to or at crustal values. In general, >95% of the iron in the Hudson was being transported in the >0.4 micron fraction (Tables 6 and 7).

The Ni/Al ratios plotted in Figure 8 are consistent with the soluble concentrations of Figure 4. That is, the ratios are essentially crustal suggesting no adsorption or desorption has taken place while the soluble distributions reflect the sewage input near Manhattan/New Jersey ($S \simeq 15\%$).

Zinc was apparently more reactive than nickel since the Zn/Al ratios were 4-8 times crustal values throughout the estuary. Furthermore, the distributions of the soluble fraction reflects an input near Manhattan. One explanation is that upstream anthropogenic zinc was being adsorbed outside the study area but that zinc discharged downstream remained soluble for the residence time of water in the lower Estuary which is a few days (Simpson et al., 1975). Although this hypothesis is consistent with these data, other explanations cannot be eliminated here.

The Cu/Al ratios were consistently 2-4 times above crustal values suggesting some adsorption may have taken place. Within reasonable limits, the soluble concentrations can be explained by simple two-source mixing of New York Bight and Hudson River waters. This suggests that any anthropogenic copper dumped in the Lower Estuary was either >0.4 microns or was being rapidly adsorbed onto particulate matter.

The distribution of soluble Mn (Figure 4) is very similar to that of reactive-phosphate. Apparently, sewage was one source of soluble Mn in the Lower Estuary. However, the average concentration of total Mn in sewage effluents being discharged here (Interstate Sanitation Commission, 1972) are large enough to account for only about 25% of this anomaly.

The Mn/Al ratios in Figure 8 suggest that some Mn was being desorbed from particulates at mid-salinities. This is also supported by the data in Figure 9 which suggests that about 50% of the particulate Mn is being desorbed near or at the bottom of the estuary. If this desorption occurs in the water column,

Table 7-1

Mile Point Locations, Depths, Salinities and the Metal Abundances of Six Metal in Particulate Matter Samples Collected from the Hudson Estuary

Mile Point	Depth *	Salinity o/oo	** APRIL, 1974 Cd	Ni	Zn	Cu	Mn	Fe
34	S	0.60	5.9	96	---	200	1300	96,500
	M	0.60	17	170	670	230	990	122,000
	B	0.62	5.0	56	300	90	400	51,500
24.5	S	1.99	4.2	240	250	110	430	48,100
	B	2.00	3.1	41	280	110	570	45,500
14	S	3.59	2.7	25	150	90	350	39,000
	M	3.62	7.1	280	270	170	520	61,400
	B	3.65	4.7	77	250	170	390	52,100
SALIN-	S	1.73	6.4	86	340	160	400	67,400
ITY	S	1.74	5.2	64	300	110	510	59,500
GRAD-	M	3.62	4.2	97	330	190	530	64,300
IENT	S	1.95	3.8	59	290	160	520	61,100
	S	2.20	4.8	60	290	180	550	61,100
	S	2.38	5.2	60	280	180	580	62,100
	S	2.63	3.6	52	260	150	460	50,800
	S	3.20	1.8	12	120	220	210	25,800
	S	3.06	3.0	34	260	120	400	46,400
	S	3.59	5.5	---	170	70	---	31,500
	S	5.09	---	80	---	und	---	----
	S	5.96	4.9	200	130	60	140	18,300
	S	5.85	2.7	und	40	und	70	8,180
	S	6.68	5.9	76	330	130	300	52,000
0.5	S	7.71	5.0	44	300	210	440	65,300
	M	12.00	18	68	440	400	570	73,700
	B	15.90	---	---	---	---	---	----
-8	B	22.33	4.5	38	160	95	320	32,000
-15	S	21.59	12	110	1090	830	820	79,000
	B	21.79	3.5	und	390	260	350	34,000
-18.5	S	29.71	---	und	---	und	---	----
	M	30.33	---	und	---	und	---	----
	B	32.26	11	und	340	und	460	33,600

* S = surface; M = mid-column; B = bottom
** All abundances are in parts per million.
und = undetectable

Table 7-2

Mile Point	Depth *	Salinity o/oo	** OCTOBER, 1975 Cd	Ni	Zn	Cu	Mn	Fe
33	S	.07	6.3	85	480	170	1330	77,700
31	S	.07	7.8	78	530	200	1300	75,200
29	S	.07	6.9	110	790	150	2210	122,000
27	S	.89	17	100	590	270	1840	103,000
26	S	1.03	---	---	---	---	---	---
25	S	.31	5.3	90	580	180	2070	86,200
	B	1.49	3.0	52	300	120	880	47,100
23	S	.48	2.6	39	220	90	710	37,400
	B	1.25	8.7	44	290	120	1070	---
21	S	.83	3.3	60	350	160	1410	63,000
	B	1.25	2.5	43	270	110	760	42,300
20	S	.89	5.8	150	710	310	2590	113,000
	B	4.90	5.3	54	400	150	980	50,600
18	S	1.10	3.0	40	260	70	1200	43,500
	B	6.29	2.6	64	350	200	1240	61,600
16	S	1.68	3.3	79	520	190	1350	62,300
	B	4.31	2.0	44	320	150	650	42,600
14	S	1.98	2.8	47	310	130	1230	50,100
	B	4.06	1.6	60	200	120	380	33,300
12	S	2.66	2.6	71	480	160	1760	55,100
	B	8.22	2.8	46	320	200	550	45,800
10	S	3.33	2.7	57	340	180	920	54,100
	B	8.17	---	44	340	190	570	45,300
8	S	4.19	3.0	52	270	200	800	---
	B	12.40	3.8	44	270	200	660	262,000
6	S	4.48	10	160	1300	880	2100	138,000
	B	17.63	4.1	58	360	300	510	57,600
4	S	6.83	3.3	59	410	180	1200	68,000
3	S	8.11	13	210	1700	580	1770	166,000
1	S	11.47	8.5	130	880	490	2120	107,000
	M	18.46	26	210	1900	1200	4000	11,100
0.5	S	12.40	4.8	68	520	190	880	64,400
0	S	13.67	8.6	64	500	170	820	46,100

Table 7-3

Mile Point	Depth *	Salinity o/oo	** OCTOBER, 1975 Cd	Ni	Zn	Cu	Mn	Fe
-1	S	13.72	43	360	2300	1200	3140	208,000
	S	13.87	16	340	2400	1400	3430	197,000
-2	S	15.43	5.4	110	630	390	810	50,700
-4	S	16.67	1.6	31	200	60	640	19,100
	S	16.70	45	67	540	260	1000	54,900
	S	16.72	14	77	710	270	1860	58,300
	B	20.69	2.7	48	310	130	1090	21,800
-6	S	18.13	4.4	96	800	420	1000	43,000
-8	S	20.52	3.6	1100	520	und	1790	31,400
-9	S	21.16	3.3	44	460	und	1000	25,100
-10	S	22.52	5.0	350	760	160	1930	60,800
	B	30.70	4.1	72	590	280	1860	68,800

* S = surface; M = mid-column; B = bottom
** All abundances are in parts per million.
und = undetectable

Table 8-1

Mile Point Locations, Depths, Salinities and the Metal to Aluminum Weight Ratios of Six Metals in Particulate Matter Samples Collected from the Hudson Estuary

Mile Point	Depth *	Salinity o/oo	APRIL, 1974 Cd/Al x10^5	Ni/Al x10^3	Zn/Al x10^3	Cu/Al x10^3	Mn/Al x10^3	Fe/Al x10^0
34	S	0.60	5.3	.86	---	1.76	14.7	.87
	M	0.60	17	1.7	6.65	2.30	9.71	1.23
	B	0.62	9.3	1.0	5.45	1.56	7.56	.94
24.5	S	1.99	6.8	3.90	4.09	1.72	7.27	.78
	B	2.00	---	---	---	---	---	---
14	S	3.59	5.7	.55	4.42	1.93	7.85	.83
	M	3.62	12	.47	6.68	2.79	7.97	1.02
	B	3.65	7.6	1.2	4.12	2.80	6.18	.85
SALIN-	S	1.73	8.5	1.11	4.53	2.17	5.17	.89
ITY	S	1.74	8.7	1.02	5.02	1.80	8.55	.98
GRAD-	M	3.62	5.8	1.32	4.44	2.53	6.78	.89
IENT	S	1.95	6.7	1.11	5.08	2.87	8.51	1.08
	S	2.20	5.9	.76	3.64	2.23	7.45	.76
	S	2.38	7.3	.74	4.82	3.12	9.66	.88
	S	2.63	5.4	.75	3.81	2.17	6.96	.75
	S	3.20	5.8	.29	3.82	0.70	7.31	.81
	S	3.06	5.5	---	4.79	2.14	7.53	.86
	S	3.59	---	---	---	---	---	---
	S	5.09	8.6	.62	4.20	---	6.71	.73
	S	5.96	16	.26	4.42	1.97	7.29	.62
	S	5.85	5.8	6.82	2.54	---	5.40	.48
	S	6.68	1.2	---	6.68	2.68	6.19	1.06
0.5	S	7.71	8.3	.77	4.95	3.39	6.37	1.07
	M	12.00	27	1.10	6.67	6.22	9.48	1.13
	B	15.90	---	---	---	---	---	---
-8	B	22.33	8.7	.73	3.11	1.80	6.10	.61
-15	S	21.59	18	1.52	16	13	11	1.20
	B	21.79	9.9	---	11	7.20	9.75	.96
-18.5	S	29.71	2.8	---	4.82	---	19	.78
	M	30.33	2.8	---	2.07	---	11	.34
	B	32.26	3.7	---	1.13	---	16	1.13

* S = surface; M = mid-column; B = bottom

Table 8-2

Mile Point	Depth *	Salinity o/oo	OCTOBER, 1975 Cd/Al x10^5	Ni/Al x10^3	Zn/Al x10^3	Cu/Al x10^3	Mn/Al x10^3	Fe/Al x10^0
33	S	.07	5.8	.78	4.36	1.58	12.2	.71
31	S	.07	7.7	.77	5.13	1.93	12.9	.74
29	S	.07	3.3	.55	3.75	.71	10.6	.58
27	S	.89	8.8	.54	3.16	1.44	9.80	.55
26	S	1.03	---	---	---	---	---	---
25	S	.31	3.8	.66	4.24	1.33	15.1	.63
	B	1.49	3.3	.57	3.32	1.28	9.82	.52
23	S	.48	3.4	.62	3.42	1.48	11.2	.59
	B	1.25	15	.76	5.04	2.08	18.5	.77
21	S	.83	2.8	.50	2.91	1.32	11.7	.53
	B	1.25	3.3	.57	3.52	1.45	10.0	.56
20	S	.89	3.2	.84	3.93	1.73	14.4	.62
	B	4.90	5.6	.56	4.14	1.60	10.4	.53
18	S	1.10	3.5	.47	3.06	.80	14.0	.51
	B	6.29	2.1	.54	3.31	2.21	10.0	.52
16	S	1.68	3.4	.80	5.24	1.94	13.6	.62
	B	4.31	2.6	.58	4.22	1.94	8.49	.56
14	S	1.98	3.1	.50	3.39	1.37	13.5	.55
	B	4.06	2.8	.11	3.43	2.11	6.64	.58
12	S	2.66	2.8	.79	5.31	1.73	19.6	.61
	B	8.22	4.0	.67	4.57	2.92	7.91	.66
10	S	3.33	3.2	.66	3.92	2.05	10.6	.62
	B	8.17	---	.63	4.86	2.69	8.23	.65
8	S	4.19	2.7	.49	3.68	1.85	7.49	---
	B	12.40	4.3	.49	2.99	2.27	7.42	.51
6	S	4.48	4.2	.63	5.40	2.00	8.53	.55
	B	17.63	4.1	.58	3.62	2.95	5.25	.59
4	S	6.83	2.6	.46	3.17	1.44	9.43	.53
3	S	8.11	4.9	.76	6.27	2.13	6.61	.62
1	S	11.47	3.9	.59	4.12	2.30	9.88	.50
	M	18.46	7.6	.63	5.47	3.61	11.6	.57
0.5	S	12.40	3.5	.48	3.74	1.37	6.40	.46
0	S	13.67	10	.76	5.92	2.06	9.90	.55

Table 8-3

Mile Point	Depth *	Salinity o/oo	OCTOBER, 1975 Cd/Al $x10^5$	Ni/Al $x10^3$	Zn/Al $x10^3$	Cu/Al $x10^3$	Mn/Al $x10^3$	Fe/Al $x10^0$
-1	S	13.72	11	.90	5.73	2.94	7.78	.53
	S	13.87	2.1	.44	3.14	1.80	4.38	.24
-2	S	15.43	4.2	.83	4.93	3.02	6.43	.40
-4	S	16.67	3.2	.57	3.82	1.09	11.9	.36
	S	16.70	---	.61	4.92	2.32	9.26	.51
	S	16.72	15	.82	7.30	2.96	20.5	.62
	B	20.69	4.5	.77	5.07	2.13	17.8	.35
-6	S	18.13	3.6	.74	6.18	3.24	7.88	.33
-8	S	20.52	3.5	1.10	5.23	---	17.9	.33
-9	S	21.16	3.6	.47	4.67	---	10.0	.26
-10	S	22.52	4.2	2.82	6.25	1.33	15.5	.48
	B	30.70	3.8	.68	5.40	2.52	17.2	.63

* S = surface; M = mid-column; B = bottom

Figure 6. Plots of salinity versus soluble cadmium concentrations for samples collected in April, 1974, and October, 1975, as well as soluble iron concentrations for October, 1975

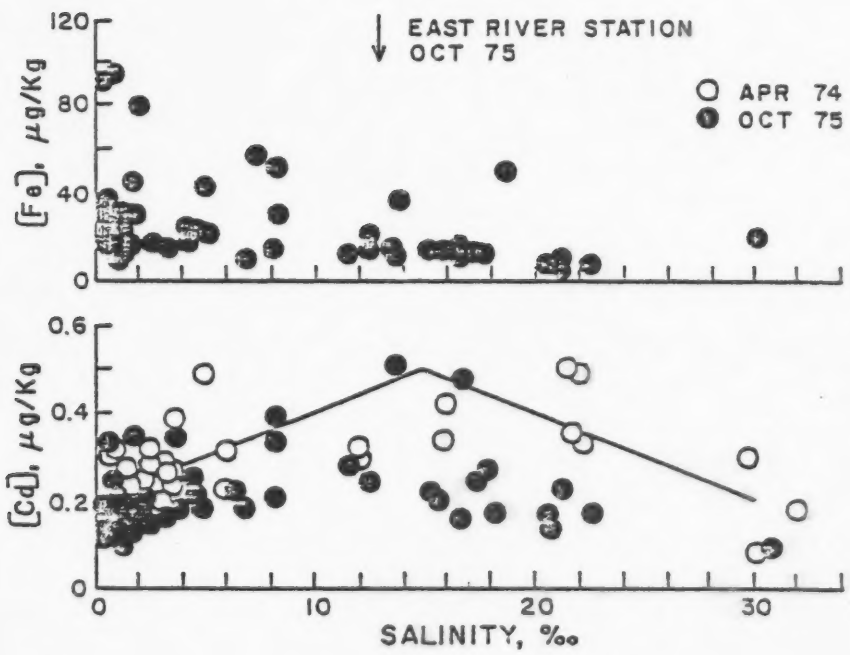

Figure 7. Plot of suspended load versus the proportion of total Cd found in the particulate phase. Also shown is the range in the partition coefficients between solid and liquid predicted by Gardiner (1973)

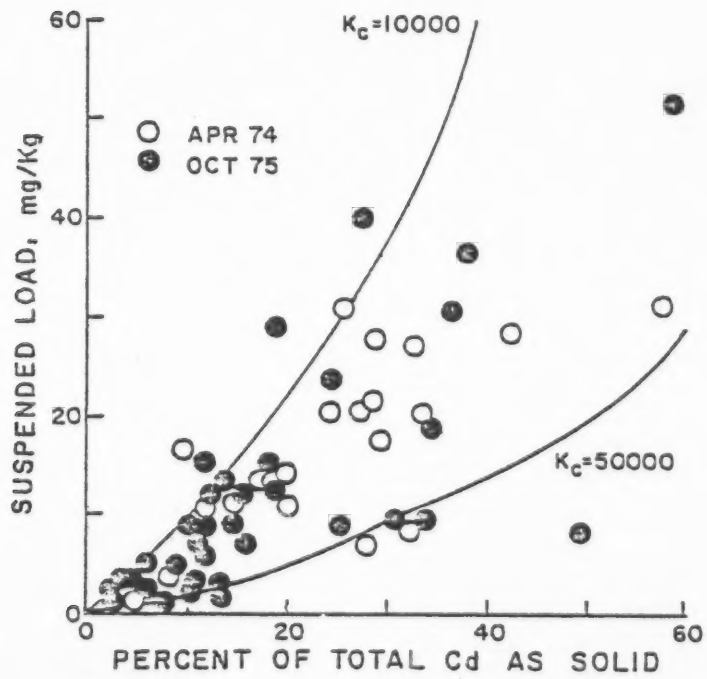

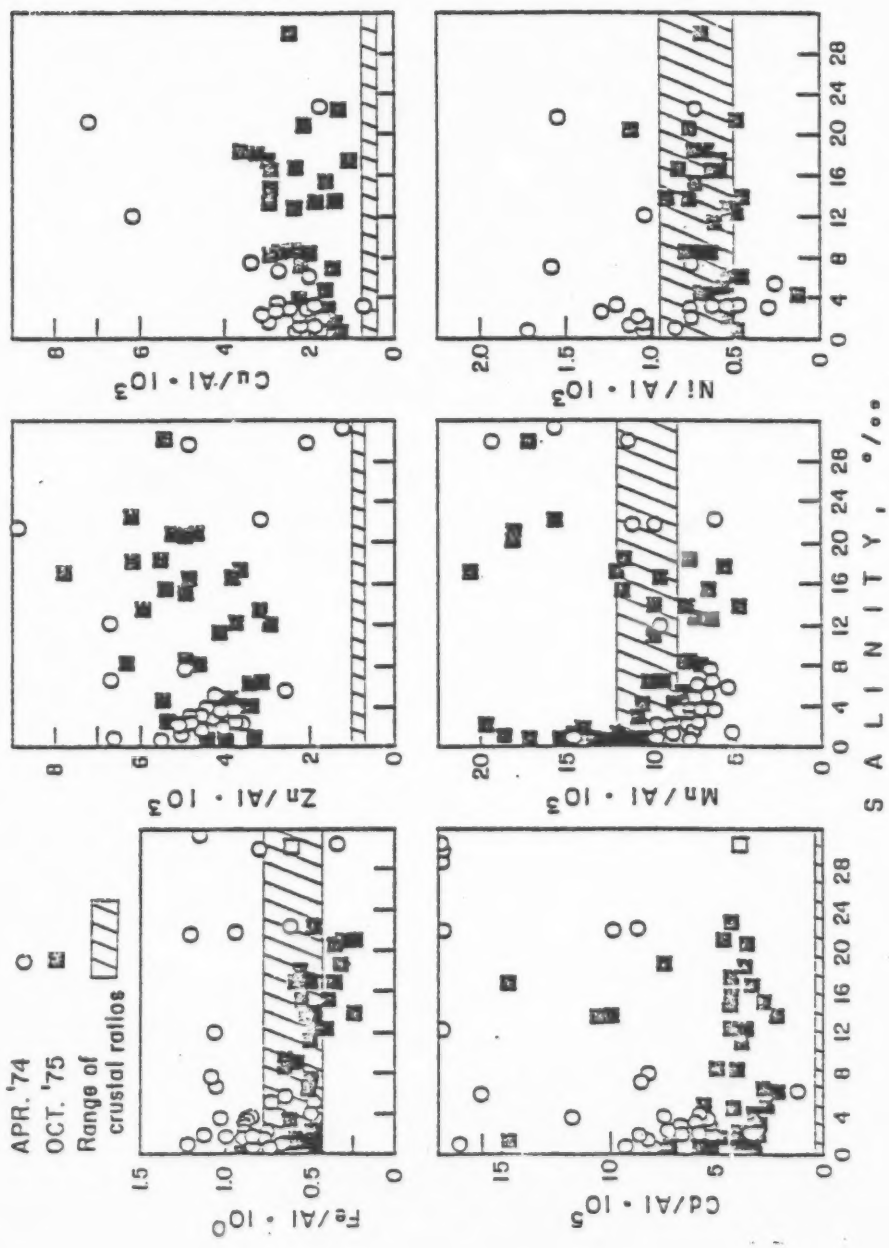

Figure 8. Metal to aluminum weight ratios of six metal in particulates filtered from the Hudson Estuary plotted versus salinity

Figure 9. Manganese abundances of surface and sub-surface particulates collected from the Hudson Estuary during October, 1975, plotted versus mile point

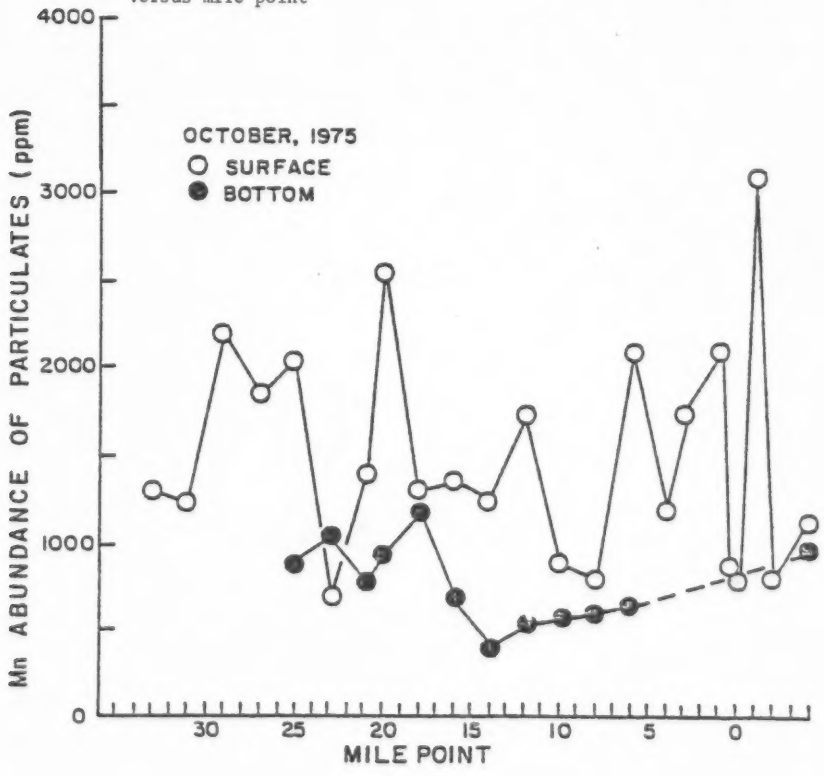

it may contribute as much as 10 µg kg to the soluble load.

Additionally, a benthic flux of Mn from reducing interstitial waters like that demonstrated in Narragansett Bay (Graham et al., 1976) would supply about 2 µg/kg. Still, only about 50% of the soluble Mn at a salinity of 15% can be accounted for with these sources. Of course, it is entirely possible that any or all these sources have been underestimated. Alternately, an additional source of dissolved Mn to the Lower Estuary such as atmospheric particles, or ground waters may have been important. Still another possibility is that the Lower Estuary may act as a trap for dissolved Mn being supplied by surges during storm runoff periods. This idea was used by Evans et al. to explain similar plots of dissolved Mn in the Newport River Estuary, North Carolina. This question must remain unresolved until additional data becomes available.

CONCLUSIONS

Using residence times for water in the Lower Estuary calculated from the distributions of reactive-phosphate (Simpson et al., 1975), it was possible to estimate the flux of these metals out of the Estuary (Table 9). These represent the total fluxes of metals out of the Upper Bay into the Lower Bay (Figure 1).

Data presented in this report was drawn from samples collected over only two periods. Although the magnitude of the anthropogenic input to some extent simplified the interpretation of trace metal distributions in the Hudson River Estuary, the chemistry of this system must be considered extremely dynamic and complex. Therefore, any broad conclusions based on these limited data must be considered tentative. Furthermore, there are undoubtedly other processes not mentioned below which may be of at least minor importance. However, to a first approximation, these observations and hypotheses are consistent with the bulk of these data.

IRON

1. The baseline concentration of 'soluble' iron in the estuary was between 10 and 30 µg/kg during October, 1975.

2. Generally, iron abundances of suspended material in the Hudson was somewhat higher in the spring (51,700 ppm) than in the fall (37,700 ppm). This is consistent with greater biological activity in October.

3. No evidence was found for an anthropogenic input of soluble iron near Manhattan. This might be explained by rapid conversion of this phase to the greater than 0.45 micron fraction by adsorption.

4. In general, more than 95% of the iron being carried through the estuary was associated with the >0.45 micron fraction. Most of this iron was apparently being deposited in the New York Harbor area (Figure 10).

CADMIUM

1. Soluble cadmium concentrations ranged from 0.1 to 0.5 µk/kg.

Table 9

The Standing Crops of the Dissolved Fractions of Five Metals in Upper New York Bay and the Fluxes of These Metals out of This Area during a High-flow Period (April, 1974) and a Fall Flooding Period (October, 1975)

Metal	Standing Crop in Metric Tons		Net Flux out in Grams/ Second	
	April, 1974	October, 1975	April, 1974	October, 1975
Cd	0.24	0.15	1.4	0.6
Ni	4.8	2.9	28	11
Zn	19	7.3	110	28
Cu	3.2	1.5	19	5.8
Mn	24	25	140	96

Figure 10. Plot of the concentration of suspended material versus salinity and mile point

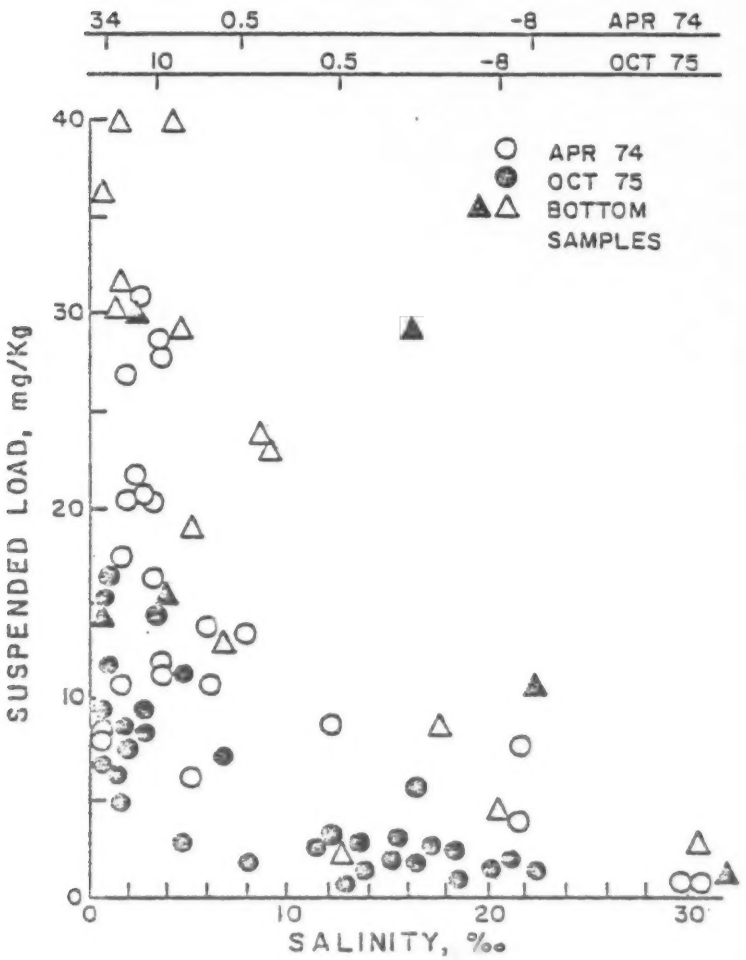

2. Somewhat higher values of soluble cadmium were found in the New York Harbor area which can be explained by a concentration of soluble cadmium in sewage effluent being discharged here of about 9 µg/kg.

3. Cadmium to aluminum weight ratios were about four times higher than those predicted by a crustal model. This can be explained by adsorption of only 3 to 6 percent of the anthropogenic input.

4. Eighty-five percent of these data had a solid to soluble ratio of between 10,000 and 50,000. This range is predicted for systems where adsorption is controlling the partitioning of cadmium between solid and liquid.

5. Approximately 80 percent of the total cadmium in the Hudson River was soluble. This increased dramatically to more than 90 percent near New York Harbor due to apparent deposition of particulates in this region.

NICKEL

1. Soluble nickel concentrations increased from an upstream average of 1 µg/kg to a maximum of about 5 µg/kg near Manhattan due to anthropogenic input.

2. During both periods, approximately 80 percent of the total upstream nickel was less than 0.45 microns. This fraction increases to greater than 90 percent downstream due to deposition.

3. Nickel to aluminum weight ratios were within the range predicted by a crustal model.

ZINC

1. Absolute concentrations of soluble zinc ranged from 2 to 30 µg/kg.

2. Soluble zinc transects can be explained by a three-source mixing model which includes a dissolved zinc concentration of 180 µg/kg in sewage effluents.

3. Zinc abundances of the particulate matter were generally higher than predicted values. This is consistent with the hypothesis that from 13 to 55 percent of the total zinc was adsorbed onto particulates.

4. Any adsorption of zinc apparently took place upstream of the study area on a time scale longer than a few days.

COPPER

1. Soluble copper concentrations ranged from about 1 to 6 µg/kg.

2. The concentrations of soluble copper are consistent with the reported sewage input if one assumes that about 34 to 57 percent of this anthropogenic copper was adsorbed on particulates in April, 1974, and October, 1975, respectively.

3. About 60 percent of the total copper in the Hudson itself was present

in the less than 0.45 micron fraction during both collection periods. This fraction generally increased toward the Bight due to increased sedimentation in the harbor area.

MANGANESE

1. A dialysis experiment was performed which further constrained the size limit of the soluble manganese species from 0.4 microns to about 20 Angstroms.

2. During April, 1974, soluble manganese increased from an upstream value of about 16 µg/kg to about 60 µg/kg at the East River station.

3. The upstream minimum during October, 1975, was about 2 µg/kg. Concentrations again increased downstream reaching a maximum of about 45 µg/kg at the East River station.

4. Transects of total manganese across the estuary were nearly the same for the two collection periods.

5. During October, 1975, the manganese abundances of suspended material collected near the bottom were systematically lower than those of surface particulates. This may suggest post-depositional diffusion of manganese followed by resuspension. Such an arguement predicts a benthic flux of manganese in Upper New York Bay of 1.3 µg/cm^2/day.

SECTION 9

MANGANESE MASS BALANCE IN NARRAGANSETT BAY

Our work on the mass balance of Mn in Narragansett has been published (see Appendices) and will only be summarized briefly here. We sampled rivers entering the Bay, Bay waters, and Block Island Sound waters. Particulate and dissolved Mn and salinity were determined in all samples. The results showed that, while total Mn was roughly conservative, there was a transformation of the element from the dissolved phase in rivers to the particulate phase in the estuary; the transformation was believed to result from oxidative precipitation of soluble Mn^{++}.

Release from sediments is a major source of dissolved Mn in Narragansett Bay: the doubling time by release from sediments is approximately 5 days, whereas the residence time of water in the Bay is about 1 month. Hence it appears that there is rapid recycling of manganese in the Bay, with manganese being released from sediments, oxidized and precipitated out, and again remobilized.

References

Bender, M.L. and Gagner, C. (1976) Dissolved copper, nickel, and cadmium in the Sargasso Sea. J. Mar. Res. Vol. 34, No. 3. 327-339.

Bender, M.L., Klinkhammer, G.P. and Spencer, D.W. (1976) Manganese in sea water and the marine manganese balance. Deep Sea Research

Boyle, E., Collier, R., Dengler, A.T., Edmond, J.M., Ng, A.C., and Stallard, R.F. (1974) On the chemical mass-balance in estuaries. Geochim. et Cosmochim. Acta Vol. 38 , 1719-1728.

Boyle, E., Edmond, J. (1977) Determination of copper, nickel and cadmium in sea water by APDC chelate coprecysitation and flameless atomic absorption spectrometry. Analytica Chimica Acta, 91, 189-197.

Evans, D., Cutshall, N., Cross, F., and Wolfe, D. (1977) Manganese cycling in the the Newport River Estuary. Estuarine and Coastal Marine Science, 5, 71-80.

Fukai, R., Murray, C.N., and Huynh-Ngoc, L. (1975) Variations of soluble zinc in the Var River and its Estuary. Estuary and Coastal Marine Science, 3, 177-188.

Gardiner, J. (1974b) The chemistry of cadmium in natural water - II. Adsorption of cadmium on river muds and naturally occurring solids. Wat. Res. 8, 157-164.

Graham, W.F., BEnder, M.L. and Klinkhammer, G.P. (1976) Manganese in Narragansett Bay. Limnol. Oceang. 21, 665-673.

Helz, G.R., Huggett, R.J. and Hill, J.M. (1975) Behavior of Mn, Fe, Cu, Zn, Cd and Pb discharged from a wastewater treatment plant into an estuarine environment. Wat. Res. 9, 631-636.

Hunt, C.D. (1973) A study of Pb, Cd and Cu Interactions at the Connecticut River/ Long Island Sound Boundary. M.S. thesis, University of Connecticut.

Interstate Sanitation Commission (1972) Report of the ISC of New York, New Jersey and Connecticut.

Klinkhammer, G. (1977) The Distribution and Partitioning of Some Trace Metals in the Hudson River Estuary. M.S. thesis, University of Rhode Island.

Martin, J.M., Jednacak, J. and Pravdic, V. (1970) The physico-chemical aspects of trace element behavior in estuarine environments. Lecture at the International Symposium on the Chemistry of the Mediterranean. "Rudjer Boskovic" Institute, Rovinj, Croatia, Yugoslavia, Sept. 24-26, 1970.

Sholkovitz, E.R. (1976) Flocculation of dissolved organic and inorganic matter during the mixing of river water and seawater. Geochim. et Cosmochim. Acta 40, 831-845.

Simpson, H.J., Hammond, D.E., Deck, B.L. and Williams, S.C. (1975) Nutrient budgets in the Hudson River Estuary. In Marine Chemistry in the Coastal Environment, ACS Symposium Series, No. 18 (editor T.M. Church).

Turekian, K.K. and Wedepohl, K.H. (1961) Distribution of the elements in some major units of the earth's crust. Bull. Geol. Soc. Amer. 72, 175.

Windom, H.L., Beck, K.C., and Smith, R. (1971) Transport of trace metals to the Atlantic Ocean by three southeastern rivers. Southeast Geol. 12, 169-181.